PHOTOPHYSICAL STUDIES ON NANOCOMPOSITE DYAD SYSTEMS BY USING TIME RESOLVED SPECTROSCOPIC TECHNIQUES.

A thesis submitted towards partial fulfilment of the requirements for the degree of

Master of Technology in Laser Technology

Course affiliated to Faculty of Engineering and Technology and
offered by Faculty Council of Interdisciplinary Studies, Law and Management,
Jadavpur University

submitted by

TOUSHIF ALAM

Examination Roll No. M4LST22007

Registration No. 154562 of 2020-21

Under the guidance of

Prof. Dr. Tapan Ganguly

(THESIS SUPERVISOR)

School of Laser Science and Engineering

Jadavpur University, Kolkata - 700032

School of Laser Science and Engineering

Faculty of Interdisciplinary Studies, Law and Management

Jadavpur University

Kolkata -700032

India

2022

M. Tech in Laser Science & Technology
Course affiliated to
Faculty of Engineering and Technology
and offered by
Faculty Council of Interdisciplinary Studies, Law and Management
Jadavpur University
Kolkata, India- 700032

CERTIFICATE OF RECOMMENDATION

I HEREBY RECOMMEND THAT THE THESIS PREPARED BY **TOUSHIF ALAM** UNDER MY SUPERVISION ENTITLED **PHOTOPHYSICAL STUDIES ON NANOCOMPOSITE DYAD SYSTEMS BY USING TIME RESOLVED SPECTROSCOPIC TECHNIQUES** BE ACCEPTED IN THE PARTIAL FULFILLMENT OF THE REQUIREMENTS FOR THE DEGREE OF MASTER OF TECHNOLOGY IN LASER TECHNOLOGY DURING THE ACADEMIC SESSION 2021- 2022.

THESIS SUPERVISOR
Prof. Dr. Tapan Ganguly
School of Laser Science and Engineering
Jadavpur University, Kolkata-7000032

Countersigned

SHRI. DIPTEN MISRA
Director
School of Laser Science and Engineering
Jadavpur University, Kolkata-700 032

DEAN
Faculty Council of Interdisciplinary Studies, Law and Management
Jadavpur University, Kolkata-700 032

M. Tech in Laser Science & Technology
Course affiliated to
Faculty of Engineering and Technology
and offered by
Faculty Council of Interdisciplinary Studies, Law and Management
Jadavpur University
Kolkata, India-700032

CERTIFICATE OF APPROVAL **

This foregoing thesis is hereby approved as a creditable study of an engineering subject carried out and presented in a manner satisfactory to warrant its acceptance as a prerequisite to the degree for which it has been submitted. It is understood that by this approval the undersigned do not necessarily endorse or approve any statement made, opinion expressed or conclusion drawn therein but approve the thesis only for the purpose for which it has been submitted.

COMMITTEE OF FINAL EXAMINATION FOR EVALUATION OF THESIS ----------

---

** Only in case the recommendation is concurred

DECLARATION OF ORIGINALITY AND COMPLIANCE OF ACADEMIC ETHICS

The author, hereby declares that this thesis contains original research work by the undersigned candidate, as part of his Master of Technology in Laser Technology studies during academic session 2021-2022.

All information in this document has been obtained and presented in accordance with academic rules and ethical conduct.

The author also declares that as required by this rules and conduct, the author has fully cited and referred all material and results that are not original to this work.

NAME: TOUSHIF ALAM

EXAMINATION ROLL NUMBER: M4LST22007

THESIS TITLE: PHOTOPHYSICAL STUDIES ON NANOCOMPOSITE DYAD SYSTEMS BY USING SPECTROSCOPIC TECHNIQUES.

SIGNATURE: DATE:

ACKNOWLEDGEMENT

First and foremost, I would like to express my sincere gratitude to my supervisor cum guru ***Prof. Dr. Tapan Ganguly***, Emeritus Professor, School of Laser Science and Engineering, Jadavpur University, for his invaluable guidance, whole-hearted support and encouragement for accomplishing the present investigation. His dynamism, fantastic stamina and day-to-day monitoring every minute detail were a constant source of inspiration to me.

I would also like to express my deep sense of thankfulness to ***Shri Dipten Misra*** providing me necessary atmosphere to work on.

I am extremely thankful to my seniors of School of Laser Science and Technology, especially **Dr. Somnath Paul** and **Ms. Ishani Mitra** for their inspiration and encouragement and helping me through the research work.

I record my acknowledgement to ***School of Laser Science and Engineering*** for giving me the opportunity to pursue my research work.

My sincere thanks to Honourable Vice-Chancellor **Dr. Suranjan Das** and Dean of FISLM, Jadavpur University, for the opportunity provided to complete my research work.

I record my gratitude to our beloved **Jadavpur University**, the vibe and positive circumstances inside and outside of it and the memories of so many in Jadavpur University.

On a final note, I record my one special acknowledgment to my Abba and Maa, my Model School Friends for their perpetual love, motivation and support.

_____

TOUSHIF ALAM

Examination Roll No. M4LST22007

Registration No. 154562 of 2020-2021

This Thesis Work Is Dedicated To:

My Beloved Mother TAJUNNAHAR BEGUM,

Father JAHANGIR ALI

My Supervisor, Friends, Seniors

ALMIGHTY

And

Science & Technology

Content

Abstract

Steady state and time resolved spectroscopic studies on a pristine short-chain dyad (E)-(((9H-fluorene-2-yl)imino)methyl)-N,N-Dimethylaniline (i.e. briefly called as NNDMBF) and its nanocomposite forms with Graphene oxide (GO), reduced Graphene oxide (RGO) as well as Graphene Quantum dots (GQD) were made to examine whether the dyad being combined with the GO or RGO or GQD would serve as efficient artificial light energy converters and charge storage systems relative to its pristine form. The time resolved measurements reveal that with dyad-GO, dyad-RGO and dyad-GQD large portion of the trans structure of the ground state dyad could be protected even on photoexcitation. On the other hand in the case of the pristine dyad NNDMBF all the ground state trans-conformers would be converted to relatively folded structure cis on photoexcitation.

The retention of elongated conformation in trans-form will help to impede energy wasting charge recombination processes within nanocomposite dyads and may serve as better candidate for artificial light energy conversion systems relative to its pristine form. From the present time resolved spectroscopic results it could be hinted that relatively stable trans-conformer in the excited state in case of the nanocomposite system of dyad NNDMBF-GO (or RGO or GQD) in comparison to the pristine form may arise from the surface trap effects.

Preface

The project work or dissertation entitled "Photophysical studies on Nanocomposite Dyad Systems by using Time Resolved Spectroscopic Techniques" deals in designing a functional device combining novel organic dyads with graphene oxide (GO), separately Reduced graphene oxide (RGO) and also deals with the photophysical studies of this composite Dyad with above mentioned nano materials for the much needed development of budget friendly light energy conversion devices with perks like highly efficient, comparatively more stable and biocompatible.

The requirement of energy will never finish, Sun's energy driven by nuclear fusion will last for at least another 5 billion years and so far only a fraction of energy has been utilized from the Sun. So even after consuming so much energy from sun, we remain with immense amounts of energy in our hand. Now this energy can be exploited to model and develop light energy conversion devices in such a manner that it would be safe and sound Biologically and compatible with nature, besides being cheap economically and efficient.

This Dissertation is then divided in several chapters which fulfils the aim and motivation of the project.

Chapter 1: *It is mostly introduction of the brief review of our existing theoretical & experimental knowledge which is relevant to present work. It also outlines the purpose behind studying in the present investigation and furthermore.*

Chapter 2*: Moving to the next chapter which contains descriptively the materials used and the methodology i.e. experimental techniques in our Present study comprising works in designing a functional device by combining synthesized novel organic dyads with graphene oxide (GO) and/or reduced graphene oxide (RGO) nanocomposite systems for fulfilment of the strong need for the much needed development of budget friendly, cheap light energy conversion devices providing high efficiency, better stability, biocompatible.*

Chapter 3: *Depicts the important results made from UV-vis absorption, steady state and time resolved Spectroscopic investigations, both in nanosecond and picosecond time domain. Worthwhile investigations are made on an organic synthesized novel dyad, E-4-(((9H-fluorene-2-yl)imino)methyl)-N,N-Dimethylaniline (NNDMBF) in its pristine form and when combined with Graphene Quantum Dots i.e. in its nanocomposite form in different concentration level.*

Chapter 4: *Concludes our worthwhile investigation of the work and compares the photophysical properties of the short chain Dyad-GQD, dyad-GO with previous known different nanocomposite dyad, e.g. Dyad-CQD and pristine Dyad in Acetonitrile.*

Chapter :1

Introduction

- **Energy**
- **Photophysical Studies and Processes**
- **Light Energy Conversion Process Using Dyads**
- **Graphene and Its Derivatives**
  - **Graphene Quantum Dots**
  - **Graphene Oxide**
  - **Reduced Graphene Oxide**
- **Aim of Thesis**
- **Literature Review**
- **Reference**

1. Energy

Energy, the term itself bears huge meaning and importance in our everyday lives. Its uses is versatile and revolutionary. We use it to produce heat and work in our daily lives, whether it is in household or factories.[1] The reason of our improved and better lives than ever before is because we use more energy to do work. Our ancestors do know little about the blessings of energy and through time and ages, we gain to know more, understand its capabilities as well as its secure uses in various innovative fields. Energy exists in Universe in various forms. On Earth, that main source is Sun, which we get directly or indirectly [2] except nuclear energy. It is little different because of it can be harnessed by using the atomic properties of atoms or molecules. Geothermal energy is different also. Fossil fuel like coal, petroleum, natural gas that we exploit hugely nowadays are derived from several types of organisms which grew over hundreds to million years and stored solar energy on planet earth's surface in layers.[3] Renewable energies like biomass, hydro, river water, wind are never ending and is very much needed in today's world more and more.

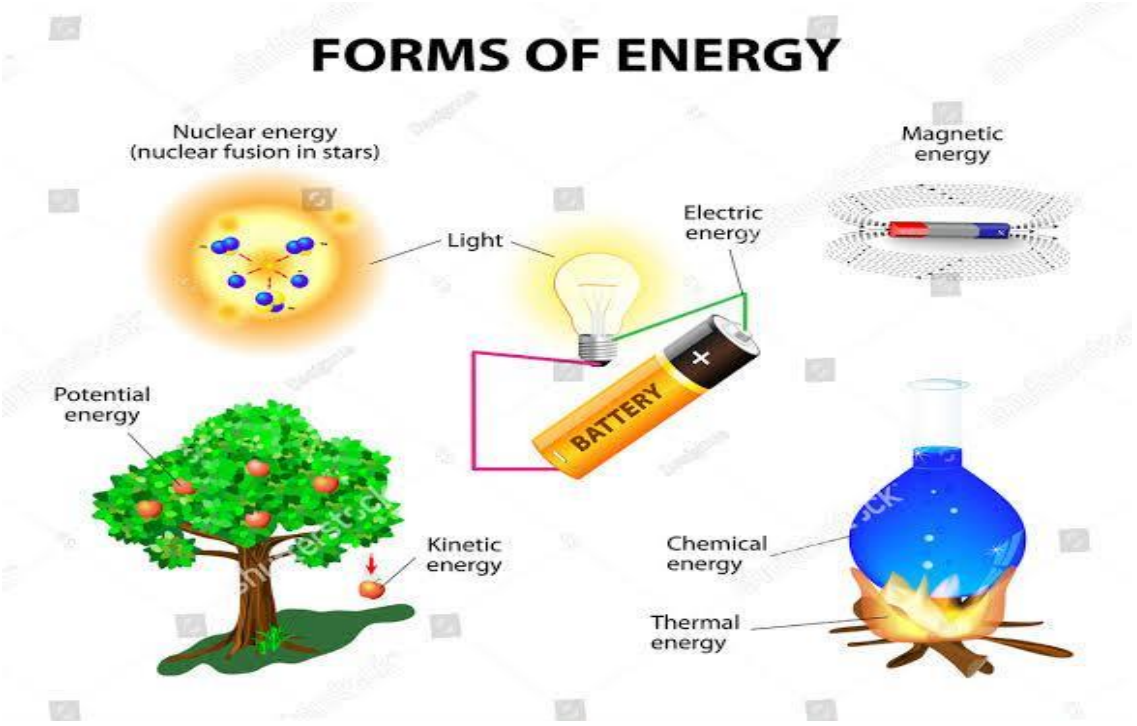

Figure 1.1: Different Forms of Energy

Physical Properties:

- It is a Quantitative property in Physics which is transferred to a physical system.
- Energy is extensive i.e. proportional to size of the system.
- SI Unit: Joule. Defined by $J= ML^2T^{-2}$ (Dimension) [1]

1.1 History and Evolution of Energy Sources

The age of stored photosynthesis has been very brief in historical terms. When coal became widely used due to a lack of wood in the late eighteenth century, it was seen as a poor substitute. Late in the nineteenth century, the era of petroleum fuels began. There are three grounds to believe that the current age is coming to an end: resource constraints, environmental challenges, and societal issues. Pessimists now believe that the peak of world oil production was in the year 2000, and that we are already on the downhill slope, according to a special series of energy reports published in New Scientist lately. There are still optimists who believe it will be another 10 years or more, but there is no significant disagreement on the geological fact that, if it hasn't already occurred, the peak of global oil production will occur in most of our lifetimes. Oil will become scarcer and more expensive in that near-future planet. So, while current assumptions are that we will have cheap petroleum for a few decades, we will have to shift the basis of our energy use. Two heroic assumptions underpin this belief. The first is that there will be continued stability in the Middle East, as well as a desire to export oil from the region. The second assumption is that the majority of the world's population will continue to live without the transportation options we take for granted while we waste scarce petroleum resources on such selfish pursuits as car races, jet skis, motor boats, and suburban trips in heavy four-wheel-drive vehicles. As a result, the first and most fundamental argument for shifting away from the current pattern of fuel energy usage is that we are wasting a finite resource, necessitating change.

The use of fossil fuels is causing serious environmental problems at all levels, from local to global.[3] This is the second reason for change. At the local level, urban fuel usage is the primary source of air pollution, which poses major health problems in many large cities (UNEP 2002). In India, Delhi is the city with the most polluted air. The problem of acid precipitation has prompted policy reforms at the regional level to limit sulphur dioxide production as a consequence of fossil fuel consumption (UNEP 2002). The burning of increasing amounts of fossil fuels is the primary

source of human-caused climate change on a global scale. Concerns about this situation led to the creation of the Framework Convention on Climate Change and its accompanying Kyoto Protocol, a deal to reduce carbon dioxide and other "greenhouse gas" emissions. According to current scientific consensus, carbon dioxide emissions are around 2.5 times the capacity of natural systems to absorb the gas (IPCC 2001). To put it another way, worldwide fossil fuel consumption needs to be cut by around 40% to bring emissions back into balance with the natural carbon cycle. Climate change, according to recent scientific thought, is speeding up and influencing other planetary cycles, posing a severe threat to human civilization's future.[4]

1.2. Energy Statistics in World

China ranked first in energy consumption amongst all the countries in the world. Whether United States of America (USA) just got below China and ranked second in this race.[6]

After China and USA, India's total energy consumption ranked third in the world[]. India is an energy importer that consumes about 3% of the world's total energy. India is the world's third-largest coal-producing country where China is the world's largest in this sector. Oil provides 30% of India's energy demands, and more than 60% of oil is imported and most of them are from middle east.[7]

Global Annual Average Change in Energy

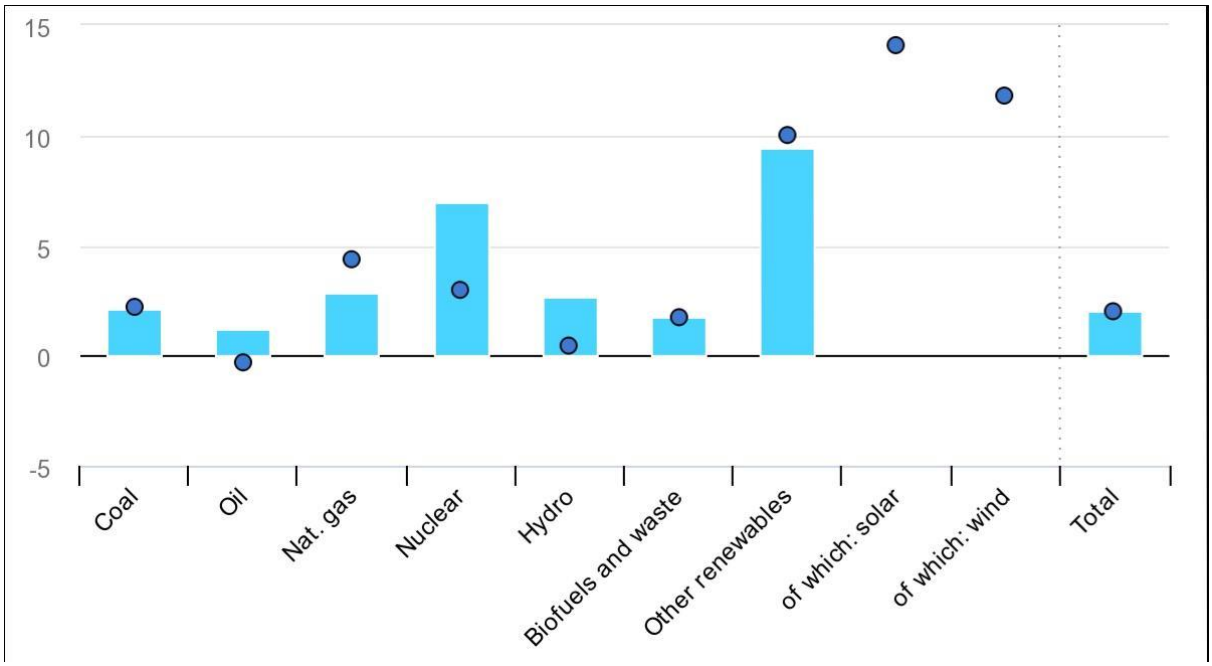

Figure 1.2: Global Change in Energy.[6] (Deep blue dots represent change in 2019-20)

The transport demand of oil fell during time in global health crisis. With 1383 TWh of power generation, India is ranked third in the world. According to Ernst & Young's 2021 RECAI (Renewable Energy Country Attractiveness Index) ranked India 3rd. In November 2021, India had a renewable energy capacity of 150 GW consisting of solar (48.55 GW), wind (40.03 GW), small hydro power (4.83 GW), bio-mass (10.62 GW), large hydro (46.51 GW), and nuclear (6.78 GW). India has made commitment for a goal of 450 GW renewable energy capacity by the year, 2030. Situation has to be improved all over the world in terms of energy.

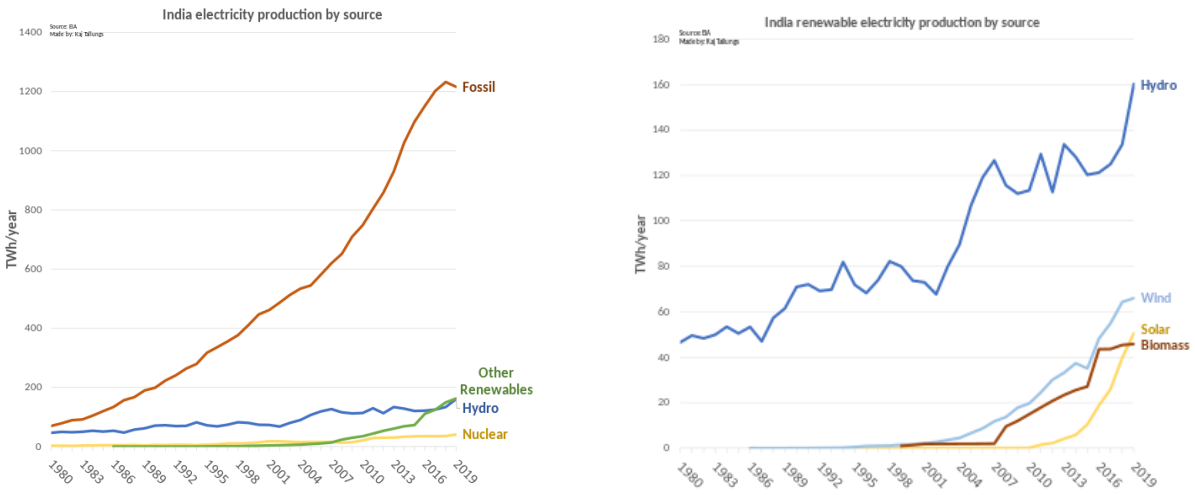

Figure 1.3: India electricity production (i) by energy source (ii) by renewable energy [7]

1.3 Energy Consumption of India:

As on March 31, 2022 Total Installed Capacity from both fossil fuel and renewable energy sources are tabled below.[5]

Table 1

Energy Source	Usage Capacity (MW)	Percentage
1. Fossil Fuel:		
Coal	2,04,080	51.1%
Lignite	6,620	1.7%
Gas	24,900	6.3%
Diesel	510	0.1%
Total Fossil Fuel:	2,36,109	59.1%

2. Non-Fossil Fuel

RES (Incl. Hydro)	1,56,608	39.2%
Hydro	46,723	11.7 %
Wind, Solar & Other RE	1,09,885	27.5 %
Wind	40,358	10.1 %
Solar	53,997	13.5 %
BM Power/Cogen	10,206	2.6 %
Waste to Energy	477	0.1 %
Small Hydro Power	4,849	1.2 %
Nuclear	6,780	1.7%
Total Non-Fossil Fuel	1,63,388	40.9%
Total: Fossil Fuel + Non-Fossil Fuel	3,99,497	100%

1.4 Energy Crisis

The first and second law of Thermodynamics is used to describe the energy flow of a system and how energy is converted to work or other dissipated heat energy. According to first law of Thermodynamics, Energy can be neither created nor destroyed. It just changes from its one form to another. But the energy consumption is closely related to the evolution of mankind. As the consumption of energy grows, the population depends more and more on fossil fuels such as coal, oil and gas day by day and today's world is mostly dependent on non-renewable fossil fuel in nature. Because the prices of gas and oil continue to rise with each passing day, it is necessary to ensure future energy supplies. Natural gas and petroleum are expected to be depleted by the end of the twenty-first century at current consumption rates.

Our current civilisation is reliant on fossil fuels to function. The ever-increasing demand for energy, coupled with the fast dwindling supply of fossil fuels, has resulted in rapid depletion of fossil fuels. This conventional energy resource shortage is slowing social and economic progress in underdeveloped and developing countries. In India, petroleum products such as kerosene, diesel, and petrol are widely used in agriculture and transportation. Aside from that, coal, natural gas, and petroleum are widely used in numerous manufacturing and large-scale businesses. As a result, we expect to be confronted with an energy crisis very soon. Conventional energy sources and non-conventional energy sources/renewable energy sources are the two categories of energy sources. For a long time, conventional energy sources have been employed to generate electricity and power numerous businesses. The majority of these energy sources are fossil fuels such as coal, oil, and natural gas. From air and water pollution to global warming, using fossil fuels for energy has taken a huge toll on humans and the environment the last 20 years, Because to the lack of usage of renewable energy sources and the fast use of fossil fuels for power generation, conventional energy will be phased out in a few years, leaving us with a massive energy crisis.

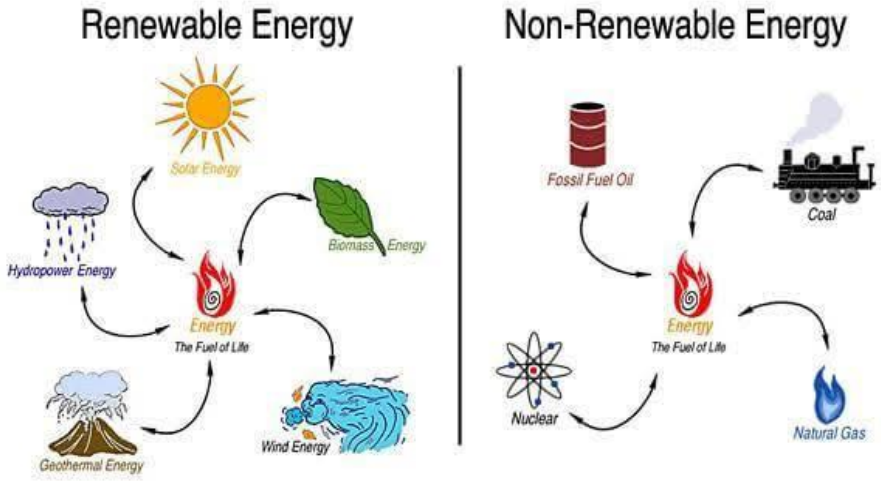

Figure 1.4: Renewable and Non-Renewable Energy

1.5 Solution to Energy Crisis

a. Renewable energy is clean, environmentally beneficial, and pollution-free. Solar power, wind power, hydropower, geothermal energy, and other renewable energy sources are among them. Electricity generation has shifted fast from conventional to renewable, owing to the benefits and promising future.
b. Photochemistry research focuses on fundamental processes aimed at capturing and converting solar energy to chemical or electrical energy. It involves chemical change

caused by the absorption or emission of visible light or ultraviolet radiation.[8] A molecule moves from the ground state to the excited state after absorbing a photon (a particle of light). Light is made up of photochemical reactions. If a molecule loses its chemical identity as a result of electronic photo-excitation, the process is called photochemical; if the molecule retains its chemical identity, the process is called photophysical. Photosynthesis, the technique by which plants obtain energy from the sun, is a well-known photochemical reaction. As a result, different types of artificial photosynthesis are effectively fighting for the right to capture incoming photons and utilize them for the benefit of the community.

c. Nanotechnology presents wide range of solutions to many existing problems and bettering the current situation, e.g. in healthcare, defense system, also in energy crisis. Traditional silicon-based solid state solar cells are one of the few commercially accessible systems for converting solar energy to electricity. Though the performance is not that much, Quantum dots (nanoscale particles) could be used as an alternative. The good thing is these devices can be fabricated in normal atmosphere and room temperature. Efficiency is improving to about 9-11%. The ability to distribute quantum dots in various materials, resulting in "sprinkle on" low-cost and large-area solar cells that may be applied to buildings or vehicles, is perhaps the most interesting aspect of quantum-dot solar cells [9].
d. Because hydrogen is clean, versatile & portable, scientists believe it could be an effective way to reduce world's reliance on non-renewable carbon-formed fossil fuels.
e. Photosynthesis is a natural but very advanced method performed by plants. It consists of several chemical reaction and mainly absorbs sunlight for nutrients synthesis. Besides giving us food and every other nutrients all of today's fossil-fuel-based energy comes from photosynthetic organisms that harvests sunlight. Photosynthesis process is divided into some important parts and factors

    i. Antenna system: Photosynthetic organisms uses its in-built antenna system for light absorption and transfer the required excitation energy to reaction center where the charge separation occurs.
    ii. Reaction factor: Reaction center build a stable charge separation system with very less charge wasted back reactions.
    iii. Oxidation: The separation of charge powers oxidation of H2O molecules.[10]

Finally the product glucose and oxygen are formed.

f. Artificial photosynthetic systems would be a significant step forward in energy generation and a vital breakthrough in addressing the growing concerns about environmental degradation caused by use in extreme quantities of fossil fuels.[4]
One appealing technique to solve this crisis is the construction of solar cells. As a result, dye-sensitized solar cells have emerged as a viable alternative to costly solid-state solar cells. Further developments would be going on there and described in this thesis.

g. A number of other promising approaches to artificial photosynthesis have emerged in recent years, based on the development of organic molecular systems that will provide photosensitized reactions such as PET i.e. photo-induced electron transfer.[11] Some chemical techniques in designing model molecules for artificial photosynthesis have been proposed in preceding years. [54,58]

h. This photosynthesis phenomenon gives rise to the idea of creating a charge storage and artificial light energy conversion system. Based on the underlying scientific principles of the natural process, e.g. Photosynthesis, the solar energy is to be captured and converted into useful forms of energy. A novel organic short chain dyad, NNDMBF was synthesized and characterized.[41] The fundamental goal is to construct supercapacitor like storage systems by combining this organic dyad with various noble metals, metal-semiconductor core/shell nanocomposite, and eventually with graphene hybrid materials. The current thesis focuses on a current research question in the field of new solar cell that uses charge electron injection separation in a short chain dyad as a light energy converter.

i. UV-vis absorption, steady state, and time resolved spectroscopic investigations were carried out in various environments on this newly synthesized dyad in its pristine form and when combined with graphene quantum dots (GQD), graphene oxide (GO) and reduced graphene oxide (RGO). When the two redox components are connected with a short chain, charge separated species arise in both ground and excited states, according to steady state measurements. It is envisaged that by coupling the short chain organic dyad system with GQD, GO and RGO, a highly efficient, stable, and low-cost artificial light energy converter might be constructed that will be safe and biocompatible. To exploit these nanostructures' full potential in the realm of energy storage, we need to fathom how the intricate interplays between the electrical and physical interactions of the active components affect the performance of these devices. This is how our current and future research will be conducted.

2. Photophysical and Photochemical Studies and Processes:

Photophysical and Photochemical processes plays pivotal role in the development of life on earth and surrounding environment with it. Simple cells became autotrophic, provided the basics of life, stored solar energy in the form of fossil fuels, and still feed us with nearly all of our food thanks to a complex set of photochemical and photophysical processes. Photochemistry has an important role in determining the composition of materials in interstellar space and in the creation of pollutants in the atmosphere. Their influence on chemical, physical, biological, and medicinal sciences and technologies, including nanotechnology, is growing at a rapid pace.

Photochemistry deals with chemical reactions.[12] These reactions caused absorption of UV i.e. ultraviolet (wavelength, λ~ 100-400 nm), visible light (λ~ 400-750 nm) or infrared radiation (λ~ 750-2000 nm). Here, photon should have sufficient amount of energy to raise the atoms from ground to excited state. In excited state atoms or group of atoms undergoes chemical reaction more rapidly as compared to ground state.

2.1 Ground States & Excited States

Electronic states i.e. ground states (g.s) and excited states (e.s) of a molecule are obtained by considering the properties of all the electrons in the unfilled shells. The electronic structure of states are commonly denoted by their multiplicities, singlet (S) or triplet (T). At natural temperatures and in normal environment most organic molecules' g.s all electrons are paired. Pauli Exclusion formula determines electrons will have opposite spin in a pair. When one of a pair of electrons is promoted to an orbital of higher energy, the two electrons no longer share an orbital, and the promoted electron can have same spin as the former or opposite spin. A quantum state in which two unpaired electrons have same spin is called a triplet (T), while one in which all spins are paired is called a singlet (S).

A molecule is promoted from its ground state to an electrically excited state by light excitation with a photon of sufficient energy. Each excited state has its own chemical and physical properties as a result of light excitation. Photophysical and photochemical processes are such processes in which the excited species dissociates, rearranges, isomerizes or react with any other molecule.

2.2 Deactivation Processes in Excited States

Radiative transitions, in which the excited molecule emits light in the form of fluorescence or phosphorescence and returns to the ground state, and intramolecular non-radiative transitions, in which some or all of the energy of the absorbed photon is eventually converted to heat are examples of photophysical processes. The schematic diagram is expressed elegantly by Jablonski Diagram [13].

Physical relaxation processes may be categorized as:

I. **Intramolecular**: These processes are

   i. Radiative Transitions: In this electromagnetic (e.m) radiation is emitted when excited molecule happens to go to ground state. Fluorescence & phosphorescence are collectively known as luminescence.

   ii. Radiation-less Transitions: In this no emission of e.m radiation is occured during relaxation process.

II. **Intermolecular**: These processes are

   i. Vibrational Relaxation: Excess energetic molecules in excited vibrational level undergoes very rapid collision with each other or with lowest vibrational energy level in solvent molecule of a defined electronic level.

   ii. Electron Transfer: A photoexcited donor molecule interacts with a ground-state acceptor molecule in this reaction. The excited donor is quenched as an ion pair forms, which may undergo back electron transfer.

   iii. ET: Energy Transfer: By transferring energy to another molecule (the acceptor), the donor's electrically excited state is deactivated to a lower electronic state, while the acceptor is promoted to a higher electronic state.

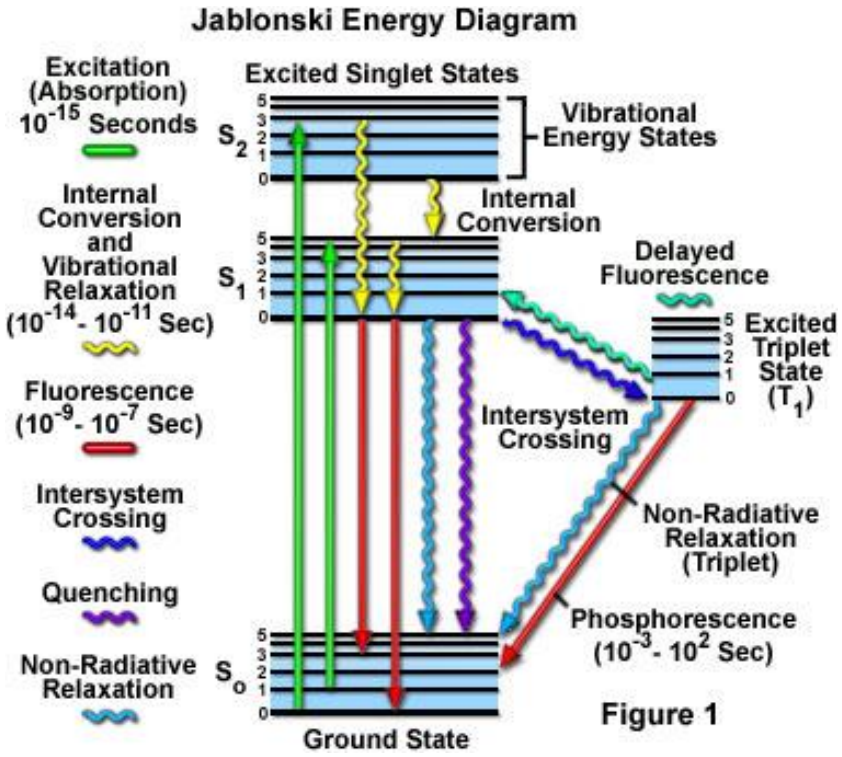

Fig. 1.5: Jablonski Energy Diagram: Physical deactivation of excited states [13]

2.3 Laws of Photochemistry:

I. **Absorption**: When an atom in a ground or lower level absorbs a photon with energy, E = hν (frequency ν) and moves to an upper level is called absorption. There are several governing laws regarding absorption of light. They are called laws of photochemistry.

a) First Law of Photochemistry: Grotthuss-Draper Law

Grotthuss-Draper Law states that Photochemistry requires the absorption of light. This is a basic notion, yet it is essential for properly conducting photochemical and photo biological investigations.. Due to its fundamentality, it is named as first law of photochemistry. Only light that is absorbed by a molecule can cause photochemical changes in the molecule, according to this theory[14].

b) Second Law of Photochemistry: Stark-Einstein's Law

Stark-Einstein's Law states that only one molecule is activated for a photochemical reaction for every photon of light received by a chemical system. It's the second photochemistry law. It also states that just one molecule is activated for a subsequent reaction for each photon of light received by a chemical system. Only one molecule is activated for a photochemical reaction for each photon of light absorbed by a chemical system[9].Albert Einstein developed the quantum theory of light and came up with this 'photo-equivalence law'.

c) Lambert's Law

When a ray of monochromatic light goes through an absorbing material, the intensity of the ray falls exponentially as the absorbing medium's length grows**.** This is known as Lambert law [9]. Mathematically it can be written as,

$$I = I_0 e^{-kx}$$

I, I_0 denotes Intensity of transmitted and incident light respectively

and 'k' is absorption coefficient.

d) Beer-Lambert Law:

Beer–Lambert law, also known as Beer's law is a relationship between light attenuation and the qualities of the substance through which it travels. The law is extensively used in chemical analysis measurements and in physical optics to understand attenuation for photons, rarefied gases. The modified form of Lambert's law comes from the consideration that decreasing rate in intensity of monochromatic light falls exponentially with the length of the medium as well as concentration (c) of solution.

$$I = I_0 e^{-\varepsilon c x}$$

ε = molar absorption coefficient or molar extinction coefficient

II. Spontaneous emission

If the transition between E2 and E1 is radiative, an atom in upper level can be able to decay spontaneously to lower level and release a photon of frequency v. Phase and direction of this photon is arbitrary.

III. Stimulated emission

An incident radiation causes an upper-level atom to decay into lower level, resulting in the emission of a "stimulated" photon with identical properties as input photon. This term ‘stimulated’ emphasizes that this type of radiation happens only when an incident photon is present. The amplification occurs because the incident and radiated photons are similar.

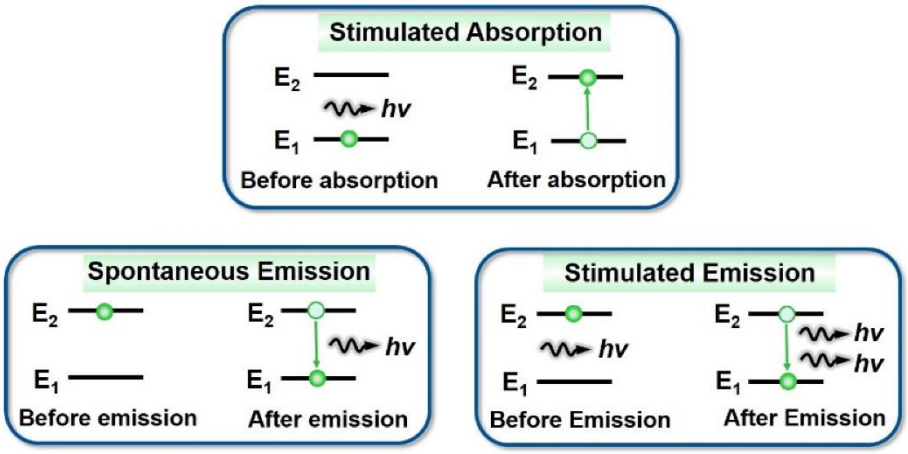

Figure 1.6: Mechanism of the interaction between an atom and a photon [14]

IV. Franck Condon Principle:

In spectroscopy and quantum chemistry, the Franck–Condon principle describes the intensity of vibronic transitions. Vibronic transitions are changes in a molecule's electronic and vibrational energy levels that occur simultaneously as a result of the absorption or emission of a photon of sufficient energy. The principle states that if the two vibrational wave functions overlap more considerably during an electronic transition, a change from one vibrational energy level to another is more likely to occur [26].

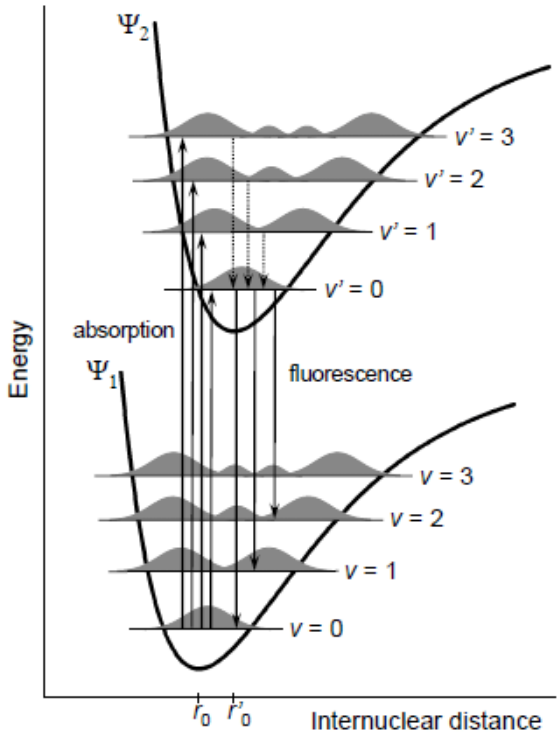

Figure 1.7 : Diagram depicting Franck-Condon principle & absorption, fluorescence emission processes[26]

V. Quantum Efficiency

The term quantum efficiency (QE) commonly refers to incident photon to converted electron ratio. In photochemical reaction it defines the efficiency of that reaction. For this photochemical reaction, QE need to be unity.

$$QE = \frac{no.\ of\ molecules\ reacted/sec}{no.\ of\ photons\ absorbed/sec} \quad ; \quad QE = \frac{rate\ of\ chemical\ reaction}{quanta\ absorbed/sec}$$

(Theoretically) **(Experimentally)**

3. Light Energy Conversion Process Using Dyads

Some donor-acceptor dyads and triads have been synthesized for light harvesting assemblies. Photosynthesis is the fundamental principle of these dyads and triads. Because the donor-acceptor system containing Chlorophyll a and porphyrin can attain a long-lasting charge separation state, it can mimic the photo-induced electron transfer process of natural photosynthesis. Some nanoparticle has clever features that protect charge separation species in diverse stimulated short chain dyads systems by limiting the energy-draining charge recombination process.[9]

Many model compounds with electron donors and acceptors coupled by covalent bonds have been created for use in light emitting diodes (LEDs), photovoltaic cells, organic solar cells, and artificial or model photosynthetic systems, among other things. The creation of numerous effective light energy conversion devices will be aided by the use of synthetic compounds in the form of organic dyad systems with electron donor and acceptor moieties connected together by short spacers. The short-chained dyads may efficiently harvest light, transfer excitation energy, transfer electrons, and produce long-lived charge-separated states. Several strategies were employed on model donor–acceptor connected dyads or multichromophoric systems to boost the charge-separation rate in order to develop various light energy conversion devices.[15]

NNDMBF– A short-chain dyad containing the electron donor 4(N,N-dimethylamine)Benzaldehyde (NNDMB) and the acceptor F (fluorene) has been synthesised. The dyad is shown in following figure.[16]

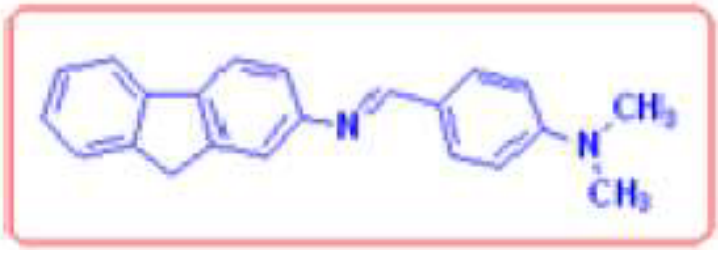

Figure 1.8: Novel short-chain dyad (NNDMBF)[16]

4. Graphene and Its Derivatives

4.1 Introduction

Graphene is allotropes of carbon. This name was introduced by Boehm, Setton, and Stumpp in 1994 .[17] Graphene is a monolayer of carbon atoms arranged in a hexagonal lattice. It's a two-dimensional substance made up of carbon atoms that have undergone sp2 hybridization. Its bond length (molecular) is 0.142 nm. It has attracted a lot of attention in recent years due to its unique electrical, optical, magnetic, thermal, and mechanical capabilities, as well as its enormous specific surface area. Because graphene is widely utilised in nanoelectronics, it is critical to generate high-quality graphene. By mechanically cleaving a graphite crystal, Geim and Nosovelov were able to synthesise single layers of graphene in 2004.

Graphite is made up of layers of graphene stacked on top of each other with an interplanar spacing of 0.335 nm. Van der Waals forces hold the individual layers of graphene in graphite together, which can be overcome during graphene exfoliation. In terms of thermal and electrical conductivity, graphite has a remarkable anisotropic behaviour.

Graphene has some unique features that distinguish it from other carbon allotropes. It is around 100 times stronger than the strongest steel in terms of thickness, yet its density is far lower than any steel. This conducts heat and electricity very well and is practically translucent. Graphene has a large and nonlinear diamagnetism, even stronger than graphite, which can be levitated by Nd-Fe-B magnets.

Graphene has extraordinary electronic, chemical, mechanical, thermal, and optical properties, making it a crucial material in the twenty-first century. It is also known as the world's 'thinnest' material. Graphene is now used in a wide range of applications, including energy storage materials, supercapacitors, nanoelectronics, drug delivery systems, polymer composites, liquid crystal devices, biosensors, and many others.[18]

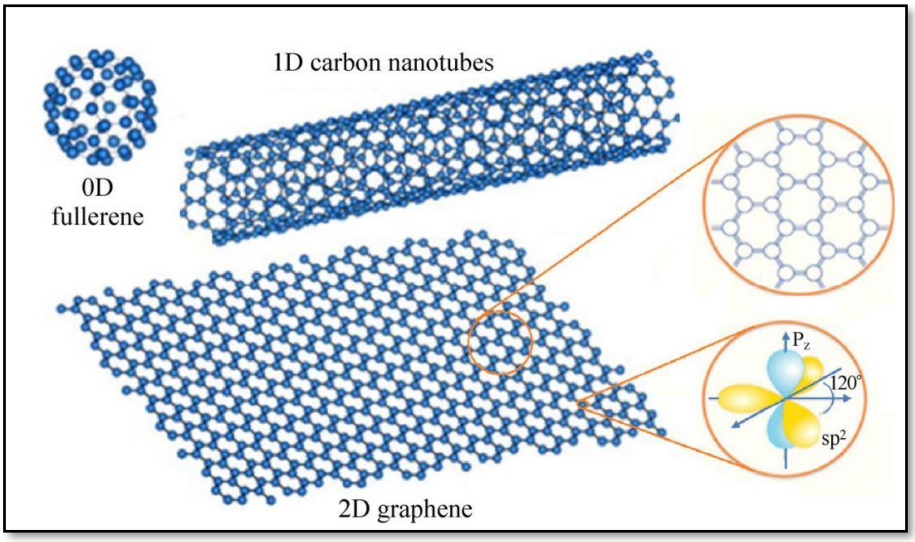

Figure 1.9: Graphene structure[18]

4.2 Graphene Quantum Dots (GQD)

Graphene quantum dots (GQDs) are a type of 0D material formed from small fragments of graphene. Due to quantum confinement and edge effects, GQDs display new phenomena akin to semiconducting QDs. Graphene and similar materials utilised for chemical sensing, such as GO or RGO, offer a lot of potential. This is owing to the 2-dimensional structure, which provides a large sensing surface per unit volume and low noise in comparison to conventional solid state sensors.

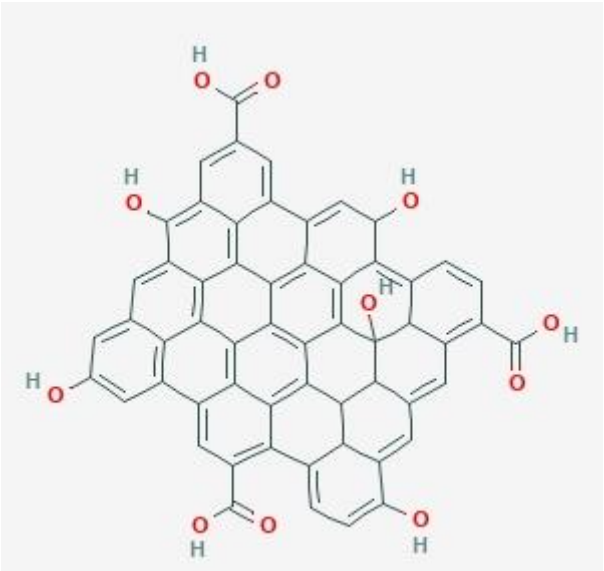

Figure 1.10: Molecular Structure of GQD. [20]

Properties:

1. GQD consist of one or a few layers of graphene and are smaller than 100 nm in size.
2. Less toxicity, having quantum confinement property.
3. They are chemically and physically stable,
4. GQD has large surface to mass ratio
5. It can be dispersed in water easily due to functional groups at the edges.
6. Fluorescence emission of G-dots has broad spectral range, includes IR, visible & UV.

4.3 GQD Synthesis Method

A variety of approaches have been created to make GQDs.[20] These methods are usually classified as either top down or bottom up. Different techniques, such as graphite, graphene, and carbon nanotubes, were used to turn bulk graphitic materials into GQDs via top-down methodologies. Electron beam lithography, chemical oxidation, graphene oxide (GO) reduction, ultrasonic assisted exfoliation method are some of the more useful ones.[21] Because of strong mixed acids are used in top-down methods, substantial purification is frequently required. Bottom-up techniques, on the other hand, construct GQDs from small organic molecules such as citric acid and glucose. The biocompatibility of these GQDs is improved.

Top- Down Method

Hydrothermal Method:

The hydrothermal approach is a simple and quick way to make GQDs. Using a range of macromolecular or tiny molecular compounds as starting ingredients, GQDs can be produced at high temperatures and pressure. To make GQDs, high temperature and high pressure are used to disrupt the bonds between carbon components.

Electrochemical Oxidation

In this particular process, carbon–carbon graphite bonds, graphene are oxidized and decomposed in high redox voltage circumstance (1.5-3 V) into making GQD.

Chemical Exfoliation:

It is one of the suitable methods for GQD synthesis. In this method c-c bonds of graphene, carbon nanotubes are destroyed by adding acids like H_2SO_4, HNO_3. Then it oxidises or exfoliates graphene in layers and GQDs are formed.

Bottom-Up Process:

Electron-beam lithography:

Electron-beam lithography or EBL is a process of scanning a focused beam of electrons to draw custom shapes on a surface covered with an electron-sensitive film. It requires costly and professional equipment. By this method GQD can be synthesized even at room temperature. [21]

Microwave Method:

Because the hydrothermal method's long reaction time is a typical issue, microwave technology has evolved into a quick heating method that is widely employed in the fabrication of nanomaterials. It not only cut the reaction time in half, but it also boosted the yield. GQDs are purified by microwave irradiation utilising Asp (Aspartic acid), DI water and NH_4HCO_3. High fluorescence (blue) is observed in produced GQD.

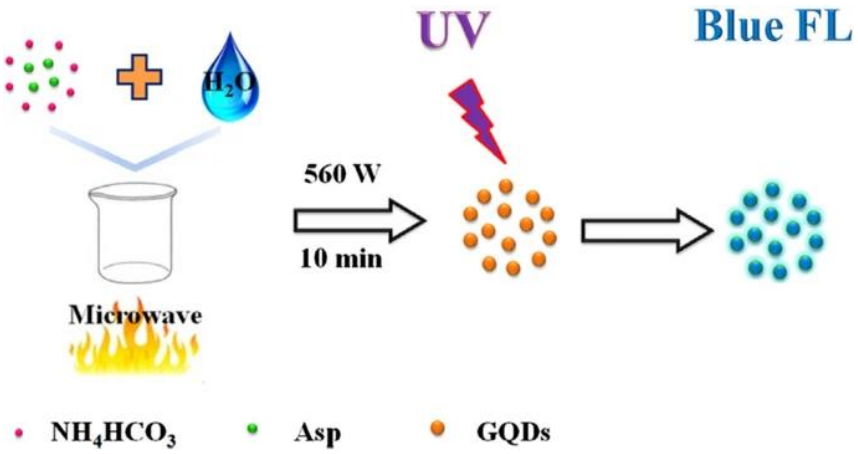

Figure 1.11: Preparation Process of GQD by Microwave Method [30]

4.4 Graphene Oxide (GO)

An oxidised form of graphene is called graphene oxide (GO). Since GO exhibits a strong hydrophilic behaviour, water molecules can pass through the graphene layers, further extending the interlayer gap brought on by oxidation. Graphite oxide and GO are frequently referred to as electrical insulators since sp2 also breaks the bonding network in them. Graphite oxide can be exfoliated into monolayer sheets using a variety of mechanical and thermal processes to produce GO. However these techniques have some drawbacks due to the serious harm they do to GO platelets, particularly by shrinking the surface area to nanometers. GO is a poor conductor, but it can regain most of the legendary pristine graphene's characteristics by being exposed to light, heat, or chemical reduction. The first synthesis of GO is often attributed to Brodie, Staudenmaier, and Hummers and Offeman each of whom derived graphite oxide via the oxidation of graphite using various techniques.[22] Hummers and Offeman made a number of improvements on the original two techniques to make them safer, including the use of KMnO4 as an oxidizer (rather than KClO3, which evolves toxic ClO2 gas) and the addition of sodium nitrate (to form nitric acid in situ rather than using nitric acid as a solvent). Due to the safer and more scalable nature of the Hummers' method, this is the one that is generally used (or, in most cases, slightly altered) to generate GO.

4.5 Reduced Graphene Oxide (RGO)

Graphene's redox component is reduced graphene oxide (RGO). The method of reducing GO to create RGO is crucial because it greatly affects the quality of the RGO that is created; as a result, it will influence how similar the structure of the RGO is to that of pure graphene. There are several ways to reduce something, but they are all based on chemical, thermal, or electrochemical processes. [23] While some of these methods can yield RGO of extremely high quality, comparable to pure graphene, their execution can be difficult or time-consuming. Surface area and conductivity yields for RGO made through chemical reduction are comparatively low. It has been demonstrated that RGO, which is produced by thermally reducing GO at temperatures of 1000 ^{0}C or higher, has a very large surface area that is comparable to that of pure graphene. As pressure increases from the heating process, the graphene platelet suffers damage, emits CO2, and loses mechanical strength due to structural flaws like vacancies. High quality RGO, which resembles pure graphene, is produced through

the electrochemical reduction of GO. The main advantage of this procedure is that no harmful waste is produced because no hazardous chemicals are used.

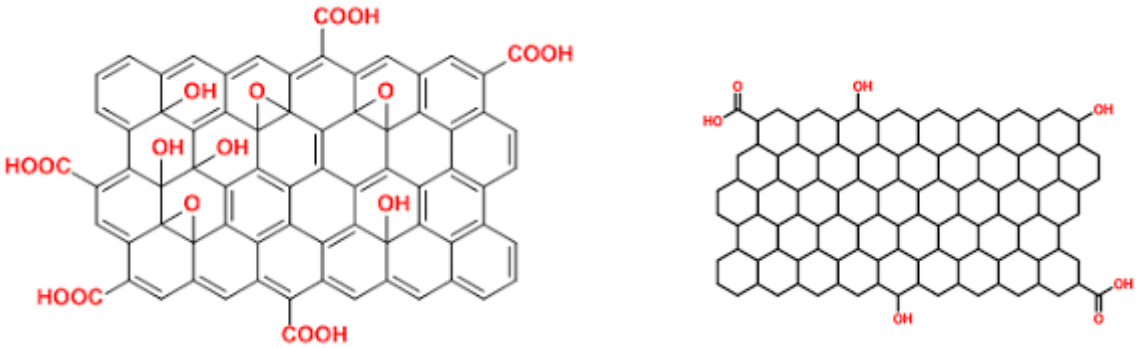

Figure 1.12: a) Molecular Structure of GO b) Structure of RGO

Properties of GO and RGO

i. GO is easily dispersible in water and organic solvents because of the presence of oxygen functionalities. This solubility of GO remains a very important property when it is mixed with other material to improve their conductivity.

ii. GO is often described as an electrical insulator because of the disruption of its sp^2 bonding networks. To recover, The reduction of GO yields RGO and hence electrical conductivity and honeycomb hexagonal lattice structure regained.

iii. Modified graphene can be achieved by functionalization of GO and chemical properties are changed. This makes it more adaptable for so many applications e.g. optoelectronics, bio utilized devices, or importantly as a drug-delivery material.

4.6 Synthesis Methods of GO and RGO

The discovery of GO & RGO brings new method of synthesis in light. Several methods are introduced through ages and in research papers. Synthesis of GO can be divided into two main categories--- i) bottom-up methods where simple carbon molecules are used to construct pristine graphene; ii) top-down methods where layers of graphene derivatives are extracted graphite or other carbon source. The effective and useful methods are described here below---

Bottom-Up Methods:

Chemical Vapor Deposition (CVD):

By this bottom-up method GO can be produced. In this process the substrate is exposed to one or more volatile precursors, which react and/or decompose on the substrate surface to produce the desired thin film deposit. The waste gases pumped out from the reaction chamber. Here temperature is the vital physical quantity which is controllable. Depending, Requirement of precursors and the structure depends on the material quality. There are many various types of CVD processes like thermal, plasma enhanced (PECVD), hot wall etc. [24]

Silicon Carbide:

Silicon carbide (SiC) is one of the candidate materials for use in the first-wall and blanket component of fusion reactors, and is used in nuclear fuel particle coatings for high-temperature gas-cooled reactors.[25]

Top-Down Methods:

The focus on top-down methods, which first generate GO and/or RGO are more popular for yielding graphene derivatives, in particular for use in nanocomposite materials.

Mechanical Exfoliation:

This is a top-down technique in nanotechnology, by which a longitudinal or transverse stress is created on the surface of the layered structure materials. mechanical method of exfoliation can be done by sonicating graphite oxide in water or polar organic media. Especially, sonicating and mechanical stirring can be combined together to exfoliate graphite oxide with a better efficiency than using any individual method. But the sonication has a great disadvantage that it causes substantial damage of GO platelets.

Thermal Exfoliation:

During heating, the oxygen-containing functional groups attached on carbon plane decompose into gases such as H2O, CO2 and CO, which will diffuse along the lateral direction. This exfoliation occurs only if the decomposition rate of functional groups surpasses the diffusion rate of evolved gases. Here the interlayer pressure existing among adjacent layers is large enough to overcome their van der Waals interactions and pushes the layers separated from each other. Generally, a minimum temperature of 550 °C is necessary for the successful exfoliation at atmospheric pressure. [56]

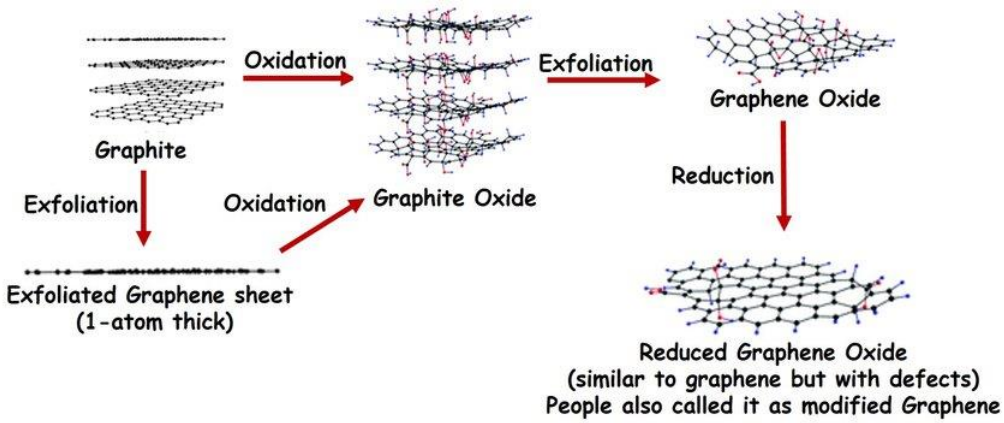

Fig. 1.13. Exfoliation of graphite oxide [58]

These two methods lack of quality and control. Due to that some other methods are introduced.

Modified Hummers Method

Any method which changes or improves upon the synthesis route proposed by Hummers is regarded ubiquitously as a "modified Hummers method".[27] In general, a carbon source (often graphite flakes or powders) is put into a protonated solvent (such as sulfuric acid, phosphoric acid, or some mixture of these) and a strong oxidizing agent (usually KMnO4) is introduced. Following a dilution step, it is common to treat the resulting mixture with H2O2 to remove any metal ions from the oxidizer; this results in a yellow bubbling and ultimately a yellow-brown liquid. The resulting solids are then separated and treated with dilute hydrochloric acid to further remove any metal species, and the solution is washed and centrifuged several times with water until the pH of the solution is essentially neutral.

Tour Method:

GO (Graphene oxide) iss prepared by mixing 90 mL concentrated H2SO4 (sulfuric acid) and 10 mL concentrated H3PO4 (Hydro-phosphoric acid). GO was reduced by using ascorbic acid as a reducing agent and distilled water. Then it is centrifuged and RGO is formed. This process involves several other similar or little different steps. That is being discussed below.

(i) Oxidation or intercalation: GTO (graphite oxide) need to be prepared from graphite powder by mixing H_2SO_4 with potassium permanganate (strong oxidizing agent).

(ii) Exfoliation: Oxidized form of graphite should be dispersed into distilled water to form single-layer graphene oxide (GO). Then heating it with magnetic stirrer, black paste formed collected by filtration and followed centrifugation and drying a day at 60°C.

(iii) Reduction: In order to synthesize reduced graphene oxide (RGO), the GO was dispersed and ascorbic acid was added as the reducing agent, and same procedure followed. At Last, the black product should be washed with ethanol and distilled water, respectively.[28]

4.7 Applications of GQD, GO & RGO

Biomedical Applications:

i. **Drug delivery system**– Medicine delivery or drug distribution also possible by GQD, GO & RGO. GQD has a greater chance in biomedical applications than graphene or graphene oxide because of its small size (GO). There are efficient GQDs-based drug delivery systems e.g. EPR-pH delivery-release mode, EPR-Photothermal delivery-Release mode.[30]

ii. **Bio imaging –** Bio-imaging and fluorescent bio-imaging using GQD or GO of cells and tissues shows great performance because fluorescent nano materials are biocompatible and bio-toxic less. [29].

iii. **Biosensor** – GQD have some great properties like high solubility in water, flexibility in surface modification, nontoxicity, multicolour emission, excellent biocompatibility, good cell permeability, and high photostability, reason of its being used in biosensors. GQD and GO biosensors are used for visual monitoring of glucose, phosphate, cellular copper, iron and nucleic acid.

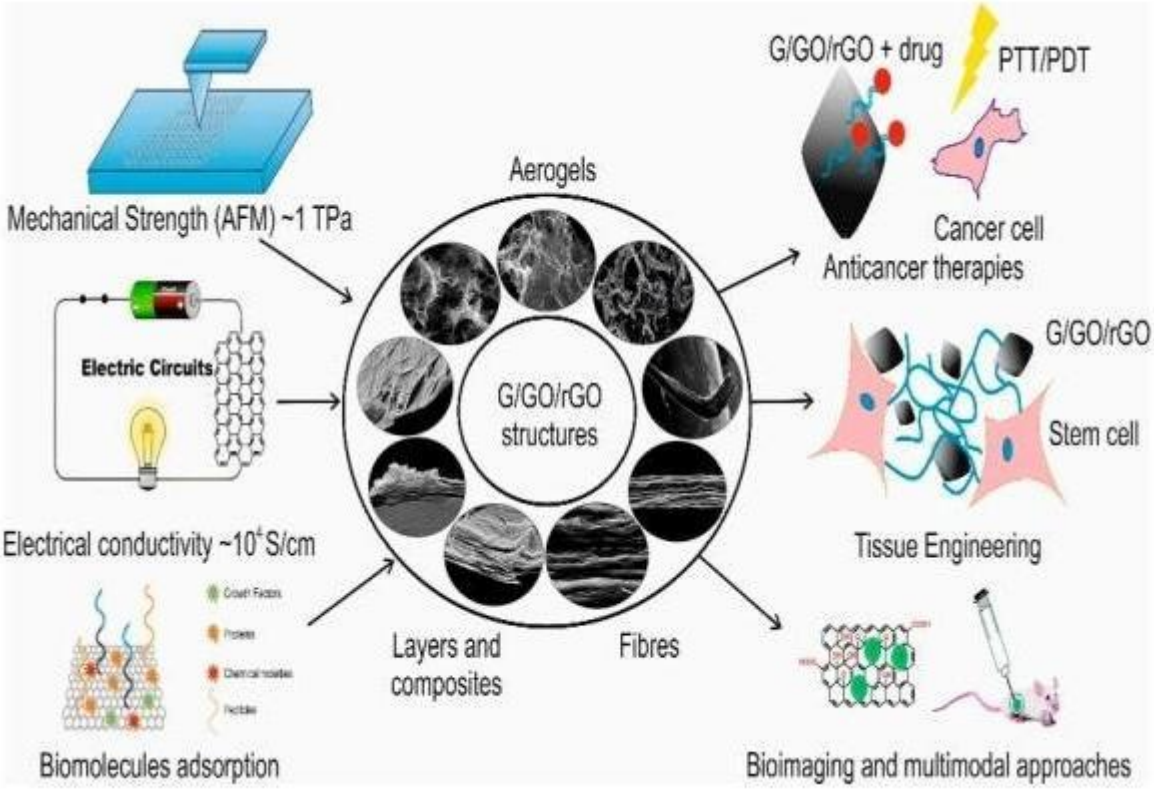

Figure 1.14: Applications of GQD, GO [29]

Optoelectronics Applications:

i. **LED: Light Emitting Device–** GQD are great material for LEDs due to their stable light emitting, low cost and eco-friendliness. Nitrogen-rich GQD show broad and bright visible light under UV illumination that would be worth utilizing in phosphor applications.

ii. **OSC: Organic solar cells –** By GQD organic solar cells can be made and this type of solar cell are very light weight, flexible and light harvesting capacity is high because it can absorb near infrared light. It has special optical properties to control efficiently by changing their quantum dot size [29].

iii. **DSC: Dye-sensitized solar cells –** DSCs are very popular because the making process is very easy and the making cost also very low. It is an organic dye and the efficiency also grate. GO or GQD with stable light absorption made from broad and cheap sources show its potential in DSCs [29].

iv. **Supercapacitor –** GO & GQD can be electrode for supercapacitors. These and some of its hybrid performs electrochemical performance achieved by efficient dispersion of reduced GO. It is useful in charge–discharge process and charge transportation [12].

5. Aim of thesis

Our primary aim of this thesis would be to fabricate new nanocomposite hybrid by combining organic novel short-chain dyad i.e. NNDMBF with GQD, GO and RGO. At first synthesis and characterization of NNDMBF are to be made. NMRNMR studies, theoretical predictions and some software calculations of this dyad are also performed and very important to it. Keen investigations are also worked out by using Ultraviolet-Visible absorption, steady state & time resolved spectroscopic (TCSPC) and Transient Absorption Spectra on same pristine dyad and also when combined with graphene quantum dots/ graphene oxide / reduced graphene oxide in order to check results of suitable form of nanocomposite dyad. Finally we do utilize the result to know whether it is an effective energy storage candidate and in future if we can use it as a budget and eco-friendly supercapacitor way or machine to solve the global energy crisis phenomenon.

6. Literature Review

NNDMBF– short-chain synthesized dyad has suitability in so many fields. As a candidate in LEDs, solar cells, data storage and Also it has the potential to serve as better candidate for artificial light energy conversion systems relative to its pristine form. From the present time resolved spectroscopic results it could be hinted that relatively stable trans-conformer in the excited state in case of the nanocomposite system of dyad NNDMBF-GO (or RGO or GQD) in comparison to the pristine form may arise from the surface trap effects. In future it may able to solve the global energy crisis phenomenon. [31]

T. Ganguly et al.[32] investigated the photophysical characteristics and the nature of the photoinduced electron transfer (PET) reactions using electrochemical, steady state, and time-resolved spectroscopic methods, in a synthetic anisole (A)-thioindoxyl (T) dyad system (24MBTO). The outcomes show how the charge separation reactions produced the two types of isomeric species, Z- and E- forms. According to the thorough investigations, the current thioaurone may function as a flexible photoswitchable system.

F. Wang et al. [33] stated that new photophysical phenomena had been introduced together with the optimization of existing photophysical processes, such as charge separation during light absorption. The use of fundamental concepts for converting solar energy into chemical energy, selective chemical synthesis, e-/h+ excitation of semiconductors and biological system self-replication are also examined. The intensity of the incident light and the higher temperature will both affect how much the nanoparticles' localized temperature increase. This practical method of fusing natural and artificial systems results in very effective and long-lasting solar to chemical energy conversion.

T. Ganguly et al. [34] demonstrates using steady state and fluorescence lifetime measurements that singlet-singlet energy transfer occurs to populate the lowest excited singlet of carbazole as a result of photoexcitation of the benzotriazole (BZ) part of the bichromophore, 9(1-H-benzotriazole-lylmethyl)-9H-carbazole (BHC) (CZ). As a result of this indirect energy transfer process, CZ is indirectly stimulated and conducts a strong charge transfer reaction (CT) with the polar medium acetonitrile (CAN). BHC behaves as a triad system of BZ-CZ-CAN when dissolved in CAN, with BZ serving as an antenna molecule and CZ serving as a reaction centre. It has been suggested that the bichromophoric system BHC may function as a synthetic photosynthesis or solar energy conversion mechanism.

Chakraborty et al. [35] claimed that core-shell nanostructures had typically been discovered to have enhanced qualities, leading to the development of a more effective light energy conversion device using chore-shell nanocomposites rather than just nanoparticles.

T. Asahi et al. [36] used femtosecond laser spectroscopy to investigate photoinduced intramolecular charge separation (CS) and charge recombination (CR) of the product ion pair (IP) state of a number of fixed-distance dyads composed of zinc or free-base porphyrin and quinines in order to ascertain the energy gap and temperature dependences of CS and CR reactions in nonpolar media. The obtained CS and CR rates were in the normal and inverted regions, respectively. They have verified that when the energy gap narrows, the activation barrier for the CS reaction rises. Here, the CS rate constant shows negligible solvent polarity dependence while the CR rate constant exhibits an increase in solvent reorganisation energy with solvent polarity.

T. Ganguly et al.[37] used steady state, time-resolved spectroscopic methods, and fluorescence anisotropy decay to observe the photophysical properties of the synthesised short-chain organic dyad, 1-(4-chlorophenyl)-3-(4-methoxy-naphthalen-1-yl)-propenone (MNCA) in isotropic media and gel (P123) environment. According to NMR and time-resolved spectroscopic studies, the charge-transfer species of the dyad MNCA appear to have only one isomeric form in the ground state, and this conformation persists even after photoexcitation, regardless of the environment's characteristics, such as whether it is an isotropic solution or a micro-heterogeneous medium (gel phase of P123).

T. Ganguly et al. [38] studied the nature of charge separation as well as the energy-wasting charge recombination processes within a short-chained organic dyad 1-(4-bromo-phenyl)-3-(2-methoxynapthalen-1-yl)-propenone (MNBA) have been revealed by using electrochemical, steady state and time resolved fluorescence (by TCSPC), nanosecond laser flash photolysis methods. On photoexcitation, further conformers probably of the nature of folded type isomeric species (Z-form) were also obvious from time resolved fluorescence studies, even if in the ground state elongated type structure (E-form) is observable from NMR spectra. However, this time-resolved study has revealed a predominance of elongated shape in the excited singlet state. The charge separation rate was found to be much higher than the energy-wasting charge recombination rate, which was calculated from the transient absorption measurement using nanosecond laser flash photolysis technique. This finding suggests that MNBA may be a good candidate for building artificial light energy conversion devices or molecular photovoltaic cell components.

T. Torres et al.[39] looked at the photophysical characteristics of a new dyad molecule made up of a donor Zn-phthalocyanine and a C_{60} derivative that are covalently bonded (acceptor). They provided experimental proof of charge separation with a long half-life in solid state, which is many orders longer than in solution. The foundation for potential photovoltaic applications is it.

T. Ganguly et al.[40] investigated steady state and time resolved spectroscopic measurements on the organic dyad 1-(4-Chloro-phenyl)-3-(4-methoxy-naphthalen-1-yl)-propenone (MNCA) at ambient temperature. When the surrounding medium is changed from being only chloroform to being a mixture of chloroform and Ag@TiO2 (noble metal-semiconductor) nanocomposites, time resolved fluorescence and absorption measurements show that the rate parameters associated with charge separation within the dyad increase while charge recombination rate reduces significantly. According to the results, a dyad and core-shell nanocomposites may be coupled to create an organic-inorganic nanocomposite system that may be used to create light energy conversion devices.

According to *T. Ganguly et al.* [41], different photophysical properties could be measured using UV-vis absorption, steady state spectroscopic experiments, and time-resolved spectroscopic experiments. When the results of the silver (Ag)-dyad MNTMA and gold (Au)-MNTMA hybrid nanocomposites systems were examined, a striking difference was found between the two.

T. Ganguly et al.[42] measured various photophysical properties of the silver (Ag)-dyad MNTMA system and compared the results to the gold (Au)-MNTMA hybrid nanomaterials by using UV-vis, steady state, and time resolved spectroscopic techniques, Ag-dyad systems have a significant amplification of the plasmonic absorption band, whereas the other Au-dyad systems do not. In the case of the Ag-dyad hybrid nanocomposite system, the preponderance of folded conformation, which enables charge recombination, was detected even in the excited state from the measured fluorescence lifetime values. According to transient absorption tests using the laser flash photolysis method, the Ag-dyad system's rate of energy destruction is significantly higher than that of the Au-dyad nanocomposite device.

Bhattacharya et al. [43] reported on the nature of the charge separation and recombination processes in an organic dyad with a short spacer. This inquiry shown that an effective light energy conversion device may be created using the 1-(4-Bromo-phenyl)-3-(2-methoxynaphthalen-1-yl)-propenone (MNBA) candidate. Therefore, this technique can be used to create low-cost, effective energy conversion devices in the future.

Bhattacharya et al. [44] looked at the possibility of employing metal-semiconductor nanoparticles to modulate the charge recombination process in light energy conversion devices. It was discovered that a significantly enhanced version of the light energy conversion device was implied by the use of TiO2 nanoparticles. Charge-separated organisms could be protected for a long time under this system.

T. Ganguly et al. [45] looked and studied pure dyads, dyad-spherical gold nanoparticles (GNP), and dyad-star shaped gold nanoparticles using UV-vis absorption, steady state, and time-resolved spectroscopy examinations (GNS). Although the pristine form of the dyad has a trans-(elongated and planar) isomer in the ground state, it was found that during photoexcitation, the trans- transforms into the cis- structure (folded). It's interesting to note that the dyad behaves differently whether it combines with GNP or GNS. Due to the stimulation of the dyad-GNS system, 60% of the trans-species remain unaltered in the excited state. In the current experiment, the dyad-GNS nanocomposite appears to be a better light energy storage device than the dyad-GNP and the pure form of the dyad.

Mitra et al. [46] noticed the impact of short chain dyad carbon quantum dots (CQD) and their capacity for storing energy. The research on the pure short chain dyad €-4-(((9H-fluorene-2-yl)imino)methyl)-N,Ndimethylaniline (NNDMBF) and its nanocomposite forms with CQD or NCQD was done using time resolved spectroscopic approach. The experiment's findings demonstrate that the ground state dyad's more than 80% trans structure can be maintained in the presence of photoexcitation in the CQD environment and functions as a powerful energy storage system.

Gust et al. [47] claimed that a biomimicry system may lessen the complexity of natural photosynthesis. The liposomal device, a biometric nanoscale machine, converts solar energy into chemical energy. The system has a very high level of efficiency. A photosynthetic bacterium's solar energy conversion method is similar to how the liposomal system transfers energy overall.

Rozzi et al. [48] noted that the main issue is how effectively light energy can be turned into electrical power or chemical fuels. This conversion is typically believed to occur on extremely fast, femto-to-pico second time scales in artificial photosynthesis and solar devices. They also looked into the primary charge transfer process in a prototypical artificial reaction centre called a supramolecular trio.

Sen et al. [49] stated that time-resolved and steady-state spectroscopy has been used to examine the surface energy transfer between confined dye and Au nanoparticles. Analysis shows that the energy transfer from the dye to the Au nanoparticles is a process of surface energy transfer. It may be possible to create novel light harvesting systems using this energy transfer between restricted dye and Au nanoparticles.

Dutta et al. [50] recognised that photoexcitation of a donor molecule followed by electron transfer to an accepter is a typical pathway for energy storage. They confine trisbipyridine ruthenium (II), the light sensitizer donor, in the super cages of zeolite.

Zhang et al. [51] found that a variety of advantages exist for nanostructured materials, including high surface-to-volume ratios, favourable transport characteristics, altered physical properties, and confinement effects brought on by the nanoscale size. Thus, it has a wide range of applications, including in solar cells, catalysts, thermoelectric devices, lithium-ion batteries, and super capacitors, among others. Some applications gain from this review, such as increasing electrochemical reaction by increasing surface area, or improving solar cell optical absorption by producing optical effects.

Balaya et al. [52] discussed the cutting-edge idea at the nanoscale for the creation of superior materials that perform effective energy conversion and storage. The use of nanostructured materials in thermoelectric devices for efficient waste heat conversion is highlighted. He claimed that metal oxides of the nanoscale can improve the performance of supercapacitors.

Edward et al. [53] mentioned were fuel cells and hydrogen's usage and applications. Energy storage, distributed heat and power generation, and transportation are all applications for hydrogen and fuel cells. Using fuel cells, electricity is produced by converting hydrogen or a fuel rich in hydrogen into an oxidant. It involves an electrochemical reaction at low temperature. It has a promising future because it is a sustainable energy source with low CO2 emissions.

Brudving et al. [54] ventured that relying on fossil fuels has a number of disadvantages, including concerns about energy security and greenhouse gas emissions. By directly transforming solar energy into fuel, it might be avoided by artificial fuel-producing systems that replicate natural photosynthesis. The three key aspects of photosynthesis—light capture, charge separation, and catalysis—were discussed. Here, we describe the design of dye-sensitized solar cells for fuel production.

Eustis et al. [55] studied the noble metal surface plasmon resonance and its radiative and non-radiative properties of different forms of nanocrystals, as well as its contemporary applications. The characteristics of nanoparticles can change when their size or form is altered. Future applications may be created by implementing them.

T. Ganguly et al. [56] noticed the photo switchable properties of the unique self-synthesised dyad system, i.e. 1-(4-chloro-phenyl)-3-(1-methoxy-3,4-dihydro-naphthalen-2-yl) propene (MNCADH). They claimed to have discovered this dyad's "trans" isomer in its ground state. Both the "cis" and "trans" isomers are present in the excited state, according to steady state and time resolved spectroscopic techniques. The energy barrier for trans-cis interconversion is discovered to be lower in the excited state than in the ground state, and trans-cis conversion is more effective in the excited state.

Mandal et al. [57] reported on the synthesis and technique of 3-(1-Methoxy-3,4-dihydro-naphthalyn-2-yl)-1-p-chlorophenyl propane, a new chemical dyad. By mixing the organic dyad with various noble metals, semiconductor nanoparticles, and noble metal-semiconductor core/shell nanocomposites, they create new hybrid nanocomposites.

Paul et al. [58] discovered that the pristine dyad, dyad-spherical gold nanoparticles (GNP), and dyad-star shaped gold nanoparticles (GNS), underwent UV-vis, steady state, and time resolved spectroscopic investigations. In the ground state, the dyad in its pristine form possesses trans-type isomer, but on photoexcitation trans-form converts into cis-structure. When the dyad combines with GNP or GNS, it behaves differently. The best light energy conversion or storage system available is the dyad-GNS nanocomposite.

Olabi et al. [59] observed that graphene exhibits exceptional performance in the majority of energy storage device applications. Performance can be improved with graphene, and it has excellent durability. This work emphasises the use of graphene in electrochemical, absorbance, and energy storage devices.

Park et al. [60] ventured that in order to fully benefit from the use of graphene in micro-scale devices, it is crucial to include two-dimensional graphene nanosheet into a micro/macro sized structure. In order to do this, a brand-new high temperature organic solvent spray aided self-assembly technique is used to produce a spherically integrated graphene microstructure.

References

1. Wikimedia Foundation. 2022. Energy. Wikipedia. https://en.wikipedia.org/wiki/Energy

2. C. Ngo and J. B. Natowitz, “Our energy future – resources, alternative and the environment”, Wiley, 1, 2009.

3. Vaclav Smil, “Energy in World History”, Routledge, 1994.

4. N.S. Lewis and D.G. Nocera, “Powering the planet: Chemical challenges in solar energy utilization”, Proc.Natl.Acad Sci. U.S.A, 103, 15729, 2006.

5. Central Electricity Authority (CEA) https://powermin.gov.in/en/content/power-sector-glance-all-india

6. World Energy Balances. https://www.iea.org/reports/world-energy-balances-overview/world

7. Wikimedia Foundation. 2022. Energy in India. Wikipedia.https://en.wikipedia.org/wiki/Energy_in_India

8. E.A. Rohlfing, W.J. Stevens, M.E. Gress, “Project of Chemical Sciences, Geosciences and Bio-sciences”, 2003.

9. Gopa Dutta Pal, Somnath Paul, Munmun Bardhan, Asish De and Tapan Ganguly. Designing of an artificial light energy converter in the form of short-chain dyad when combined with core-shell gold/silver nanocomposites. Spectrochimica Acta Part A: Molecular and Biomolecular Spectroscopy. (2017). 180:168-174. https://doi.org/10.1016/j.saa.2017.03.015

10. G.M. Whitesides, The right size in nanobiotechnology, Nat. Biotechnol, 21, 1161, 2003

11. J. Pan, G. Benkö, Y. Xu, T. Pascher, L. Sun, V. Sundström, T. Polivka, Photoinduced electron transfer between a carotenoid and TiO2 Nanoparticle, J. Am. Chem. Soc, 124, 13949, 2002.

12. V. Balzani, P. Seroni, A. Juris, “Photochemistry and Photophysics: Concepts, Research, Applications”, Wiley-VCH, 2014.

13. St. Pius X College. 2022. Photochemistry. http://stpius.ac.in/crm/assets/download/Photochemistry.pdf (accessed 26 May, 2022)

14. Wikimedia Foundation. 2022. Photochemistry. Wikipedia.https://en.wikipedia.org/wiki/Photochemistry (accessed 26 May, 2022)

15. M. Julliard, M. Chanon, Photoelectron transfer catalysis: its connection with the thermal and electrochemical analogues, Chem. Rev., 83, 425, 1983.

16. Sudeshna Bhattacharya, MunmunBardhan, Avijit Kumar De, Asish De, Tapan Ganguly. Photoinduced electron transfer within a novel synthesized short-chain dyad. Journal of Luminescence 130 (2010) 1238–1247. doi:10.1016/j.jlumin.2010.02.032

17. H.P. Boehm, R. Setton and E. Stumpp, Nomenclature and terminology of graphite

18. Md. Sajibul Alam, Md. Nizam Uddin, Md. Maksudul Islam, Ms. Bipasha & Sayed Shafayat Hossain. Synthesis of graphene. Crossmark. Int Nano Lett 6, 65–83 (2016). DOI 10.1007/s40089-015-0176-1

19. K. K. Rohatgi-Mukherjee, "Fundamentals of Photochemistry", New Age International'78

20. PubChem, National Library of Medicine. https://pubchem.ncbi.nlm.nih.gov/compound/Graphene-quantum-dot

21. Graphene Quantum Dot. https://en.m.wikipedia.org/wiki/Graphene_quantum_dot

22. W.S. Hummers and R.E. Offeman, Preparation of Graphitic Oxide, J Am. Chem. Soc., 80, 1339, 1958.

23. C.H. Chuang, Y.F. Wang, Y.C. Shao, Y.C.Yeh, D.Y. Wang, C.W. Chen, J.W. Chiou, S.C. Ray, W.F. Pong, L.Zhang, J.F.Jhu and J.H. Guo, The effect of thermal reduction on the photoluminescence and electronic structures of graphene oxides, Sci. Rep., 4, 4525, 2014.

24. Peter M. Martin, "Handbook of Deposition Technologies for Films and Coatings", 3rd Edition, Elsevier, 2010

25. Advanced Materials '93, IIA: Biomaterials, Organic and Intelligent Materials. https//doi.org/10.1016/C2013-1-15211-2

26. Wikimedia Foundation. 2022.Frank-Condon-Principle. Wikipedia.https://en.wikipedia.org/wiki/ Frank-Condon_Principle (accessed 28 May,'22)

27. Alam, S., Sharma, N. and Kumar, L. (2017) Synthesis of Graphene Oxide (GO) by Modified Hummers Method and Its Thermal Reduction to Obtain Reduced Graphene Oxide (rGO)*. Graphene, 6, 1-18. Doi: 10.4236/graphene.2017.61001.

28. Adere Tarekegne Habte, Delele Worku Ayele, Synthesis and Characterization of Reduced Graphene Oxide (rGO) Started from Graphene Oxide (GO) Using the Tour Method with Different Parameters, Advances in Materials Science and Engineering, vol. 2019, Article ID 5058163, 9 pages, 2019. https://doi.org/10.1155/2019/5058163

29. Gity Behbudi, Mini review of Graphene Oxide for medical detection and applications, September 2020. DOI:10.47277/AANBT/1(3)66

30. Zhao, C., Song, X., Liu, Y. et al. Synthesis of graphene quantum dots and their applications in drug delivery. J Nanobiotechnol 18, 142 (2020). https://doi.org/10.1186/s12951-020-00698-z

31. S. Paul, C. Samajdar and T. Ganguly, Attempts to Build Light Energy Conversion Devices, 6th chapter of the book, Photonics and Fiber Optics (pp.149-156), DOI: 10.1201/9780429026584-6.

32. S. Bhattacharya, T.K. Pradhan, A. De, S.R. Choudhury, A.K. De and T. Ganguly, Photophysical processes involved within the anisole-thioindoxyl dyad system, J. Phys. Chem. A, 110, 5665, 2006.

33. Feifan Wang, Qi Li, and Dongsheng Xu. Recent Progress in Semiconductor-Based Nanocomposite Photocatalysts for Solar-to-Chemical Energy Conversion. Advanced Energy Material.(2017), 7, 1700529, DOI: 10.1002/aenm.201700529

34. P. Mondal, T. Misra, A.De, S. Ghosh, S.R. Choudhury, J. Chowdhury and T. Ganguly, Phtophysical processes involved within the bichromophoric system 9-benzotriazole-1-ylmethyl-9H-carbazole and its role as an artificial photosynthetic device, Spectrochim Acta Part A, 66, 534, 2007.

35. Amrita Chakraborty, Tapan Ganguly.Developments of novel nanomaterials by combining shortchain dyad with semiconductor nanoparticles. Optics: Phenomena, Materials, Devices, and Characterization. American Institute of Physics. AIP Conf. Proc. 1391, 31-32 (2011). Doi: 10.1063/1.3646772

36. T.Asahi, M. Ohkohchi, R. Matsusaka, N. Mataga, R.P. Zhang, A. Osuka and K. Maruyama, Intramolecular photoinduced charge separation and charge recombination of the product ion pair states of a series of fixed-distance dyads of porphyrins and quinones: energy gap and temperature dependences of the rate constants, J. Am. Chem. Soc., 115, 5665, 1993.

37. M. Bardhan, T. Misra, J. Chowdhury and T. Ganguly, Comparative studies by using spectroscopic tools on the charge transfer (CT) band of a novel synthesized short-chain dyad in isotropic media and in a gel (P123), Chem. Phys. Lett., 481, 142, 2009.

38. S. Bhattacharya, J. Chowdhury and T. Ganguly, Nature of charge separation and recombination processes within an organic dyad having short spacer, J. Lumin., 130, 1924, 2010.

39. M.A. Loi, P. Denk, H. Hoppe, H. Neugebauer, C. Winder, D. Meissner, C. Brabee, N.S. Sariciftci, A. Gouloumis, P. Vazquez and T. Torres, Long lived photoindused charge separation for solar cell applications in phthalocyanine-fulleropyrrolidine dyad thin films, J. Mater. Chem., 13, 700, 2003.

40. G. Mondal, S. Bhattacharya, S. Das and T. Ganguly, The rates of charge separation and energy destructive charge recombination processes within an organic dyad in presence of metal-semiconductor core shell nanocomposites, J. Nanosci Nanotechnol., 12, 187, 2012.

41. Gopa Dutta (Pal), Abhijit Paul, Somnath Yadav, MunmunBardhan, Asish De, Joydeep Chowdhury, Aindrila Jana, and TapanGanguly. Time Resolved Spectroscopic Studies on a Novel Synthesized Photo-Switchable Organic Dyad and Its Nanocomposite Form in Order to Develop Light Energy Conversion Devices. Journal of Nanoscience and Nanotechnology Vol. 15, 5775–5784, (2015). doi:10.1166/jnn.2015.10290

42. G. Dutta, P. Chakraborty, S. Yadav, A De, M. Bardhan, P. Kumbhakar, S. Biswas, H.S. DeSarkar and T. Ganguly, Time resolved spectroscopic investigations to compare the photophysical properties of a short-chain dyad when combined with silver and gold nanoparticles to form nanocomposite systems, J. Nanosci Nanotechnol., 16, 7411, 2016.

43. Sudeshna Bhattacharya, Joydeep Chowdhury, Tapan Ganguly. Nature of charge separation and recombination processes within an organic dyad having short spacer. Journal of Luminescence 130 (2010) 1924–1934. doi: 10.1016/j.jlumin.2010.05.007

44. Sudeshna Bhattacharya, Gopa Mandal, Mrinal Dutta, Durga Basak, and Tapan Ganguly. Is Dye Mixture More Suitable Rather Than Single Dye to Fabricate Dye Sensitized Solar Cell?. Journal of Nanoscience and Nanotechnology Vol. 11, 1–9, (2011). doi:10.1166/jnn.2011.5115

45. Somnath Paul, Ishani Mitra, Rituparna Dutta, MunmunBardhan, Mridul Bose, Subrata Das, MithuSaha, and Tapan Ganguly. Comparative Analysis to Explore the Suitability of a Short Chain Dyad in Its Pristine and Nanocomposite Forms for Designing Artificial Light Energy Conversion Device. Journal of Nanoscience and Nanotechnology Vol. 18, 1–9, (2018). doi:10.1166/jnn.2018.15533

46. I. Mitra , S. Paulb, M. Bardhanc, S. Dasd, M. Sahae, A. Sahaf, T. Ganguly. Effects of carbon quantum dots (CQD) on the energy storage capacity of a novel synthesized short-chain dyad. Chemical Physics Letters 726 (2019) 1–6. https://doi.org/10.1016/j.cplett.2019.04.025

47. DEVENS GUST, THOMAS A. MOORE, AND ANA L. MOORE. Mimicking Photosynthetic Solar Energy Transduction. Acc. Chem. Res. (2001), 34, 40-48

48. Carlo Andrea Rozzi, Sarah Maria Falke, Nicola Spallanzani, Angel Rubio, Elisa Molinari, Daniele Brida, Margherita Maiuri, Giulio Cerullo, Heiko Schramm, Jens Christoffers& Christoph Lienau. Quantum coherence controls the charge separation in a prototypical artificial light-harvesting system. NATURE COMMUNICATIONS. (2013). 4:1602. DOI: 10.1038/ncomms2603

49. Tapasi Sen, Sreyashi Jana, SubratanathKoner and Amitava Patra. Energy Transfer between Confined Dye and Surface Attached Au Nanoparticles of Mesoporous Silica. J. Phys. Chem. C 2010, 114, 707–714

50. Marlon Bhorja& Prabir K. Dutta. Storage of light energy by photoelectron transfer acress a sensitized zeolite-solution interface. Letters to nature. Vol 362 (1993)

51. Qifeng Zhang, Evan Uchaker, Stephanie L. Candelariaz and Guozhong Cao. Nanomaterials for energy conversion and storage. Chem. Soc. Rev., (2013), 42, 3127—3171. DOI: 10.1039/c3cs00009e

52. Palani Balaya. Size effects and nanostructured materials for energy applications. Energy Environ. Sci., (2008), 1, 645–654. DOI: 10.1039/b809078p

53. P.P. Edwards, V.L. Kuznetsov, W.I.F. David, N.P. Brandon. Hydrogen and fuel cells: Towards a sustainable energy future. Energy Policy 36 (2008) 4356–4362.

54. Iain McConnell, Gonghu Li, and Gary W. Brudvig. Energy Conversion in Natural and Artificial Photosynthesis. Chemistry & Biology 17, May 28, (2010). DOI 10.1016/j.chembiol.2010.05.005

55. Susie Eustis and Mostafa A. El-Sayed. Why gold nanoparticles are more precious than pretty gold: Noble metal surface plasmon resonance and its enhancement of the radiative and nonradiative properties of nanocrystals of different shapes. Chem. Soc. Rev., (2006), 35, 209–217. DOI: 10.1039/b514191e

56. A. Chakraborty, S. Chakraborty and T. Ganguly. Photoisomerization within a novel synthesized photoswitchable dyad: experimental and theoretical approaches. Indian J Phys (2013). DOI 10.1007/s12648-013-0344-y

57. Gopa Mandal, Amrita Chakraborty, Ujjal Kumar Sur, BalaprasadAnkamwar, Asish De and Tapan Ganguly. Synthesis, Characterization, Photophysical Properties of a Novel Organic Photoswitchable Dyad in Its Pristine and Hybrid Nanocomposite Forms. J. Nanosci. Nanotechnol. (2012), Vol. 12, No. 6

58. Somnath Paul, Ishani Mitra, Rituparna Dutta, MunmunBardhan, Mridul Bose, Subrata Das, MithuSaha and TapanGanguly. Comparative Analysis to Explore the Suitability of a Short Chain Dyad in Its Pristine and Nanocomposite Forms for Designing Artificial Light Energy Conversion Device. J. Nanosci. Nanotechnol. (2018), Vol. 18, No. 11

59. A.G. Olabi, Mohammad Ali Abdelkareem, Tabbi Wilberforce, Enas Taha Sayed. Application of graphene in energy storage device – A review. Renewable and Sustainable Energy Reviews 135 (2021) 110026

60. Park, S.-H., Kim, H.-K., Yoon, S.-B., Lee, C.-W., Ahn, D., Lee, S.-I., Kim, K.-B. (2015). Spray-Assisted Deep-Frying Process for the In Situ Spherical Assembly of Graphene for Energy-Storage Devices. Chemistry of Materials, 27(2), 457–465. doi:10.1021/cm50342

Chapter: 2

Materials and Experimental Methodology

- **Materials**
- **Experimental Methodology**
  - **HRTEM**
  - **UV-Vis**
  - **Fluorescence Spectroscopy**
  - **NMR Spectroscopy**
  - **TCSPC**
  - **Transient Absorption Spectra**
- **References**

1. Materials

The spectroscopic grade solvents acetonitrile (CAN) (SRL) and cyclohexane (CH) are purified using normal processes, and then tested before use for the absence of any impurity emission in the wavelength range of interest. Water is deionized using the Millipore and Milli-Q systems. The primary experimental solutions were made by dissolving the necessary amount of dyad, CAN, and CH.

1.1 Synthesis and Characterization of the Novel short-chain dyad (NNDMBF)

Figure 2.1 depicts the investigated dyad synthesis technique. 2-amino fluorene was produced during the method. In a round bottle flask, 7 mL of anhydrous ethanol was added to a combination of 1.5 mmol 2- aminofluorene and 1.5 mmol 4-(dimethylamino) benzaldehyde. The reaction mixture was stirred for 2 hours at room temperature. The solvent was removed under high vacuum after the reaction was completed (monitored by thin layer chromatography, TLC), and the crude reaction mass was washed several times with hexane to obtain the pure product, which is the dyad €-4-((9H-fluorene-2-yl)imino)methyl)-N,N-dimethylaniline (Compound 5)[1].

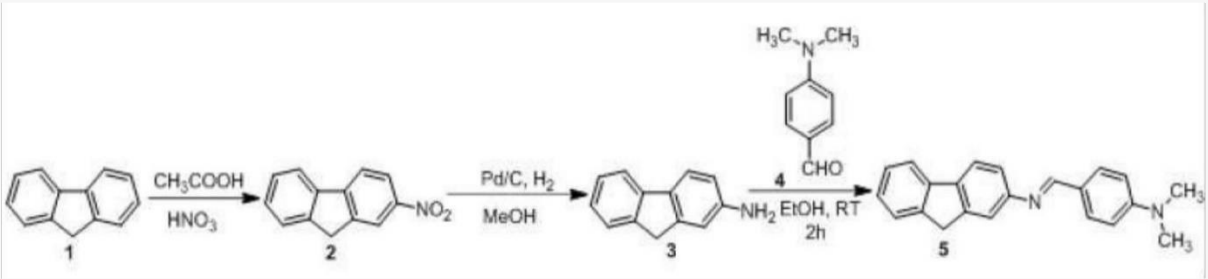

Figure 2.1: Synthesis procedure of NNDMBF dyad. [1]

On a Bruker AVIII- 500, 1H and 13C NMR spectra (Figures 2.2-2.3.) were acquired. Chemical changes were measured in parts per million (ppm). In Hertz, coupling constants (J values) were reported. The chemical shifts of 1H NMR were compared to CDCl3. The chemical shifts of 13C NMR were compared to CDCl3.

Value: ^{1}H NMR (500MHz, CDCl3): δ =2.90 (s, 6H), 3.81 (s, 2H), 6.62 (d, 2H, J = 8.5Hz), 7.13-7.18 (m, 2H), 7.24-7.28 (m, 2H), 7.41 (d, 1H, J = 7.5 Hz), 7.64-7.69 (m, 4H), 8.31 (s, 1H). ^{13}C NMR (125 MHz, CDCl3): δ = 36.9, 40.2, 111.6, 117.5, 119.5, 120.2, 120.3, 124.5, 125.0, 126.2, 126.8, 130.4, 138.9, 141.6, 144.4, 151.9, 152.4, 159.6[1].

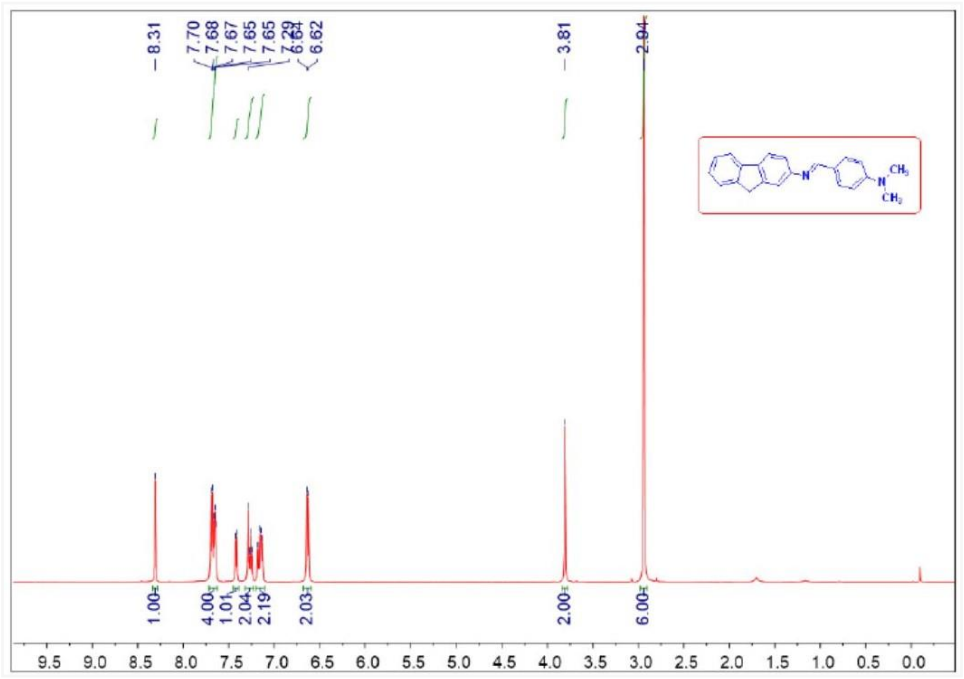

Figure 2.2: ^{1}H NMR of (E)-4-(((9H-fluorene-2-yl)imino)methyl)-N,N-dimethylaniline[1]

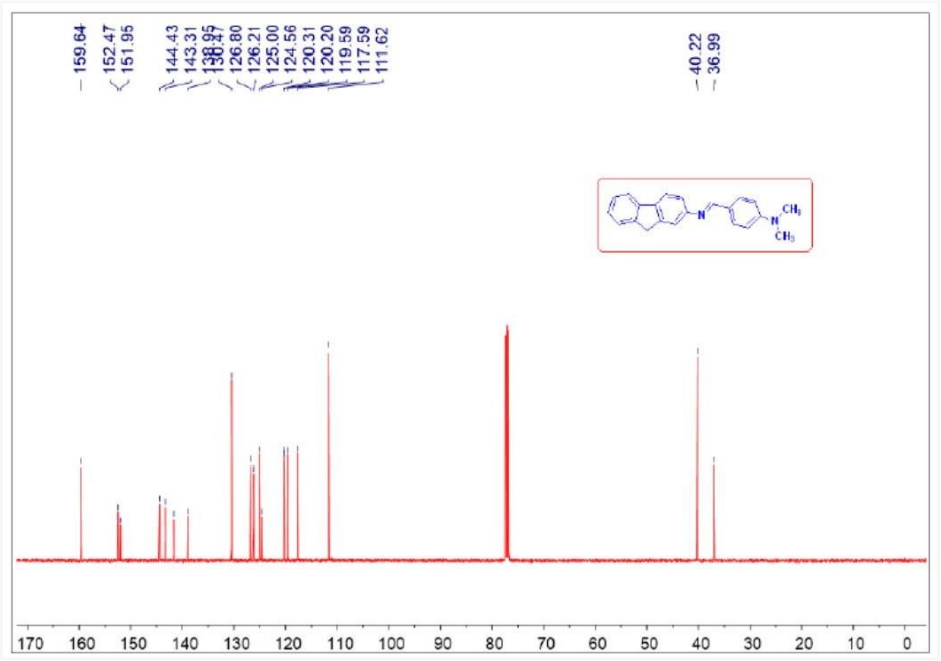

Figure 2.3: ^{13}C NMR of (E)-4-(((9H-fluorene-2-yl)imino)methyl)-N,N-dimethylaniline[1]

The astounding possibility of two conformers: Trans and Cis (Figure 2.4) of our dyad can be inferred from the molecular structure of the dyad. Because the N atom has no proton, coupling constant values from NMR cannot be used to forecast the dyad's potential ground state conformation. Theoretical simulations on the ground state optimal geometry of the dyad NNDMBF utilising the BL-LYP/6- 311g (d,p) level of theory on HOMO–LUMO surfaces reveal that there may be two types of conformers, Cis- and Trans-, with the latter being more stable in the ground state. As a result of the preceding theoretical expectations, both cis and trans forms of the dyad exist in the ground state, with the latter predominating [1].

Figure 2.4: Trans & Cis conformers of dyad[1]

The electron donor 4(N,N-dimethylamine)benzaldehyde (NNDMB) is coupled to the acceptor fluorene(F)[1] by a short chain in a novel short-chain dyad (NNDMBF) (Figure 2.5).

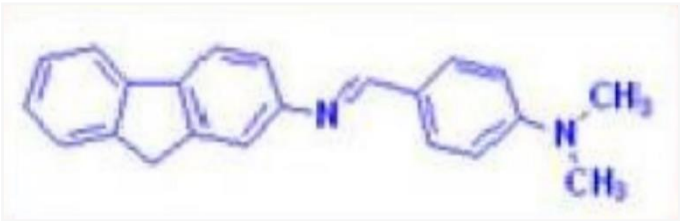

Figure 2.5: Novel short-chain dyad (NNDMBF) [1]

1.2 Graphene Quantum Dots (GQD) Synthesis

Citric acid is pyrolyzed to make graphene quantum dots (GQD) After heating and melting five grammes of citric acid, it turned a dark orange colour in 25–30 minutes. At room temperature, a 1.5 M solution of NaOH was added dropwise to a melting thick solution of citric acid.[2]

1.3 Graphene oxide (GO) and Reduced Graphene oxide (RGO) Synthesis

GO Synthesis: GO can be produced using a modified Hummer's method.[3] In this process, 2 gm of graphite powder was combined with 1 gm of NaNO3 in an ice bath. Now, 130 mL of concentrated H2SO4 was added to the mixture while swirling it. 6 gm of KMnO4 was gently added under vigorous stirring conditions, keeping the reaction temperature of the mixture around 200 C. The reaction temperature was gradually increased to 400 C, and the mixture was stirred for 6 hours. The colour of the combination shifts from dark grey to greyish green at this point. An additional 6 gm of KMnO4 were added to the mixture and stirred for another 6 h so that the color of the mixture becomes grayish brown. Now, 250 ml of triple distilled water was slowly added to the solution which raises the temperature of the solution to around 960 C at which the mixture was stirred for 30 min. The solution was then cooled down to room temperature. Now, an additional 500 ml triple distilled water and 15 ml 30% H2O2 were added to the solution to stop the oxidation. At this stage, the color of the solution becomes yellow ochre signifying the high oxidation level of graphite. Now, the yellow solution was washed two times with 1M HCl (Hydrochloric Acid) solution and repeated washing was done with triple distilled water until a pH of 5 was obtained. This was done by centrifugation of the solution and decantation of the supernatant. A rigorous washing and decantation step is necessary to exfoliate the graphene oxide layers and to remove the unexfoliated graphene oxide layers. The thick yellow brown gel was filtered and dried overnight to get a fine yellow graphene oxide (GO) powder. A stoichiometric amount of GO was then taken in triple distilled water and ultrasonicated for 30 min to get a homogeneous solution.

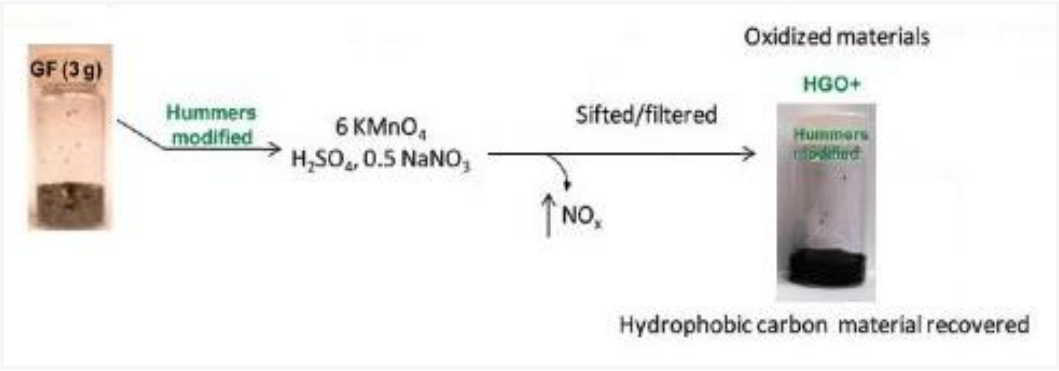

Fig. 2.6. GO Synthesis process [3]

RGO Synthesis: Oxidised material samples were reduced with hydrazine hydrate before being annealed in Ar/H2 at 300 and 900 degrees Celsius. 100 mg of enhanced GO materials are distributed in 100 ml distilled water and agitated for 30 minutes to reduce hydrazine. 1 mL hydrazine hydrate is then added. After 45 minutes of heating at 950°C in a water bath, a black solid precipitated from the reaction mixture. Filtration isolates the products, which are then washed with distilled water to yield 54 mg of chemically reduced enhanced GO i.e. RGO. NMR spectra show no signal from oxidised carbon after reduction. This signifies that RGO is of very high grade. We estimate that individual RGO flacks have a thickness ranging 1-3 nm based on AFM measurements [3].

Structural characterization of GO and RGO.

In our experiment we used GO where the level spacing is around 9.0 Å (from XRD spectra). The X-ray photoelectron spectroscopy (XPS) confirms that GO produced by modified Hammer's method is more oxidized than GO produced by Hummer's methods. XPS confirms that improved GO has 63% oxidized carbon and 37% graphitic carbon. From 13C NMR we get the apperant peak of oxidized carbon of GO at around 287 eV. TEM images confirms the structure regularity of GO. UV-Vis spectra supports the regular structure of GO is due to greater retention of carbon ring in basal plane. Large extinction coefficient of GO indicate that it has large number of aromatic ring or isolated aromatic domain.

Although the following λ_{max} results from the electronic transition show that these aromatic rings are not extended conjugation, total absorption indicates that GO produced by the modified Hummer's approach retains more aromatic rings than GO produced by Hummer's method. [3]

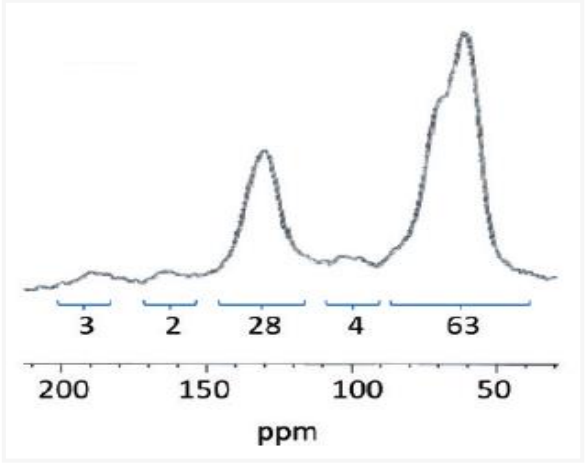

Fig. 2.7. ^{13}C NMR Spectra of GO [3]

2. Experimental Methodology

2.1 High resolution transmission electron microscope (HRTEM)

2.1.1 Introduction

It's a type of transmission electron microscopy with a modern twist (TEM). For high magnification of nanomaterials, HRTEM is utilised. HRTEM is an excellent imaging technique for nanomaterials at the atomic scale because of its high resolution. The TEM is a technique that gives morphological, compositional, and crystallographic information by using energetic electron contact with the material. HRTEM creates an interference image by using both transmitted and scattered electrons. It's a phase contrast image that can be as small as a crystal's unit cell. HRTEM has been utilised extensively and successfully for investigating crystal structures and lattice defects in a variety of sophisticated materials at the atomic level.

Point defects, stacking faults, dislocations, precipitates grain boundaries, and surface features can all be characterised with it. HRTEM has a 2D spatial resolution of around 0.05 nm. In 3D crystal, different views from various angles are combined to create a 3D map. Electron crystallography is the name for this method.

2.1.2. Working principle

TEM i.e. Transmission electron microscope has three important sections:

1. Depending on the application, the specimen system can be stationary or move slowly. The mechanical stability of the TEM plays an essential role in defining its resolution.
2. The illumination system is made up of an electron cannon and two or more condenser lenses that focus the electron beam on the sample. The diameter of the beam is determined by the specimen arrangement.
3. At least three lenses are used in the imaging system to provide a magnified image of the sample on a fluorescent screen or a monitor of an electronic camera system. The unique resolution of the microscope is determined by the imaging lens design.
4. Image recording device e.g. CCD with photodiodes is used to record the image produced.

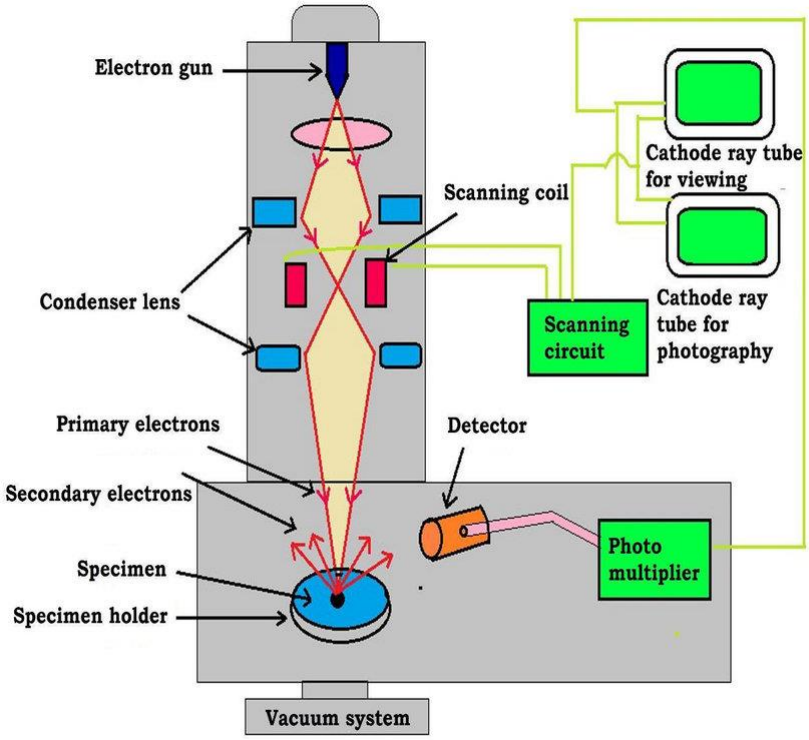

Fig. 2.8: Schematic diagram of HRTEM [14]

2.1.3 Components

a. Specimen system

Because any drift or vibration would be amplified in the final image, the specimen stage is designed to keep the specimen as still as possible. TEM specimens are always round, having a 3 mm diameter. The specimen must be perpendicular to this disc and thin enough to let electrons to pass through and generate the magnified image. The specimen is first placed in a container that can be evacuated before entering the TEM column. The specimen stage is divided into two types: side-entry and top-entry. The specimen is attached to the end of a rod-shaped specimen holder and inserted horizontally through the airlock, which is then triggered by rotating the specimen holder around its long axis. The specimen is clamped to the bottom end of a cylindrical holder with a conical collar in the top-entry stage. A sliding and tilting arm loads the holder into position through an airlock, which is subsequently removed and retracted. The cone of the specimen holder fits snugly into a conical well of the specimen stage inside the TEM, which may be manipulated in the horizontal (x and y) directions by a precision gear system.

b. Illumination system

The energy of the electron beam produced by the electron cannon is adequate to pass through the sample specimen. An electron source, a cathode (due to the high negative potential), and an electron-accelerating chamber make up this cannon. The electrons are emitted through a process known as thermo-ionic emission. A V-shaped filament composed of tungsten wire is spot-welded to straight-wire leads that are installed in a ceramic or glass socket as the electron source. The filament is heated to roughly 2700 K using a direct current (dc), at which point tungsten emits electrons into the surrounding vacuum. The electron gun's filament can be constructed of tungsten or lanthanum hexaboride (LaB6). Although LaB6 source is more expensive than tungsten filament, it has a longer lifespan. The filament is encircled by a control grid with a central aperture positioned on the column's axis; the cathode's apex is positioned at or slightly above or below this aperture. The cathode and control grid are insulated from the rest of the instrument and have a negative potential equal to the required accelerating voltage.

With the help of an electric field parallel to the optic axis, electrons are accelerated to their final kinetic energy E_0 after emission from the cathode. A potential difference V0 between the cathode and anode is used to create this field. An anode is a circular metal plate with a central hole through which an accelerated electron beam emerges [6]. Pass through the middle aperture at a constant energy if the high voltage has stabilised sufficiently. The electron gun's control and alignment are vital to its successful operation.

The condenser lens must have at least two electron lenses in order to provide a high-quality magnified image of the sample. A powerful magnetic lens is used as the first condenser lens. It creates a real image by using a virtual electron source. The spot size can be used to adjust the lens current. The weak magnetic lens used as the second condenser lens yields little or no magnification. This lens has a condenser aperture with a variable diameter that allows the angle of illumination of the electron form optic axis to be altered. The use of a small spot size reduces the effects of heating and irradiation on the specimen. In order to move the electron beam (incident on the specimen) in the y and x directions, the illumination system includes two pairs of coils that apply homogeneous magnetic fields in the horizontal (x and y) directions. A second set of coils is used to alter the incident beam's angle with respect to the optic axis.

c. Image producing system

On the viewing screen or on the digital display system, the TEM imaging system creates a magnified image of the specimen. The quality and design of these lenses, particularly the first imaging lens, the objective lens, have a significant impact on the image's spatial resolution. With a short focal length, it's a powerful lens. To avoid picture drift caused by thermal fluctuations, this lens must be kept at room temperature. The TEM also contains precision controls that allow the specimen picture to be accurately focused on the viewing screen by making small fractional adjustments to the objective current. The first condenser lens has a great deal of focusing power. The second condenser lens creates a nearly parallel beam for analytical electron microscopy.

We can restrict electrons to arrive at the specimen parallel to the axis and must remain unscattered during their passage through the specimen using parallel lighting and properly controlled tilt controls. When an electron is scattered by one or more atoms in the material, it returns to the optic axis at the same angle. The diaphragm around the aperture absorbs electrons scattered at larger angles, so they don't contribute to the final image. We can assure that practically all scattered electrons are absorbed by the diaphragm by reducing the deflection angle. As a result, parts of the material that scatter electrons strongly appear as dark areas in the final image, which is referred to as diffraction contrast. Using an objective stigmator positioned below the objective lens, the TEM operator can eliminate blurring and correct for axial astigmatism in the objective. A diaphragm, which limits the specimen region from which electron diffraction is recorded, can also be used here. Only electrons that fall within the aperture's diameter are transmitted through it. As a result, the diaphragm's introduction offers diffraction data with good spatial and angular resolution.

Between the objective and the final lens in a TEM system, there are numerous lenses. This intermediate lens is primarily used for two purposes. First, image magnification can be altered in small steps by altering the focal length, which is commonly 103-106. Second, an electron diffraction pattern can be formed on the TEM viewing screen by increasing the intermediate lens excitation. A projector lens is then used to create an image or diffraction pattern across the entire TEM screen. The final-image magnification is the algebraic product of each imaging lens' magnification factors.

d. Image Recording

The electron picture is monochromatic and must be made visible to the naked eye either by letting electrons to fall on a fluorescent screen at the foot of the microscope column or by digitally recording the image for display on a computer monitor. Computerized photographs are saved in TIFF or JPEG formats and can be examined or image-processed before being published. Charged coupled diode (CCD) sensors with a million photodiode array are used in this electronic image recording. There are various advantages to using electronic recording. The recorded image may be seen on a display screen at a high magnification, which makes focusing and astigmatism correction much easier. The image data is saved digitally in computer memory before being transferred to magnetic or optical discs, where prior photographs can be quickly accessed for comparison. The image's digital nature also allows for numerous types of image processing.

2.2 Ultraviolet–Visible Spectroscopy

2.2.1 Introduction

UV–Vis Spectroscopy, sometimes known as UV–Vis Spectroscopy, is a technique for measuring light absorbance in the ultraviolet and visible portions of the electromagnetic spectrum. It makes use of visible and near-infrared light. Incident light can be absorbed, reflected, or transmitted as it strikes materials. Atomic excitation is caused by the absorption of UV-Vis radiation, which refers to the transition of molecules from a low-energy ground state to an excited state [7].

The wavelength of light reaching the detector is measured after a light beam passes through an object. The wavelength is used to determine the chemical structure and quantity of molecules present. As a result, both quantitative and qualitative data can be collected. In the wavelength range of 160 to 3500 nm, information can be collected as transmittance, absorbance, or reflectance of radiation. Electrons are promoted to excited states or anti-bonding orbitals as a result of incident energy absorption. Photon energy must match the energy required by the electron to go to the next higher energy state for this transfer to take place. The essential operating principle of absorption spectroscopy is this mechanism.

There could be three different sorts of ground state orbitals involved:

i. Bonding molecular orbital:. σ , π
ii. Non-bonding atomic orbital: n
iii. Anti-bonding molecular orbital: σ* , π*

Transition which involves excitation of electron from s bonding orbital to σ anti-bonding orbital is called σ to σ* transition. Likewise, π to π* represents the excitation of an electron of a lone pair (non-bonding electron pair) to an antibonding π orbital. Electronic transitions occurring due to absorption of UV and visible light are:

i. σ to σ*;
ii. n to σ*;
iii. n to π*;
iv. π to π* [3].

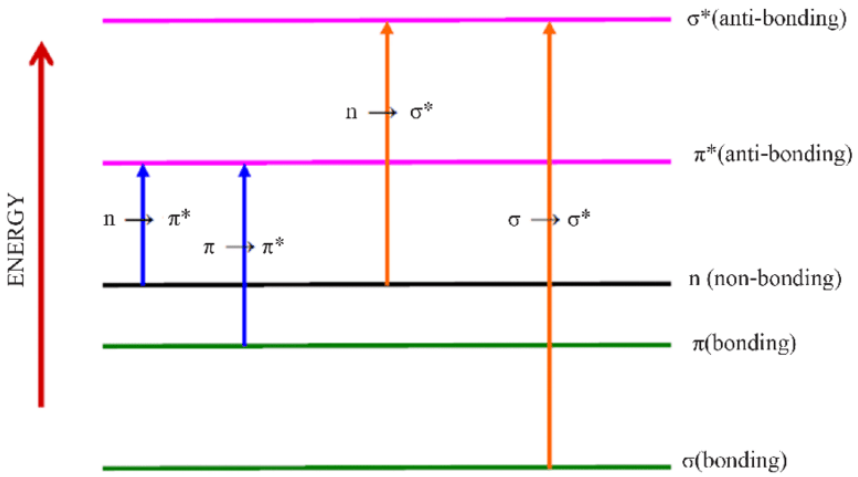

Figure 2.9: Electron transitions in UV-Vis spectroscopy

When a given wavelength and energy of light is focused onto a sample, it absorbs some of the incident wave's energy. A photodetector detects the sample's absorbance and measures the energy of transmitted light from the sample. The wavelength is used to generate the absorption or transmission spectrum of the light absorbed or transmitted by the sample. The Lambert-Beer rule (Figure 2.7), is a fundamental principle of quantitative analysis that states that a solution's absorbance scales directly with its analyte concentration. The absorbance (unit less) A is defined as the molar absorptivity of the absorbing species (M-1 cm-1), b is the sample holder path length (usually 1 cm), and c is the solution concentration (M) [8].

UV−Vis−NIR spectrometer can monitor absorbance or transmittance in UV – visible wavelength range. The relation between incident light of intensity 'Io' and transmitted light of intensity 'I' is described as follows[8].

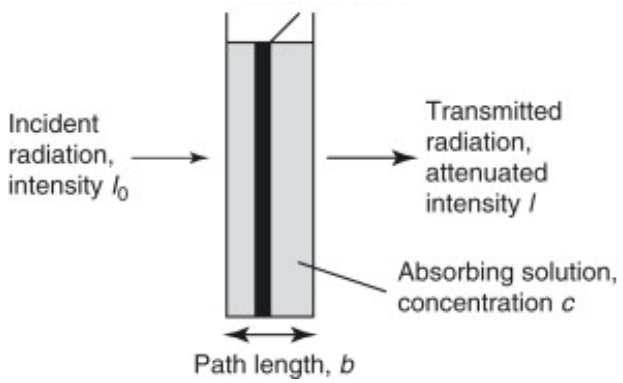

Figure 2.10: Lambert−Beer Rule

Transmittance, $T = \frac{I}{I_0}$; Transmission rate, $T\% = \frac{I}{I_0} \times 100$

Absorbance, A is defined as logarithmic inverse of transmittance, i.e. $A = \log\left(\frac{1}{T}\right)$

$$\log\left(\frac{1}{T}\right) = \log\left(\frac{I_0}{I}\right) \quad \ldots. (1)$$

we know $I = I_0 e^{-kcl}$ or, $T = \frac{I}{I_0} = e^{-kcl}$ ….. (2)

$$A = \log\left(\frac{1}{T}\right) = kcl \quad \ldots\ldots(3)$$

The constant of proportionality, 'k', is used here. While transmittance is unaffected by sample concentration, absorbance is proportional to both sample concentration (Beer's law) and optical path (Bouguer's law). Furthermore, when the optical path is 1 cm and the concentration of the targeted substance is 1mol/l, k is denoted as $'\varepsilon'$ and is characterised as molar absorption coefficient. The material's molar absorption coefficient is representative of the material under specified conditions. The Lambert Beer rule is based on the assumption that there is no stray, produced, scattered, or reflected light.

2.2.2 Components

The spectrophotometer is the instrument used in ultraviolet-visible spectroscopy. It compares the intensity of light before it goes through a sample and measures the intensity of light before it passes through the sample.

The essential components of a spectrometer are—

i. UV Light Source

Electrically igniting deuterium or hydrogen at low pressures produces a continuous UV spectrum. Both deuterium and hydrogen lamps emit light with wavelengths ranging from 160 to 375 nm [3].

ii. Visible Light Source

The radiation source is usually a Tungsten filament (300–2500 nm), a deuterium arc lamp (190–400 nm), a Xenon arc lamp (160–2,000 nm), or, more recently, light emitting diodes (LED) for visible wavelengths.

iii. Monochromator & Cuvettes

A monochromator source is employed, and light is separated into two halves of identical intensity via a half-mirror splitter before reaching the sample. One component (or sample beam) passes through a cuvette containing a clear solvent solution of the material to be studied. The second beam, sometimes known as the reference beam, travels through a comparable cuvette that contains only solvent. Containers for the reference and sample solutions must be transparent to the passing beam.

iv. Detectors

The intensity of light transmitted by cuvettes is detected by the detector, which delivers the data to a metre, which records and displays the values. The intensities of light beams are calculated and compared by electronic detectors. Several UVVis spectrophotometers contain two detectors – a phototube and a photomultiplier tube – and simultaneously monitor the reference and sample beams. CCDs (Charge-Coupled Devices) are similar to diode array detectors.

v. Recording devices

Most of the time, the amplifier is connected to a computer via a pen recorder. The computer saves all of the information and generates the spectrum of the desired molecule. The following functions can be recalled or continuously monitored by a microcomputer with completely automated equipment, depending on the sophistication of the software:

i. Base-line correction
ii. Conversion of analog to digital (a/d) data
iii. Conversion of extinction values to concentrations[8].

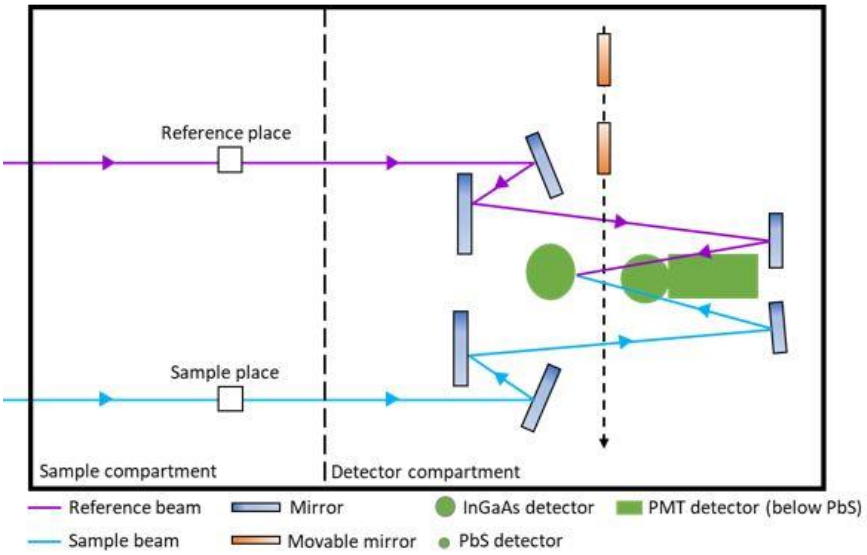

Figure 2.11: UV−Vis−NIR Spectrometer[8]

2.2.3 Applications

a) Qualitative & Quantitative analysis: UV-Vis absorption spectroscopy can be used to identify substances that absorb UV light. The absorption spectrum is compared to the spectra of recognised chemicals for identification. Aromatic compounds and aromatic olefins are commonly studied using UV-Vis absorption spectroscopy [9]. UV-Vis Spectroscopic measurements can also be used to determine the quantity of a sample.

b) Structure elucidation of organic compounds: UV-Vis spectroscopy is important in elucidating the structure of organic molecules, determining the presence or absence of unsaturation, and determining the presence of hetero atoms. The location and combination of peaks can be used to determine if the chemical is saturated or unsaturated, whether hetero atoms are present or not, and so on.

c) Impurities Detection: One of the most effective ways for determining contaminants in organic molecules is UV-Vis absorption spectroscopy. Due to contaminants in the sample, additional peaks can be seen, which can be compared to those of normal raw material. Impurities can be determined by measuring absorbance at a given wavelength as well [9].

2.2.4 Instrument Specifications

a) Name: JASCO UV-VIS Absorption Spectrophotometer
b) Model: V-630

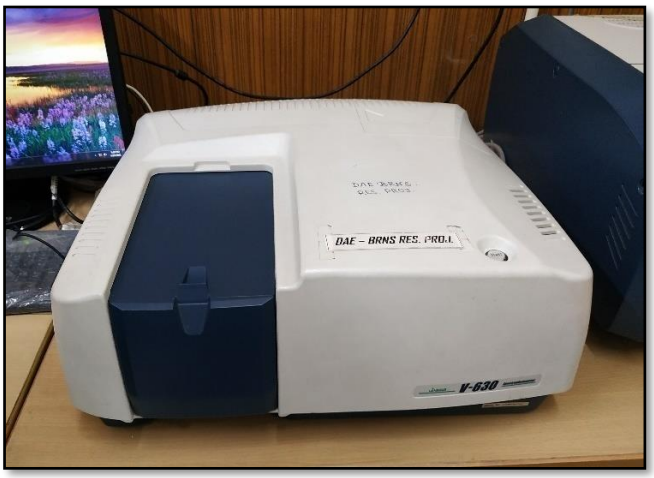

Figure 2.12: JASCO UV-VIS Absorption Spectrophotometer

2.3 Fluorescence Spectroscopy

2.3.1 Introduction

Lasers have long played a vital part in spectroscopy, which has made a significant contribution to the current state of atomic and molecular chemistry. In chemistry and physics, fluorescence spectroscopy and time-resolved fluorescence are generally used as research methods. Fluorescence is the virtually instantaneous absorption of light energy by molecules at one wavelength and subsequent reemission at another, usually longer wavelength. Fluorescent chemicals have two distinct spectra: an excitation spectrum (the wavelength and amount of light absorbed) and an emission spectrum (the wavelength and amount of light emitted). Fluorometry is a highly specific analytical technique because of this premise. Fluorescence is measured using fluorometry. A fluorometer, sometimes known as a fluorimeter, is a device that measures fluorescence. A fluorometer produces the wavelength of light needed to ignite the analyte of interest, selectively transmits the wavelength emitted, and then measures the intensity of the emitted light. When compared to other analytical techniques, fluorometry is chosen for its exceptional sensitivity, high specificity, simplicity, and low cost. Fluorometry is more sensitive than absorbance measurements in most cases. It is an important analytical tool for both quantitative and qualitative research. [10]

Photon emission mechanisms such as fluorescence and phosphorescence occur during molecular relaxation from electronic excited states. Transitions between electronic and vibrational states of polyatomic fluorescent molecules are involved in these photonic processes (fluorophores). Fluorophores are the most important component of fluorescence spectroscopy. The components of molecules that cause them to glow are known as fluorophores. Fluorophores are mostly molecules with aromatic rings, such as Tyrosine, Tryptophan, Fluorescein, and so on.

Fluorescence: Prompt fluorescence: $S1 \rightarrow S0 + h\nu$

The release of electromagnetic energy is immediate or from the singlet state.

Delayed fluorescence: $S1 \rightarrow T1 \rightarrow S1 \rightarrow S0 + h\nu$

This result comes from two intersystem crossings, at first from singlet to triplet, and then again from triplet to singlet.

Phosphorescence: $T1 \rightarrow S0 + h\nu$

Delayed release of electromagnetic energy from the triplet state.

2.3.2. Spectrofluorometer

A spectrofluorometer is a device that uses the fluorescence properties of certain substances to provide information about their concentration and chemical environment in a sample. The emission is monitored at a single wavelength or a scan is done to record the intensity versus wavelength, commonly known as an emission spectrum, when a specific excitation wavelength is chosen.

High-intensity light sources are typically used in spectrofluorometers to blast a sample with as many photons as feasible. This allows the greatest number of molecules to be in an excited state at any given time. Normally, the fluorescence is collected at a 90-degree angle to the optical axis set by the excitation light beam in all of the devices. Instead of measuring the difference in intensity of two signals, which is measured in a spectrometer, a spectrofluorometer measures a signal over a zero background. The light source, monochromator, and light detector are the three main components of a spectrofluorometer.

Light Source: A spectrofluorometer uses a high-pressure xenon arc lamp as its light source. This lamp's bulb contains high-pressure xenon, which is stimulated to a higher level by an electrical arc created by current flowing through the electrodes. The spectrum of light emitted ranges from roughly 250 nm to 1100 nm.

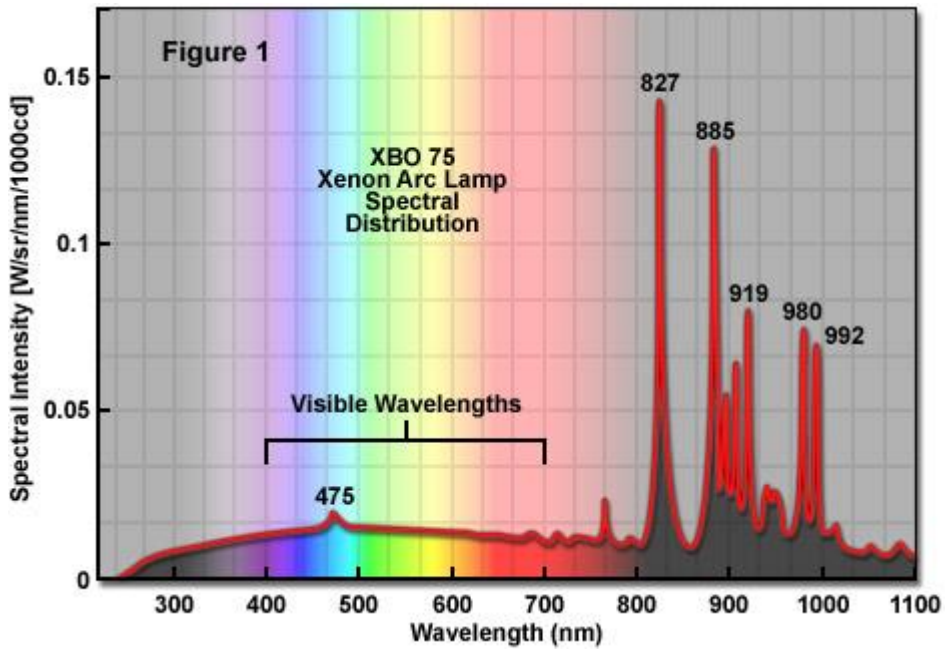

Fig. 2.13: Spectral distribution for the 300W xenon arc lamp[11]

When utilising a xenon arc lamp, monochromators are used to pick the wavelength for irradiating the sample; in the collection channel of a spectrofluorometer, they are used to record the range of wavelengths produced by a fluorophore. A diffraction grating with slits at the entrance and output make up the simplest monochromator. When light strikes the grating at an angle, it diffracts into a succession of angles, the first of which is usually chosen for measurement. When a monochromator is adjusted to deliver radiation at wavelength λ, it also delivers radiation at wavelength 2λ. The second order's strength is typically roughly a tenth of the first order's; yet, this is enough to pollute the emission spectrum. With a judicial selection of filters, the second order can be removed. The amount of stray light, or radiation present at any wavelength other than the targeted wavelength, is a characteristic of every monochromator. For reducing stray light, various solutions are possible, the first of which is a judicious grating selection. The ruled grating and the holographic grating are the two types of grating. To construct a monochromator, gratings can be arranged in a variety of ways, the two most prominent being the Czerny-Turner and the Seya-Namioka.

A photomultiplier tube (PMT) or photodiode is a light detector that converts light into an electrical signal. The PMT can be used in the wavelength range of 230 nm to 830 nm. It is clear that the sensitivity is not the same even within the working wavelength range, and the results must be corrected.

Polarizers are used in spectrofluorometers to measure anisotropy. The superposition of the wavelength transmission of the various parts of the instrument defines the operational zone of the instrument. Even when measuring fluorescence parameters inside this zone, the variance in transmission must be taken into account. Photomultiplier tubes are used to detect the fluorescence, which is then quantified using the proper electronic instruments. Typically, the output is presented in a graphical format and saved digitally [11].

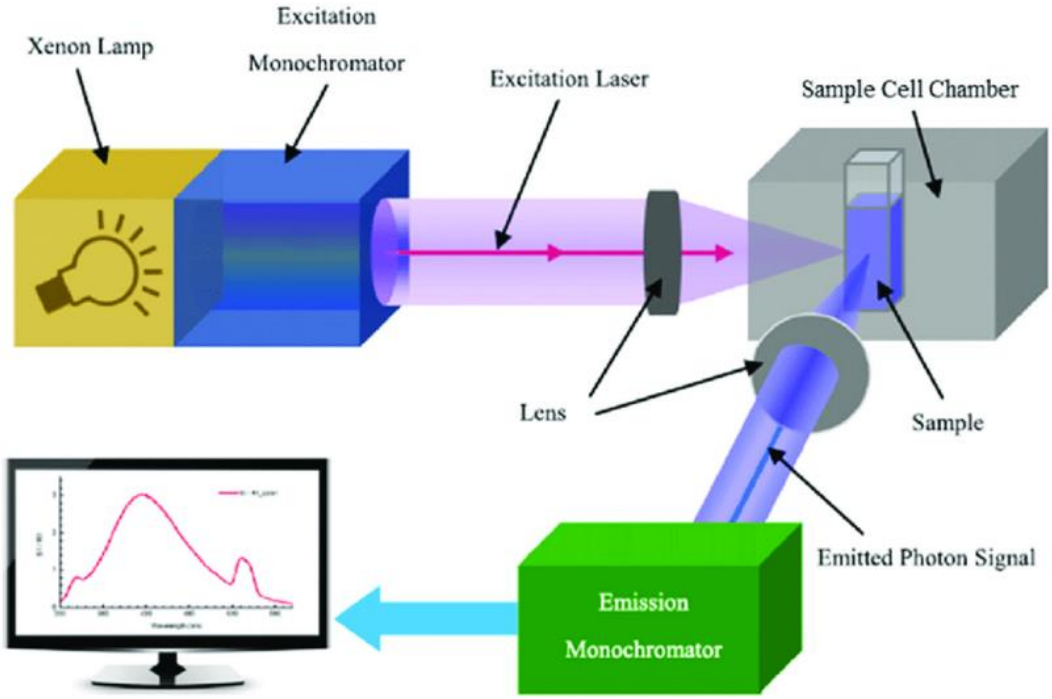

Fig. 2.14: Schematic Diagram of Arrangements in a Spectrofluorometer [12]

2.3.3 Applications of Fluorescence Spectroscopy

a) **LIF Spectroscopy in cancer diagnosis:** Laser spectroscopic techniques have the potential for in-situ, near real-time diagnosis, and the use of non-ionizing radiation assures that the diagnosis can be repeated without harm. In two techniques, laser induced fluorescence (LIF) has been used to diagnose cancer. One strategy is to give a medication like hematoporphyrin derivative (HpD) to the patient, which is selectively retained by the tumour. When the medicine is photo stimulated with the right wavelength of light, it fluoresces in the tumour. The tumour is detected and imaged using this fluorescence. Intersystem crossover also leads to the populating of the triplet state as a result of photo excitation. The molecule in the excited triplet state can either react directly with biomolecules or produce singlet oxygen, which is harmful to the host tissue. Photodynamic treatment of tumours takes advantage of the resultant damage of the host tissue [10].

b) **Glucose Determination:** Blood glucose levels (fasting, pp) are a very good predictor of human health. An abnormally high level of glucose can reveal a lot about disorders like diabetes or hypoglycaemia. Fluor photometry is frequently utilised because to its ease of use and great sensitivity.

c) **Bioscience:** Fluorescence spectroscopy can be used to sequence DNA. A DNA sample is put into a fluorescence spectrometer with an extrinsic fluorophore to acquire a reading of the sample's concentration.

d) **Agriculture:** Spectroscopic techniques are frequently used to identify various crop kinds. Citrus seedling varieties can be identified using the laser-induced fluorescence emission approach.

e) **Study of Marine Petroleum Pollutants:** Fluorescence spectroscopy is a useful technique for detecting oil slicks on the water's surface, determining petroleum pollutants in saltwater, determining specific petroleum derivative compounds, and identifying pollution sources [10].

2.3.4 Instrument Specifications

i. Instrument Name: JASCO Spectrofluorometer
ii. Instrument Model: 8200

Figure 2.15: JASCO Spectrofluorometer

2.4 Nuclear Magnetic Resonance (NMR) Spectroscopy

2.4.1 Introduction

The spectroscopic technique of nuclear magnetic resonance spectroscopy is used to study local magnetic fields surrounding atomic nuclei. Certain nuclei resonate at a specific frequency in the radio frequency band of the electromagnetic spectrum when exposed to a strong magnetic field. Slight fluctuations in this resonance frequency provide extensive information about the atom's molecular structure. According to the NMR principle, many nuclei have spin and all nuclei are electrically charged. When an external magnetic field is applied, energy can be transferred from the base energy to a higher energy level [10].

i. Nucleis are electrically charged and many of them have spin.
ii. Upon applying external magnetic field, energy transfer is possible from minimum base energy to higher energy levels.
iii. Energy transfer takes place at a frequency that resonates with radio frequency.
iv. Energy is emitted at the same wavelength when the spin comes back to its base level.
v. As a result, the processing of the NMR spectrum for the concerned nucleus is yielded by measuring the signal that matches this transfer [13].

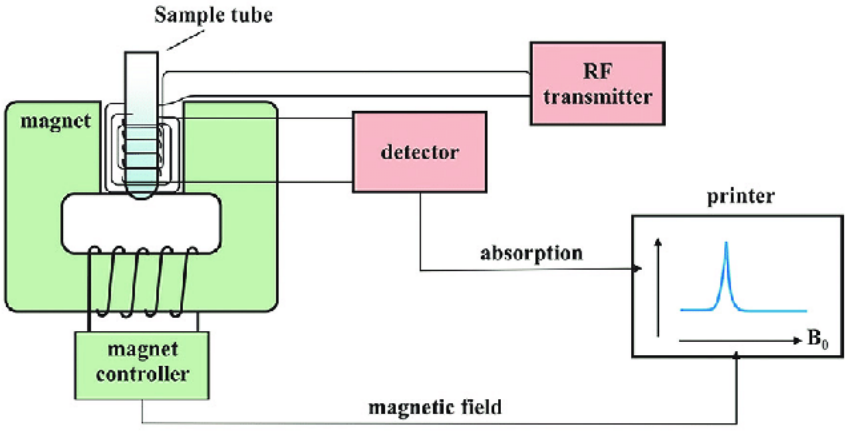

Figure 2.16: Diagram of a NMR Spectrometer [13]

2.4.2 NMR Spectroscopy Hardware

Hardware in NMR spectroscopy consists of nine major parts. In the following, they have been briefly discussed:

i. **Sample tube –** It is a glass tube which is 8.5 cm long and 0.3 cm in diameter.

ii. **Magnetic coils –** Magnetic coil generates magnetic field whenever current flows through it

iii. **Permanent magnet –** It helps in providing a homogenous magnetic field at 60 – 100 MHZ

iv. **Sweep generator –** Modifies the strength of the magnetic field which is already applied.

v. **Radiofrequency Transmitter –** It produces a powerful but short pulse of the radio waves.

vi. **Radiofrequency Receiver–** It helps in detecting receiver radio frequencies.

vii. **RF Detector –** It helps in determining unabsorbed radio frequencies**.**

viii. **Recorder –** It records the NMR signals which are received by the RF detector.

ix. **Display system –** A computer that display the records the data[13].

2.4.3 Applications

i. NMR spectroscopy is a spectroscopic technique used by chemists and biochemists to study the characteristics of organic molecules, while it can be applied to any sample with spin-containing nuclei.

ii. NMR can be used to analyse mixtures containing known substances quantitatively. NMR can be used to compare unknown chemicals to spectral libraries or to derive their basic structure directly.

iii. NMR can be used to assess molecule conformation in solutions as well as to examine physical features at the molecular level such as conformational exchange, phase shifts, solubility, and diffusion after the basic structure is known.[13]

2.5 Time Resolved Spectroscopy

Time Resolved Spectroscopy is a type of **spectroscopy that is used to track interactions between molecules and short-term motions. It is a helpful approach in biomolecular structure characterization and dynamics because it can quantify changes in the picosecond or nanosecond time range.**

2.5.1 TCSPC: Time correlated single photon counting

TCSPC [15] is based on the detection of single photons in a periodic light signal, measurement of the individual photon detection times, and reconstruction of the waveform from the individual time measurements. The method takes advantage of the fact that the light intensity for low-level, high-repetition-rate signals is typically so low that the likelihood of detecting one photon in a single signal period is substantially lower than one. As a result, the detection of multiple photons can be ignored, and the method depicted in Figure 2.13 can be employed instead:

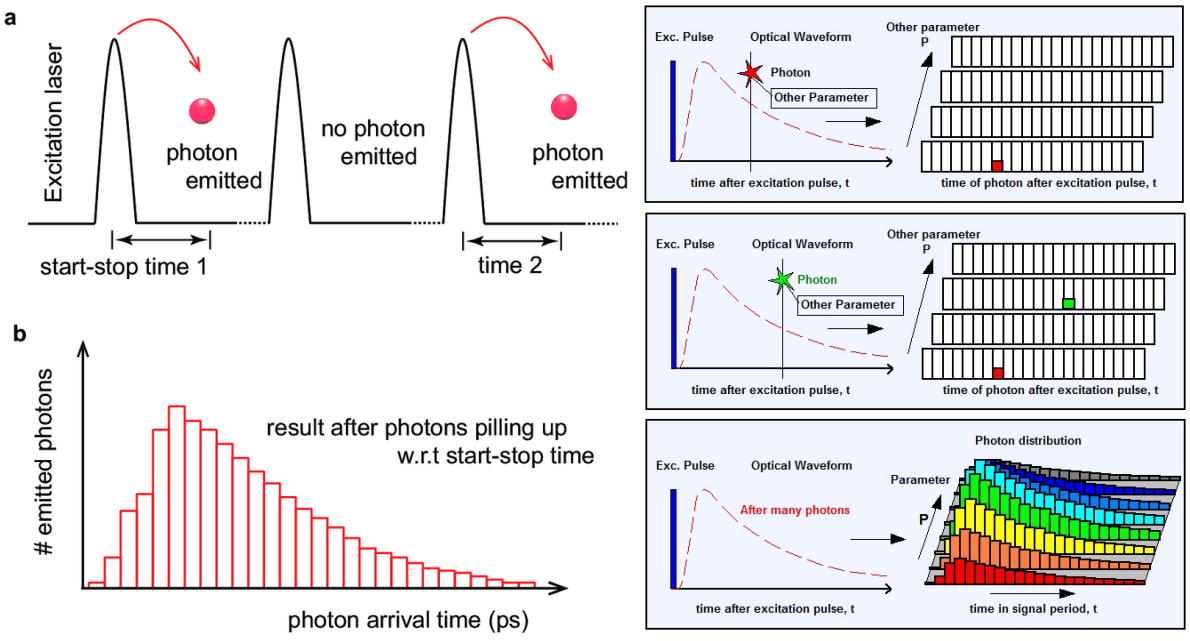

Figure 2.17: a) TCSPC Measurement Technique [16] b) Multi-Dimensional TCSPC [15]

Due to the detection of individual photons, the detector signal consists of a train of randomly distributed pulses. Many signal intervals are devoid of photons, whereas others contain a single photon pulse. Periods with multiple photons are extremely rare. The time of the matching detector pulse is measured when a photon is detected. The events are stored in memory by inserting a '1' in a memory location according to the detection time. The histogram of detection timings, i.e. the waveform of the optical pulse, grows up in the memory after many photons. Despite the fact that this approach appears to be hard at first glance, it has a number of significant advantages:

i. TCSPC's temporal resolution is limited by the transit time spread, not the width of the detector's output pulse.
ii. Because TCSPC has a near-perfect counting efficiency, it achieves the best signal-to-noise ratio for a given number of photons detected.
iii. TCSPC is able to record the signals from several detectors simultaneously
iv. TCSPC can be employed in confocal and two-photon laser scanning microscopes as a high-resolution high-efficiency lifetime imaging (FLIM) technology when paired with a fast-scanning technique.
v. TCSPC can collect fluorescence lifespan and fluorescence correlation data at the same time.
vi. TCSPC devices with cutting-edge technology achieve count rates in the MHz range and acquisition times of a few milliseconds. [15]

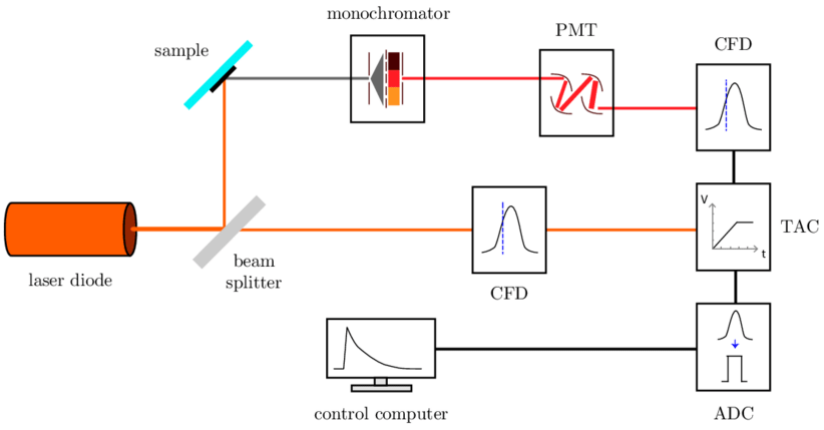

Figure 2.18: Block diagram of TCSPC using Laser Diode. [17]

Here, CFD = Constant Fraction Discriminator, TAC = Time to Amplitude Converter, ADC = Analog to Digital Converter

2.5.2 Applications

i. Fluorescence microscopy. [18]
ii. TCSPC also has many applications in diverse areas of Science & Technology.
iii. Wide-field photon counting detectors are used in optical communications systems, and recent breakthroughs in superconducting detector and SPAD array technology can be credited to the rapidly expanding applications in these fields.

2.6 Transient Absorption Spectral Measurements

2.6.1 Introduction

The transient absorption spectral measurements of the dyad-GQD (and GO) were made by using the third harmonic of Nd: YAG laser as excitation source (355 nm) at the different delay times of the excitation and analysing or probing pulses. It is to be pointed out that the peaking of the transient absorption spectra observed at around 540 nm region could be assigned to the fluorene anion of the contact ion-pair. [19] The direct evidence of occurrence of photo induced electron transfer (PET) process is provided from the observations of transient donor cationic and acceptor anionic species. Data obtained from the transient absorption decays at the ambient temperature can also be used to calculate KCR (charge recombination rates) values. From the decays the ion-pair lifetimes (τip) along with the corresponding charge recombination rates (KCR) (approximately $KCR \sim 1/\tau ip$) were computed.

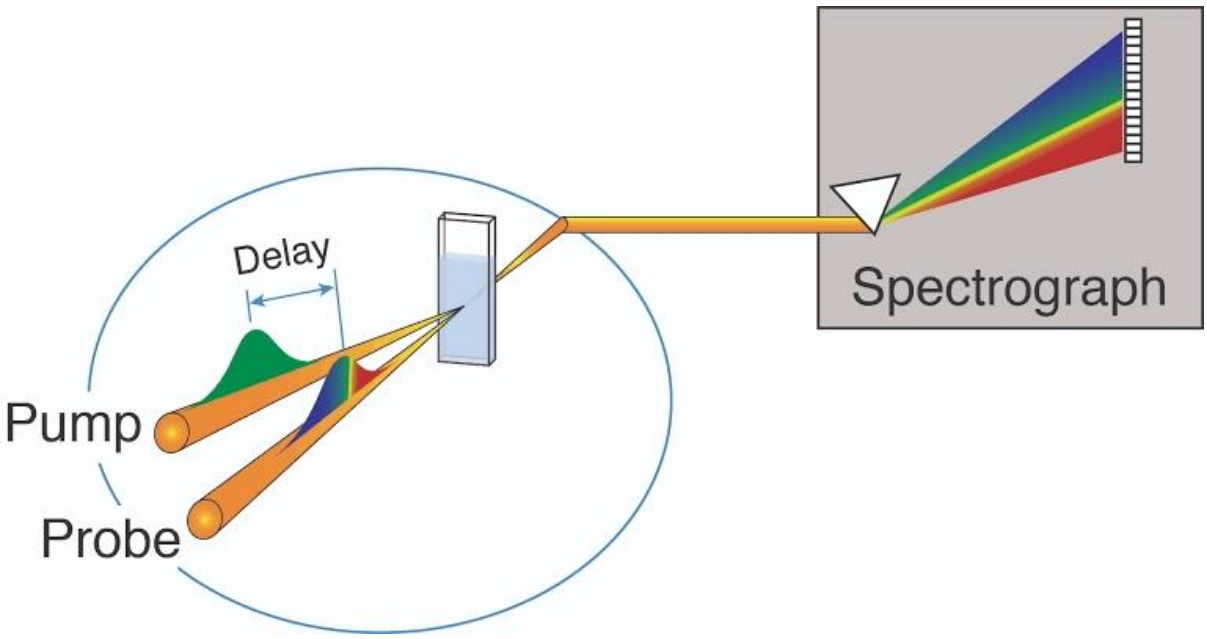

Figure 2.19: Transient Absorption Spectra Analysis. [19]

2.6.2 Applications

There are several uses of transient absorption spectra analysis. These are—

i. **Spectroelectrochemistry**: In this process it collects transient absorption spectra on a semiconductor surface submerged in electrolyte solution under an applied potential, sheds light on how the interfacial electronic structure affects the transport of photogenerated charges.

ii. **Microscopy**: In order to study the effects of film morphology on local excited state dynamics and image directly charge transport in solution-processed organic and hybrid organic-inorganic lead-halide perovskite semiconducting films, ultrafast transient absorption microscopy was used. This technique measures excited state dynamics with sub-micron spatial resolution.

iii. **Thermal Signatures:** Transient absorption spectra in organic and metal oxide semiconductor films can reveal significant heat contributions. [20]

References

1. Park, K. K.; Jung, H.; Lee,T.; Kang, S. K. Bull. Korean Chem. Soc.2010, 31, 984-988.

2. Sujuan Zhu ORCID logo*ab, Xuexue Bai a, Ting Wang a, Qiang Shi a, Jing Zhu a and Bing Wang, "One-step synthesis of fluorescent graphene quantum dots as an effective fluorescence probe for vanillin detection", RSC Adv., 2021, 11, 9121-9129. DOI: 10.1039/D0RA10825A (Paper)

3. D.C. Marcano, D.V. Kosynkin, J.M. Berlin, A. Sinitskii, Z. Sun, A. Slesarev, L.B. Alemany, W. Lu and J.M. Tour, "Improved synthesis of graphene oxide", Am. Chem. Soc., vol-4, 8, 2010.

4. A. Mallick, A.S. Mahapatra, A. Mitra, J.M. Greneche, R.S. Ningthoujam and P.K. Chakrabarti, "Magnetic properties and bio-medical applications in hyperthermia of lithium zinc ferrite nanoparticle integrated with reduced graphene oxide", Journal of Applied Physics, 123, 055103, 2018.

5. https://www.britannica.com/technology/transmission-electron-microscope
6. R. F. Egerton, "Physical principles of electron microscopy", springer, 2005.

7. Wikimedia Foundation. 2022. Ultraviolet–visible spectroscopy. Wikipedia. https://en.wikipedia.org/wiki/Ultraviolet_visible_spectroscopy [accessed 15 Jun, 2022]
8. https://www.eag.com/wp-content/uploads/2019/08/UV-Vis-Optical-System-in-Lambda-1050.jpg
9. PharmaTutor Edu Labs. 2020. Applications of Absorption Spectroscopy (UV, Visible). PharmaTutor Pharmacy Infopedia. https://www.pharmatutor.org/pharma-analysis/analytical-aspects-of-uv-visible-spectroscopy/applications.html[accessed 15 Jun, 2022]

10. E.D. Becker, "High resolution NMR: theory and chemical application", Third edition, Academic press, 2000.

11. Michael W. Davidson, “Fundamentals of Xenon Arc Lamps”
12. https://upload.wikimedia.org/wikipedia/commons/thumb/0/0f/Schematic-diagram-of-the-arrangement-of-optical-components-in-a-typical_Spectrofluorometer.png

13. Nuclear Magnetic Resonance Spectroscopy for Medical and Dental Applications: A Comprehensive Review - Scientific Figure on ResearchGate. Available from: https://www.researchgate.net/figure/Schematic-presentation-of-a-typical-nuclear-magnetic-resonance-spectrometer-showing-the_fig1_333657432 [accessed 20 Jun, 2022
14. SYNTHESIS OF SILVER NANOPARTICLES USING SILK FIBROIN: CHARACTERIZATION AND POTENTIAL ANTIBACTERIAL PROPERTIES. https://www.researchgate.net/figure/Schematic-diagram-of-HR-TEM_fig23_341277064 [accessed 21 Jun, 2022]
15. TCSPC Laser Scanning Microscopy - Upgrading laser scanning microscopes with the SPC730 TCSPC lifetime imaging module. Becker & Hickl GmbH, www.becker-hickl.com [accessed 19 Jun, 2022]

16. Nanophotonic antennas for enhanced single-molecule fluorescence detection and nanospectroscopy in living cell membranes - Scientific Figure on ResearchGate. Available from: https://www.researchgate.net/figure/TCSPC-technique-for-fluorescence-lifetime-analysis-a-TCSPC-technique-is-a-fast_fig8_321568911 [accessed 20 Jun, 2022]

17. Exploring and Exploiting Charge-Carrier Confinement in Semiconductor Nanostructures - Scientific Figure on ResearchGate. Available from: https://www.researchgate.net/figure/Simplification-of-the-time-correlated-single-photon-counting-TCSPC-method-used-to_fig19_314236894 [accessed 20 Jun, 2022]

18. Liisa M Hirvonen and Klaus Suhling, Wide-field TCSPC: methods and applications, Meas. Sci. Technol. 28 (2017) 012003
19. Elles Research Group, https://ellesgroup.ku.edu/ta_spectroscopy.
20. Journal of Materials Chemistry. C, https://doi.org/10.1039/C8TC02977F.

Chapter: 3

Effects of Graphene Quantum Dots on the Energy Storage Capacity of a Short-Chain Dyad.

Abstract

In this present chapter the steady state and time resolved spectroscopic studies along with transient absorption spectroscopic measurements at the different delay times were measured on the short-chain dyad ((E)-4-(((9H-fluorene-2-yl)imino)methyl)-N.N dimethylaniline (NNDMBF)-graphene quantum dot (GQD) nanocomposite system. The results observed from this system have been compared with the pristine dyad and graphene oxide (GO)-dyad nanocomposite. On comparing the dyad-GQD with the pristine dyad and dyad-GO system, the former looks better light energy converters due to greater ability of retention of trans-conformers even on photoexcitation. Additional ET reactions in case of dyad-GQD nanocomposite occurs due to involvement of two ET reactions of the donor (amino) part of the dyad with fluorene as well as GQD which also acts as electron acceptor. The simultaneously occurrences of the two reactions facilitate the formation of relatively stable charge-separated species, as evidenced from both the transient spectra, and observed larger fractional contributions, f (Table 1) of fluorescence lifetimes in comparison to pristine as well as dyad-GO nanocomposite systems.

Key words: Graphene quantum dots; Nanocomposites; Transient absorption; Electron transfer; charge-separated species. Pristine dyad.

1. Introduction

Investigations on photoswitchable short-chain dyads[1-8] reveal great applications in molecular electronics, designing of molecular components of photovoltaic cells and artificial light energy converters, energy storage devices etc. Recent studies by steady state and time resolved spectroscopic techniques demonstrate that when the short-chain dyads combine with nanoparticles of noble metals such as silver, gold, gold/silver core-shell nanocomposite systems[2] and carbon quantum dots[1] they show efficient artificial light energy conversion materials. Investigations with the dyad MNTMA, where methoxynaphthalene donor is attached with the electron acceptor p-methoxyacetophenone, it was observed[3] that the dyad, in its pristine form, does not suffer any conformational changes even on photoexcitation. But when the dyad combines with the noble nanometals, significant conformational changes in the excited states occur. In these changes, the elongated conformer of the dyad facilitates the lowering of the energy destructive charge recombination rate processes as the two redox components donor and acceptor tend to divert from each other minimizing the overlapping of the charge clouds of both the redox components. In the present investigation, a novel synthesized dyad, organic (E)-4-(((9H-fluorene-2yl)imino)methyl)-N,N-dimethylaniline (NNDMBF) has been chosen where N,N-dimethyl amino donor (NNDMB) is being attached with the acceptor fluorene (F) **(Figure 1a**). The primary aim of this chapter is to perform comparative analysis to examine the suitability for designing efficient artificial light energy converter when the dyad is in its pristine form and when combined with graphene quantum dots (GQD). Further the efficiency of the dyad would be considered when the quantum dot would be replaced from GQD to CQD. From the NMR measurements and analysis it is apparent that there is a possibility of the co-existence of two conformers: Trans- and Cis- (**Figure 1b**) of the dyad in its ground state. Detailed steady state and time resolved spectroscopic studies were made to determine the two parameters, charge separation (k_{CS}) and

energy wasting charge recombination rates (k_{CR}), without and in presence of GQD (or CQD) to compare the efficiency of light energy conversion of the pristine dyad and when it adsorbs the nanosurfaces of GQD and CQD i.e., of the same dyad in different nanocomposite forms.

2. Experimental Details

2.1. Materials

The method of synthesis and characterization of the short chain dyad (E)-4-(((9H-fluorene-2-yl)imino)methyl)-N,Ndimethylaniline(NNDMBF) are described elsewhere[9] . The solvents acetonitrile (ACN) (SRL), and cyclohexane (CH) (Sigma Aldrich) of spectroscopic grade were purified following the standard procedures and tested before use for the absence of any impurity emission in the concerned wavelength region. Water was deionized using a Millipore Milli-Q system. The solutions were prepared by dissolving the appropriate amount of dyad in ACN and CH. The synthesis and characteristics of GQD have been described elsewhere[10].

Fluorescence lifetimes were determined by using a time correlated single-photon-counting (TCSPC) technique with the model FLUOROLOG TCSPC HORIBA JOBIN YVON using nanosecond diode lasers of 375 nm and 440 nm (Horiba scientific, DD-375L) as excitation source profiles. The decay kinetics are monitored at emission wavelengths of 480 nm. 520 nm and 550 nm. The quality of fit is assessed over the entire decay, including the rising edge, and tested with a plot of weighted residuals and other statistical parameters e.g., the reduced $\chi 2$ and the Durbin- Watson (DW) parameters. All the solutions prepared for room temperature measurements were deoxygenated by purging with an argon gas stream for about 30 mins.

Femtosecond broadband TA measuring system was based on a femtosecond Ti: Sapphire amplifier (wavelength ~ 800 nm and pulse width < 35 fs). The output from the amplifier (Spitfire Ace, Spectra physics) was divided into two components to generate pump and probe pulses. Pump pulses (at 610 and 532 nm) were obtained from the nonlinear optical parametric amplifier (TOPAS). The probe beam was a white-light continuum (WLC), which was

generated by focusing a small fraction of 800 nm light (from Spitefire Ace) on a sapphire crystal. To obtain a stable and continuous white-light probe, the 800 nm beam was adjusted using an iris and neutral density filter. The probe beam was split into two beams, named the reference and the sample beams. These two beams were detected separately so that the unsolicited noises can be eliminated. The detection of the probe beam was carried out in both conditions: with probe and without probe with the help of a mechanical chopper of frequency 500 Hz. The time delay between pump and probe pulses was controlled with an optical delay line driven by a stepper motor. TA spectra were recorded by dispersing the beam with a grating spectrograph (Acton Spectra Pro SP 2358) followed by a CCD array. The WLC probe confronted group velocity dispersion (GVD), which was compensated with the help of a chirp correction program (Pascher Instrument). Light pulses of a particular wavelength from another TOPAS were used as a probe during the measurement of TA kinetics. Two photodiodes having variable gain were used to record TA kinetics. TA decay traces were fitted with multiexponential functions by taking into account the instrument response function.

3. Results and Discussion

3.1 UV-Vis Absorption and Steady State Fluorescence Measurements

From the theoretical computations on ground state optimized geometry of the dyad NNDMBF (**Fig 2a and 2b**) by using B3 -LYP/6-311 g (d,p) level of theory on HOMO –LUMO surfaces it appears that there may be the two types of conformers Cis- and Trans- , in which the latter form is found to be more stable in the ground state. Thus the above theoretical predictions suggest that both cis- and trans- forms of the dyad exist in the ground state (Figure 2) with the preponderance of the latter. Moreover trans-form of the dyad NNDMBF appears to be more planar.

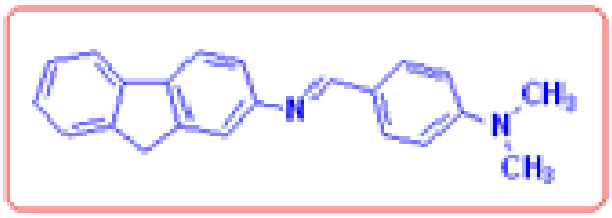

Fig 1a. Molecular structure of the dyad NNDMBF

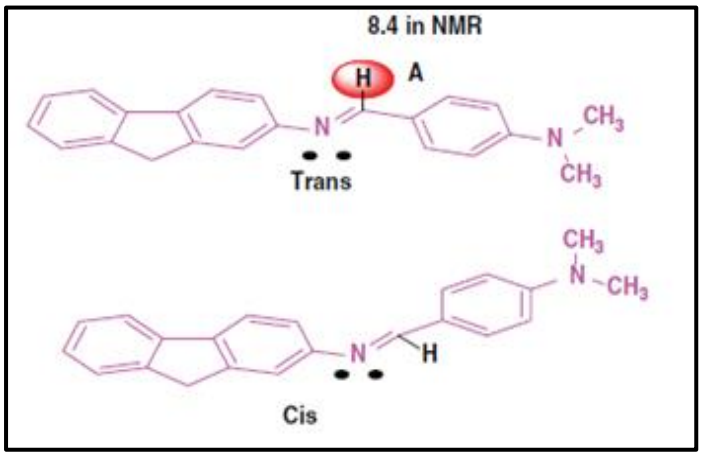

Fig 1b. Cis- and Trans-structure of the dyad

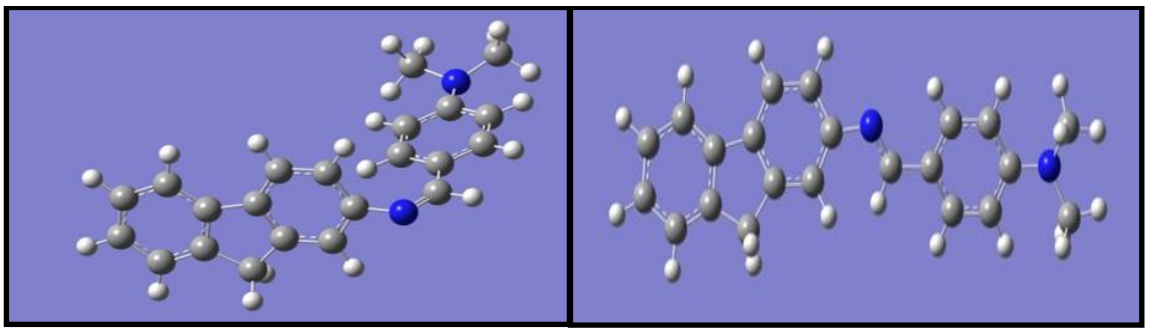

(a) (b)

Figure 2 (a) Cis form of dyad NNDMBF in vacuum**;** (b) Trans form of dyad NNDMBF in vacuum

Trans-form of the dyad appears to be more planar than the cis-one; **(b) Cis form of dyad NNDMBF in vacuum from the theoretical computations on ground state optimized geometry of the dyad by using B3-LYP/6-311g (d,p) level of theory on HOMO–LUMO surfaces; (d)Trans form of dyad NNDMBF in vacuum.**

UV-vis absorption spectra of the pristine dyad in ACN solvent exhibits a broad long wavelength band at around 365 nm region **(curve 0 of Fig 3)**. The charge transfer nature of this broad band has been confirmed from solvent polarity effect which shows blue shift in nonpolar environment relative to ACN solvent. This CT band originates due to partial transfer of electron from the highest occupied molecular orbital (HOMO) of the donor chromophore (D) to the lowest unoccupied molecular orbital (LUMO) of the acceptor fluorene (A). It is to be pointed out here that the UV-vis absorption spectra of the mixture of the free donor and acceptor components (when not present in the dyad) in ACN medium correspond to the superposition of the corresponding spectra of the donor and the acceptor moieties.

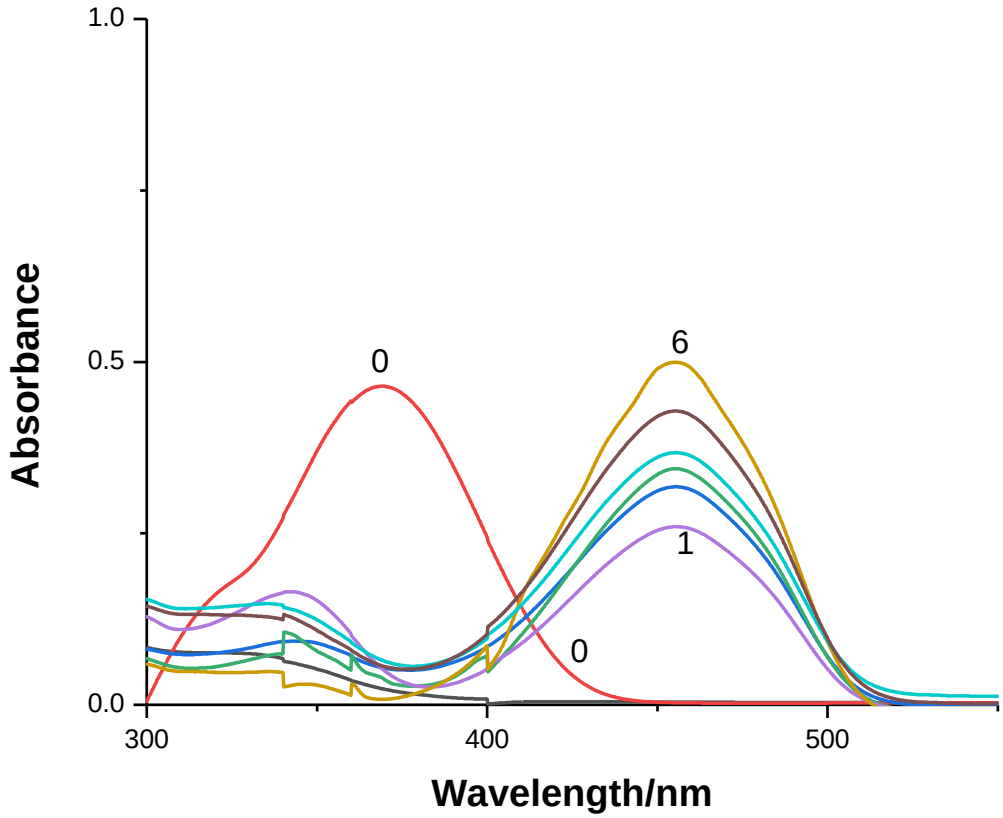

Fig 3: UV-vis absorption spectra of the dyad NNDMBF in ACN at the ambient temperature in presence GQD of concentrations (µg/ml) in 0:0; 1:0.1 ; 2: 0.2; 3: 0.4 ; 4: 0.6 ; 5: 0.8; 6: 1.0 ;

This indicates the lack of formations of any intermolecular ground state complex between the donor NNDMB and acceptor (F). However, in case of the dyad, intramolecular interaction between the donor NNDMB and the acceptor Fluorene (F) leads to the formation of Charge transfer band (broad band at 365 nm region). This indicates that within the dyad, the alignment of the donor and the acceptor moieties are such that it facilitates the formation of CT spectra in the ground state.

With addition of GQD the 365 nm band diminishes gradually with the concomitant development of another band near 450 nm region (**curves 1-6, fig 3**). Following the observations made earlier with gold nanoparticles of different morphologies, it appears that when the dyad adsorbs on the surface of GQD, the band associated with the cis- conformation develops, peaking at about 440 nm, through interconversion (trans to cis) process in the ground state.

On exciting the CT absorption band of the dyad NNDMBF-GQD system (CT nature has been conformed from the solvent polarity effect) at 365 nm region, CT fluorescence band envelop develops peaking at around 450 to 470 nm region (**Figs 4 (a)**) along with a very weak shoulder –like band at 550 nm. The 470 nm as well as 550 nm band become gradually enhanced with increase of concentrations of GQD. However the increment in 550 nm region appears to be relatively slower. The above findings demonstrate that even with the 365 nm excitation (region of mostly trans-isomers) emitting region of cis-isomer at 550 nm appear to be formed in the excited state. This observation demonstrates that in the ground state photoswitchable conversion of the trans-dyad to the cis-form facilitates when combined with graphene quantum dots (GQD).

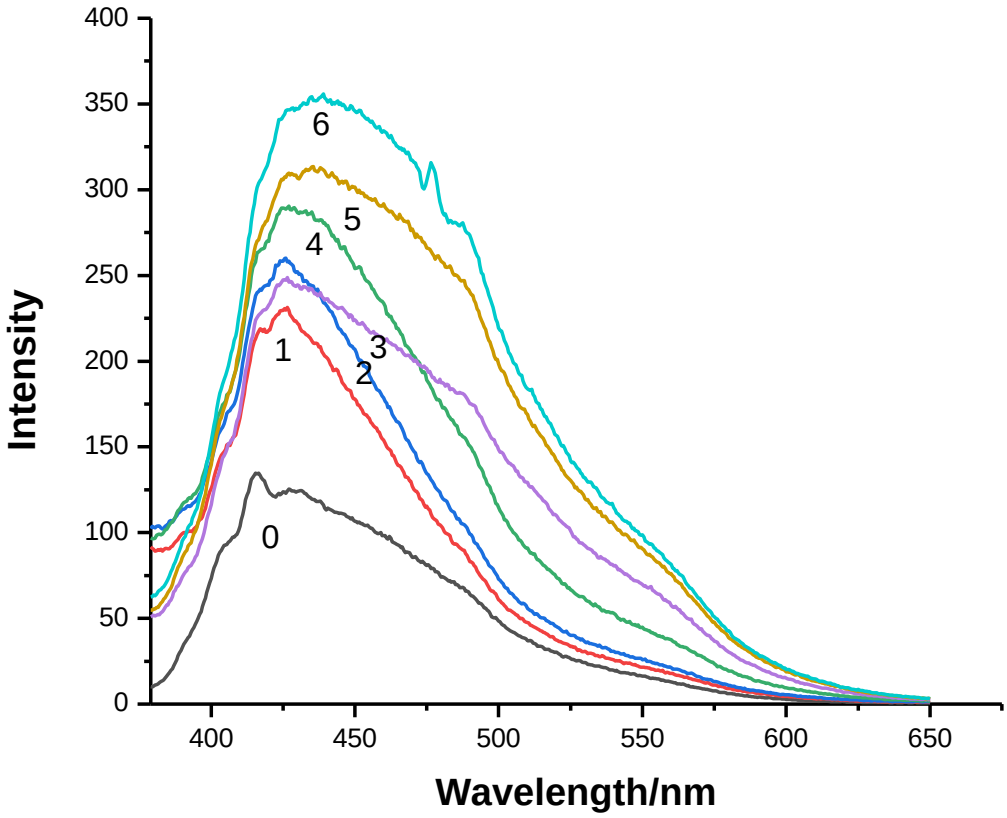

Figure 4(a) Fluorescence CT emission spectra (exc~ 370 nm) of dyad NNDMBF at the ambient temperature in presence of GQD nps of conc. (µg/ml) in 0: 0; 1: 0.1; 2: 0.2; 3: 0.4;4: 0.6; 5: 0.8; 6: 1.0 (Exc. wavelength~ 370 nm)

From the observed enhancement of the fluorescence band throughout its entire region **(Figs 4(a) and 4 (b))** indicates that both trans- and cis –species are formed by exciting the ground state trans-conformers. It is apparent from the fig 4 that due to excitation of the ground trans species, two morphologies, trans and cis, are jointly formed but the former one develops more considerably than the latter ones. This shows in presence of GQDs, the photoswitchable character of the dyad lessen in the excited state.

On the other hand, when the excitation was made at 450 nm wavelength (the region of cis isomer of UV-vis absorption spectra) of CT absorption band of the dyad-GQD system, the CT fluorescence emission mostly originates from 550 nm region (**Fig 4(C))** indicating in this region mostly excited cis-isomeric species of the dyad predominates.

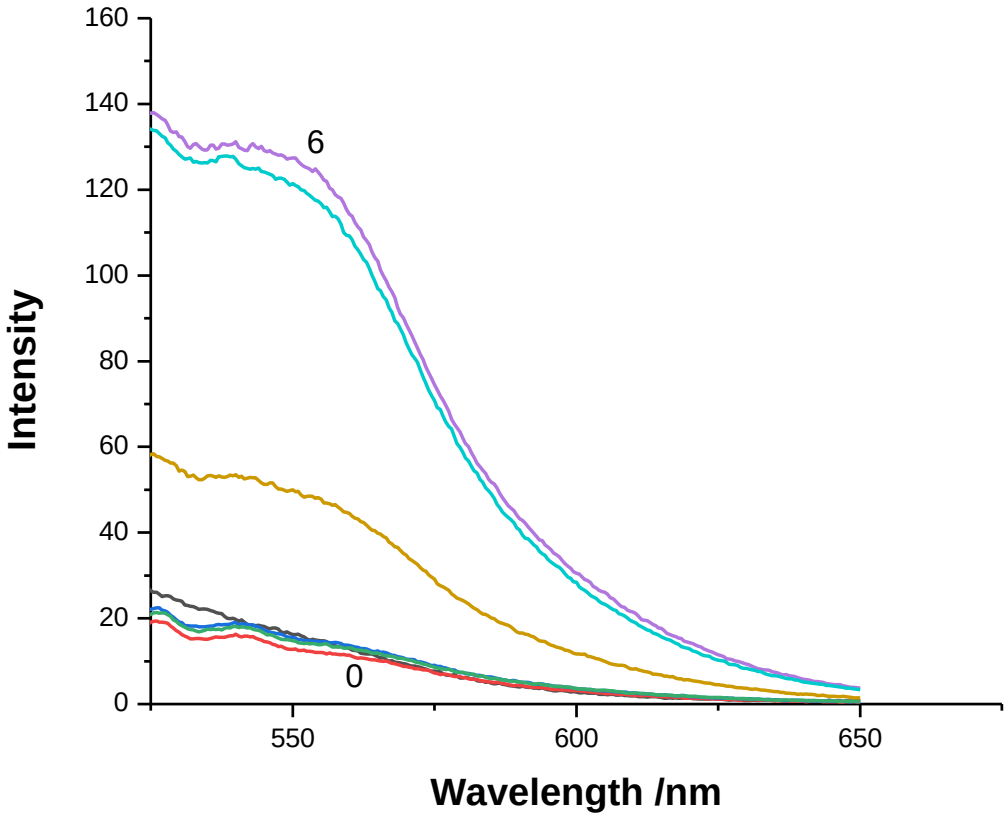

Figure 4(b) Fluorescence CT emission spectra (exc~ 450 nm) of dyad NNDMBF in presence of GQD of conc. (µg/ml) in 0:0; 1: 0.1; 2:0.2; 3: 0.4; 4:0.6; 5: 0.8; 6: 1.0 at the ambient temperature ((Exc. wavelength~ 440 nm)

:

From this Figure it is apparent that though the pristine dyad (curve 0 of **Figure 4a**) exhibits very weak emission at 550 nm but the emission becomes significantly strong when the dyad adsorbs the surface of GQD. This indicates in this environment formation of cis-isomer facilitates largely and the production of cis-species in the excited state occur directly from the

ground state cis-isomer and also from ground trans-isomer through interconversion process. This observation indicates the photoswitchable character of the dyad NNDMBF.

The fluorescence excitation spectra of the pristine dyad and its nanocomposite forms with GQD were measured by monitoring at 480 nm, 520 nm and 550 nm wavelengths (**Figs 5 (a) –(c))**. In the cases of the monitoring wavelengths 480 nm and 550 nm (**Fig 5 (a) and (c))** the observed excitation spectra correspond well to the CT absorption band of the dyad-GQD system where both the bands at 365 nm and 440 nm region were present. In the case of the pristine dyad (where no GO and RGO were present) the excitation spectra show only 375 nm band, which corresponds only CT absorption species having trans-nature whatever be the monitoring wavelength 480 nm or 550 nm. This observation infers that in the case of the pristine dyad, the excited cis-species are mostly formed due to photoconversion originate from the ground state trans-isomers. In the case of the nanocomposite dyads (dyad-GO or dyad-RGO), from the **figures 5b and 5d** where monitoring wavelength is at 550 nm, the region of mostly cis-conformer) the excitation spectra clearly show that cis-forms in the excited state are produced from the ground trans-state on photoexcitation., through interconversion processes. Moreover, presence of 440 nm band in the excitation spectra (possesses clear resemblance with the corresponding absorption spectra of the nanocomposite dyad) indicates that some direct conversion of ground state cis to excited cis is also possible. Figure 5 of excitation spectra clearly demonstrates that the steady state intensities of two excited conformers, trans-and cis-, could be varied by changing the excitation wavelength from 375nm (region of mostly trans-isomer) to 440 nm regime, the domain of primarily cis-conformers. The fluorescence lifetime measurements by TCSPC techniques further corroborate this view. The results obtained from TCSPC method has been discussed below.

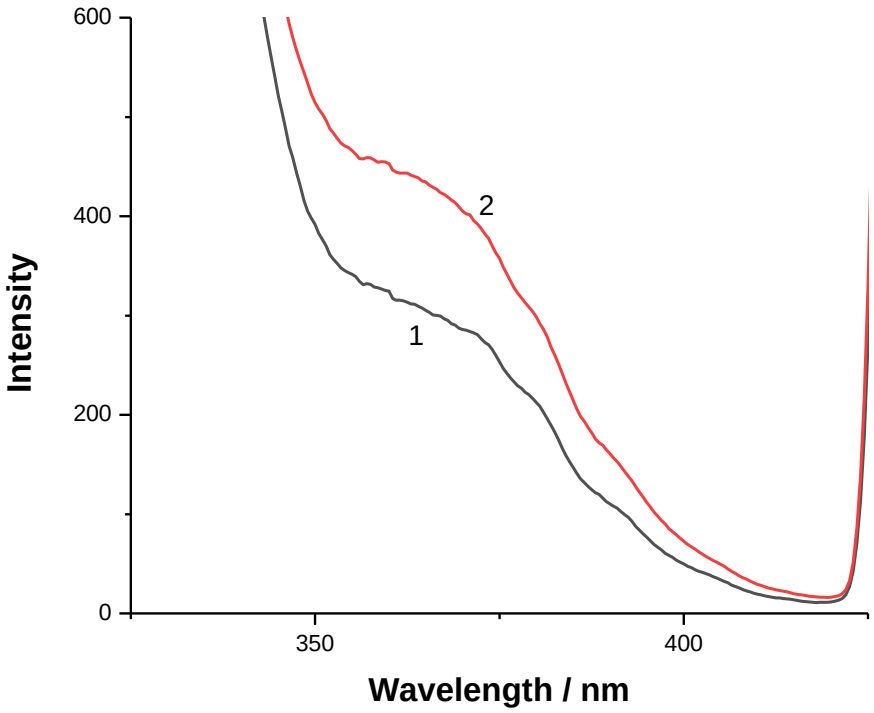
600
400
200
0
Intensity
2
1
350
400
Wavelength / nm

Fig 5 (a)

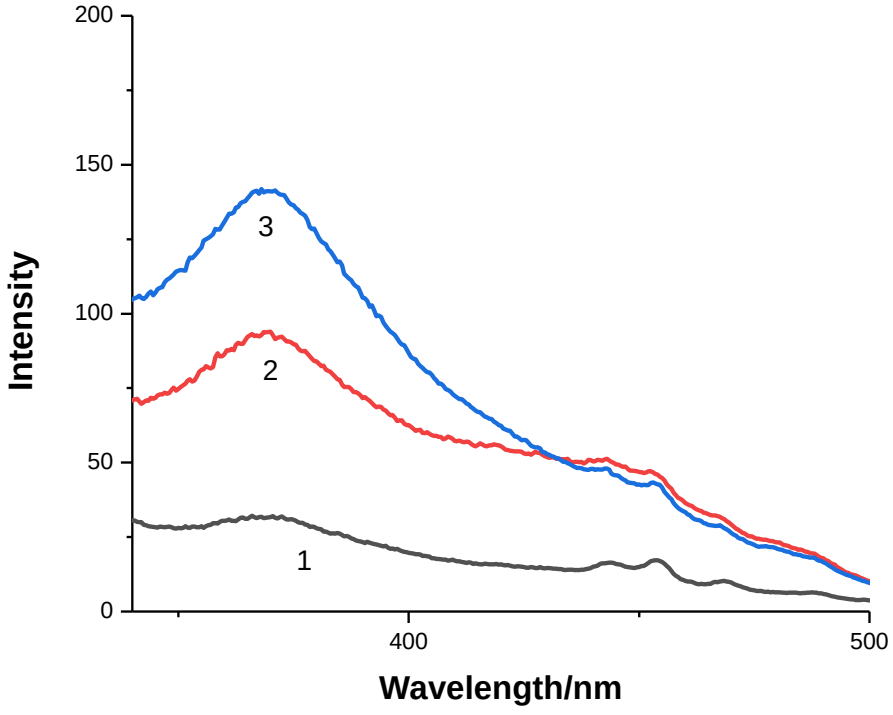
200
150
100
50
0
Intensity
3
2
1
400
500
Wavelength/nm

Fig 5 (b)

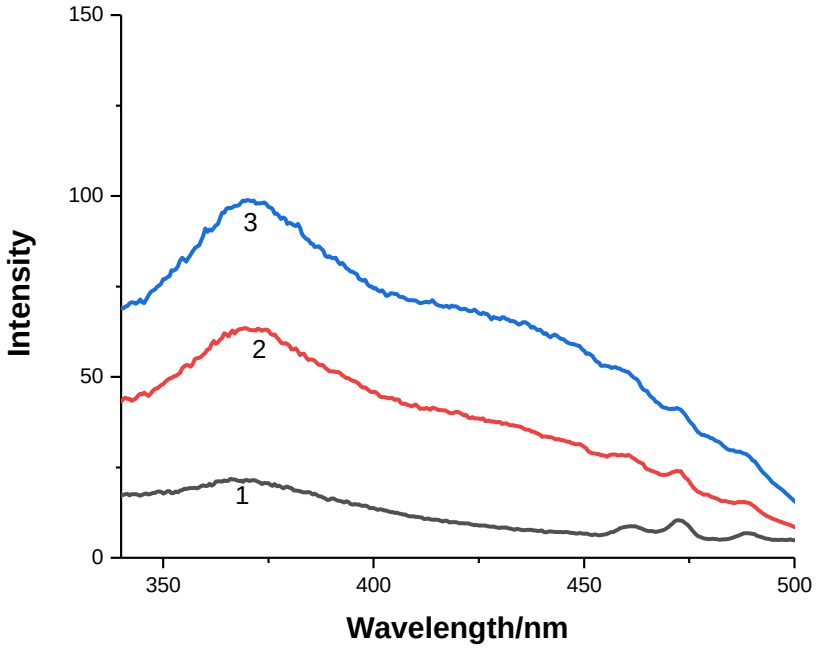

Fig 5 (c)

Fig. 5: Fluorescence excitation spectra of the dyad-GQD nanocomposite system in (a) mon wavelength ~ 480 nm, (b) mon wavelength ~ 520 nm, (c) mon wavelength ~ 550 nm. GQD concentration in $\mu g/ml$: 1:0.1 (1), 2:0.6 (2), 3:1 (3)

(mon wavelength – monitoring wavelength)

3.2 Fluorescence lifetime measurements by TCSPC method

Measurements of the fluorescence lifetimes of the dyad NNDMBF were made by using the time correlated single photon counting (TCSPC) technique. By monitoring the different positions of the steady state fluorescence spectra the possibility of formations of different conformer, apart from trans- one, in the excited state due to photoexcitation has been examined. These findings further provide us the idea that the present short-chain dyad NNDMBF possesses photoswitchable character, especially in its pristine form.

When excitation was made at 375 nm (by using diode laser) in case of the pristine dyad NNDMBF, it was found that at the monitoring wavelength 480 nm (the peak region), majority emission originates from a species having lifetime of 15 ps. (**Table 1**).

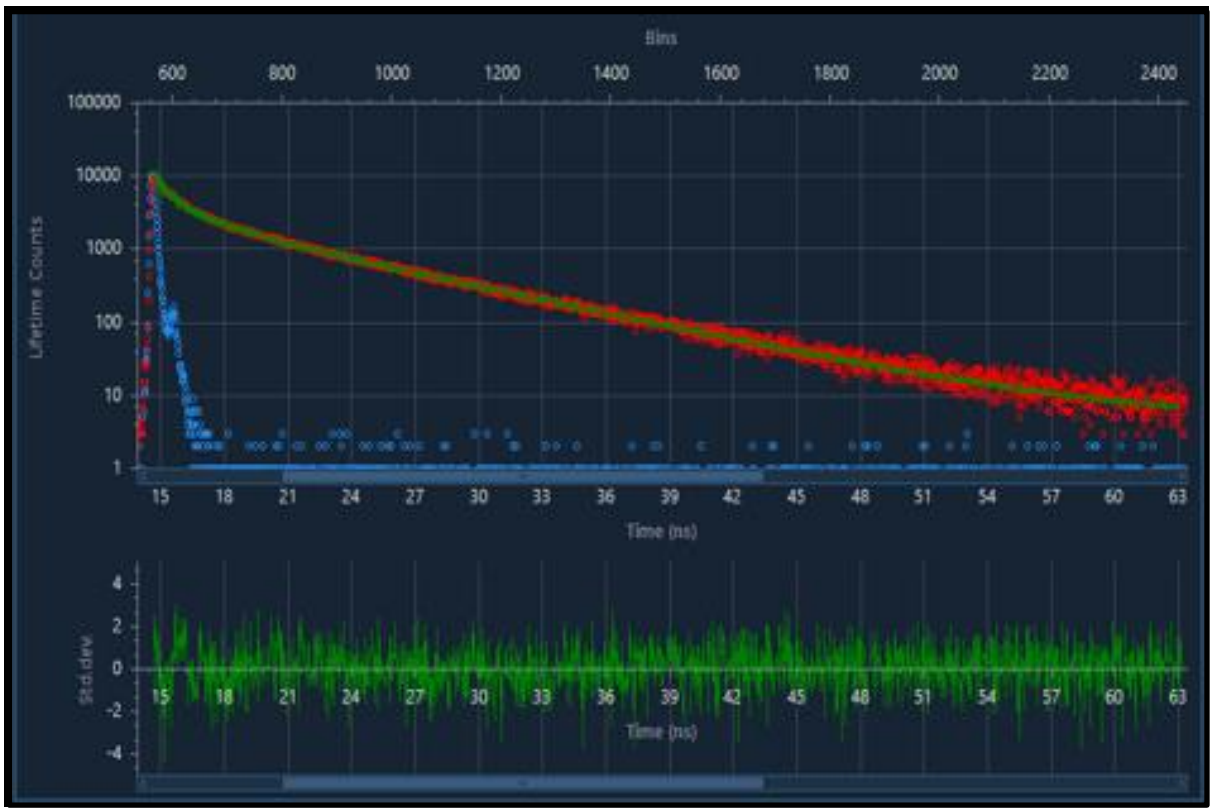

Figure 6: Fluorescence decay of the dyad –GQD system in ACN ex =375 nm, em = 480 nm, the fast (blue) decaying component represents impulse response (diode laser). The residual is also shown. (χ^2 ~ 1.12)

On monitoring at the 550 nm region again only faster component of lifetime of picoseconds (ps) order was observed (table 1). We measured the fluorescence lifetimes of the dyad in presence of GQD (nanocomposite systems) by using the excitation wavelength at 375 nm (Fig 6), the region of mostly trans-isomer. By monitoring at the different positions of the steady state fluorescence band on the longer wavelength side of the excitation wavelength 375 nm, primarily two lifetimes, both in the range of picoseconds, one in the range of 50 ps and the other in the 20 ps domain (**Table 1**).

From the previous investigations we confirmed the latter one originates from the cis-conformer[1]. By exciting the 440 nm wavelength and monitoring at 550 nm region, mostly 25 picosecond component was apparent. This it further substantiates the fact that the picoseconds species, in high probability, should originate from cis-conformers which are of folded nature. Another interesting finding is that in presence of GQD (Table 1) contribution from the 50 ps component decreases, though the decrement is not very significant, along with concomitant increase of the 25ps component (in ns order).as one moves from 480 nm to the position of 550 nm of the dyad fluorescence emission band produced by the excitation at 375 nm.

Hence the above findings demonstrate that when the trans-type dyad in its pristine form is excited by using 375 nm wavelength, most ground state trans isomers convert to the cis-type isomers having ~ 25 ps lifetime component. Thus, the dyad NNDMBF appears to behave as photoswitchable dyad. However, **in the case of nanocomposite dyads i.e.,** when the dyad combines with GQD i.e., quantum dots, 50 ps component, appearing to possess trans-type structure, are found to be present along with the 25 ps component which corresponds to cis-isomer. Thus, by developing nanocomposite systems with grapheme quantum dots, photoconversion (from trans to cis) could be retarded significantly (72 %), whereas from Table1 shows that in the cases of dyad-CQDs systems more than 80% trans-conformation retain in the excited state.

Table 1: Fluorescence Lifetime data of the the short chain dyad NNDMBF in absence (pristine) and presence of GQD at the different excitation and emission wavelengths at the ambient temperature. Values in parentheses besides lifetimes correspond to fractional contributions (f) of the particular species in the total steady state fluorescence emission intensity

Samples	λ_{exc} **(nm)**	λ_{em}**(nm)**	τ_1 **/** (f_1)	τ_2 (f_2)	χ^2
Dyad in ACN	375	480	1.5 ns (0.06)	15 ps (0.94)	1.13
		550	-	1.9 ps (1.0)	1.12
	440	550	-	-	---
Dyad + GQD (1μg/ml)	375	480	54 ps (0.72)	25 ps (0.28)	1.11
		520	50 ps (0.67)	25 ps (0.33)	1.13
		550	56 ps (0.63)	22 ps (0.37)	1.13
	440	550	56 ps (0.10)	26 ps (0.90)	1;07
Dyad + CQD[1]	375	480	6.4 ns (0.84)	256 ps (0.16)	1.156
		550	6.0 ns (0.77)	260 ps (0.23)	1.077
	440*	550			
Dyad + GO (1x10^{-6} M)	375	480	3.61ns(0.21)	91 ps (0.79)	1.080
		550	3.44ns(0.17)	82 ps (0.83)	1.09
	440	550	3.01ns(0.09)	100 ps (0.91)	1.16

Comparison of the results of GQD is done with those of carbon quantum dots (CQD) and GO

Thus dyad- CQDs systems appear to be more efficient light energy converter than dyad-GQD nanocomposites as in the former case **dominated** elongated nature (trans) of the conformers retard **significantly** energy wasting charge recombination processes.

Thus the experimental observations made from the fluorescence lifetime measurements **of the pristine dyad** reveal that though trans-isomer primarily dominates in the ground state but on photoexcitation, most of the trans components convert (photoconversion) to the cis-form in the excited level. However this photoconversion is somewhat impeded when the dyad adsorbs the grapheme quantum dots (GQDs).

From the above results and following the observations made earlier[1]it could be hinted that relatively stable trans-conformer in the excited state in case of the nanocomposite dyad NNDMBF-GQD in comparison to the pristine form may arise from the surface trap effects[11]. The phenomenon should be clearly understood if one compares with dyad-CQD systems where the situations were more prominent. As smaller size of carbon quantum dot (CQD)[12] (~2-5 nm) **exists** relative to GQDs, a larger fraction of the atoms in the former case being on the surface may form electronic states which may act as traps[13] for electrons or holes. These trap states may hinder the photoconversion of trans-to cis- isomeric forms of the dyad.

The theoretical predictions along with the steady state and time resolved spectral measurements clearly reveal that in the ground state trans-isomer of the dyad prevails but on photoexcitation cis-isomeric species of the dyad predominates. This cis-form having folded in nature generates from the relatively planar trans conformer through interconversion processes. In presence of GQD, the photoconversion is somewhat hindered resulting the presence of excited trans-isomers along with the cis-ones. The hindrance effect for photoconversion is not as efficient as observed in the case of carbon quantum dots (CQDs) where more than 80% of the ground state trans-conformers were able to retain their identity of trans-configuration even on

photoexcitation[1]. Thus dyad-CQD systems appear to be better artificial light energy conversion devices relative to the present dyad-GQD nanocomposites. Nevertheless developments of artificial energy conversion devices with graphene[14-16]could not be avoided. Being very strong due to its electrostatic forces resulted from delocalized electrons flowing through positively charged carbon atoms, Graphenes are the excellent candidates which may be used to form chemically and physically stable artificial devices. However, if the light energy conversion efficiencies of the dyad-GQD is compared with the pristine dyad system, the former looks better light energy converter due to **relative stability or** ability of retention of trans-conformers even on photoexcitation, as evidenced **from the observed** value of fractional contributions, f (Table 1). This conformation **of elongated nature** will help to impede energy wasting charge recombination processes and **thus nanocomposites** may serve as better candidates for **designing** artificial light energy **converter** relative to the pristine form.

Ghosh et al[17] reported the negative values of the free energy change of electron transfer process within aniline derivatives and GQDs. This observation suggests that photoinduced electron transfer (PET) processes from aniline derivatives to GQDs is feasible and could be responsible for the luminescence quenching of GQDs. The PET has been confirmed by detecting radical cations for certain aniline derivatives, using a nanosecond laser flash photolysis set up.

The direct evidence of occurrence of photoinduced electron transfer (PET) process is provided from the observations of transient donor cationic and acceptor anionic species from the measurements of transient absorption spectra at the different delay times between exciting and analysing or probing pulses. The excited singlet CT state of the dyad, $^{1}(D^{\delta+}\text{-sp-}A^{\delta-})^{*}$, initially formed by laser photoexcitation of the ground CT, will suffer nonradiative relaxation to form full electron transfer (ET) species, $^{1}(D^{+}\text{-sp-}A^{-})^{*}$ in the excited singlet state.

3.3 Transient absorption spectra from laser flash photolysis measurements

The **femtosecond** transient absorption spectral measurements of the dyad-GQD were made by using a **femtosecond Ti: Sapphire amplifier as excitation source (360 nm)** at the different delay times of the excitation and analysing or probing pulses. It is to be pointed out that the peaking of the transient absorption spectra observed at around 540 nm region could be assigned to the fluorene anion of the contact ion-pair, as confirmed earlier by Ganguly and Durocher [19]. The direct evidence of occurrence of photoinduced electron transfer (PET) process is provided from the observations of transient donor cationic and acceptor anionic species. The transient spectra peaking at around 400 nm of the pristine and nanocomposite dyad NNDMBF in ACN correspond to donor cationic species ($NNDMB^{+}$) **(Fig. 7 a, b and c).** This was confirmed from the production of the oxidized species of NNDMB (NNDMB +) artificially by constant current charger (model DB 300 DB Electronics, India).

This electron transfer (ET) possibility could be tested for the present system, Dyad-GQD by using Rehm-Weller relation [18,19]:

$$-\Delta G^{0} = E^{ox}(D/D^{+}) - E^{RED}(A^{-}/A) - E_{0\,0}^{*}$$

where the symbols have their usual meanings

The potential parameters were determined ($E^{OX}1/2\,(D/D^{+})) \sim +1.85$ V, $E^{RED}1/2(A^{-}/A) \sim -0.72$ V) and E_{00}^{*} is chosen at 3.35 eV (370 nm). The driving energy, ΔG^{0} or exergonicity value was computed to be −0.78 eV. This shows there is a possibility from thermodynamic point of view the occurrence of electron transfer reactions within the dyad in the excited singlet state.Now, since the back ET for formation of the ground state is also largely possible from charge recombination mechanism as evidenced from negative value (−2.57 eV) of ΔG^{b} (G), estimated from the relation,

$$\Delta G^{b}(G) = -E_{1/2}^{OX}(D/D^{+}) + E_{1/2}^{RED}(A^{-}/A) \quad (\text{"G" for ground state})$$

It appears that the formation of ground state dyad through charge recombination would be largely facilitated in case of pristine dyads (which have only cis structure in the excited state). The situation would be less favoured in case of trans-structure of the excited dyad (due to elongated form, the redox partners will be far apart). Thus it seemingly indicates that the yield of charge separated states would be lower in case of pristine dyad and due to stability the charge separated yield will become larger in case of the nanocomposite dyads where the dyad combines with GQDs. Interestingly in case of dyad-GQD nanocomposite system, the band near 400 nm , which corresponds to cationic species of the donor part (amino) of the dyad, remain nearly undiminished with increase of delay times. Whereas, the 550 nm region of the acceptor fluorine anionic part significantly diminishes showing the possible occurrences of charge recombination reactions. As the donor part of the dyad NNDMBF has high probability to undergo efficient PET reactions with both the acceptor F as well as GQD, which is also known to act as electron acceptor, the trans structure of the dyad may undergo additional PET reactions relative to the situation in pristine form. The significant fluorescence lifetime quenching of the trans conformer occurs from ns to ps. Thus it appears that due to involvement of PET reactions of the dyad with GQD (acceptor GQD interacts with the amino donor part of the dyad NNDMBF) the shape of the trans structure may be changed altering or quenching the fluorescence lifetimes from ns to ps order. This additional nonradiative transitions photoinduced ET reactions may facilitate the formations of stable charge-separated species and consequently be helpful to build efficient artificial light energy converters. In case of grapheme oxide (GO) nanocomposite dyad (Fig 7c) the situation differs from GQD and but is similar to pristine dyad (Fig 7a) where both the cationic donor and anionic acceptor lower down in intensity with increase of delay times due to charge recombination processes within the redox partners of the dyad. This shows that though GQD acts as efficient acceptor with the amino donor of the dyad NNDMBF but GO possesses no such role.

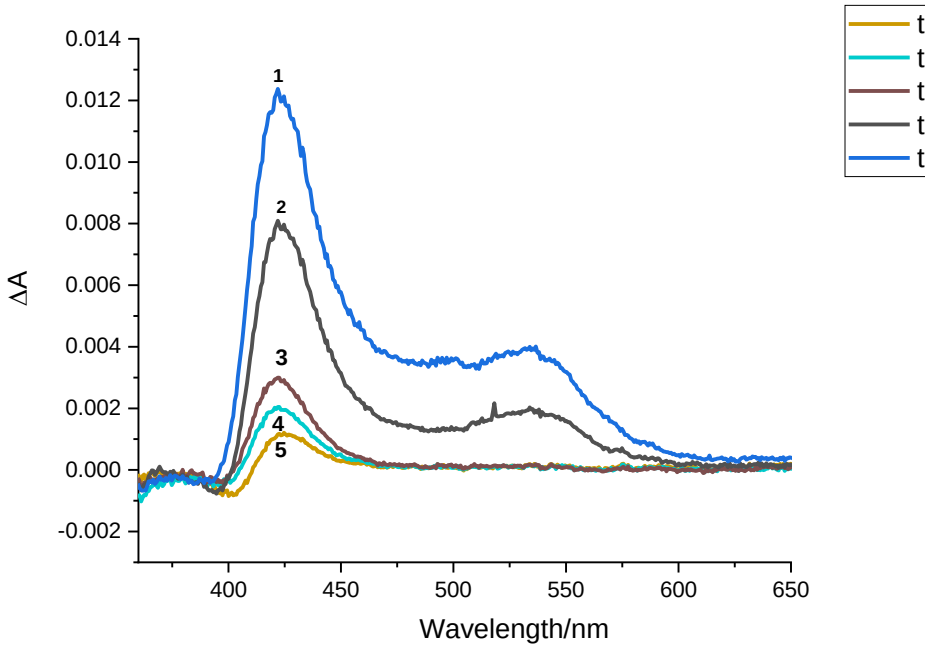

Fig.7a Transient absorption spectra of the pristine dyad in ACN at the different delay times shown in: 1, 0.3 ps; 2, 0.5 ps; 3, 3 ps; 4, 6 ps; 5, 10 ps.

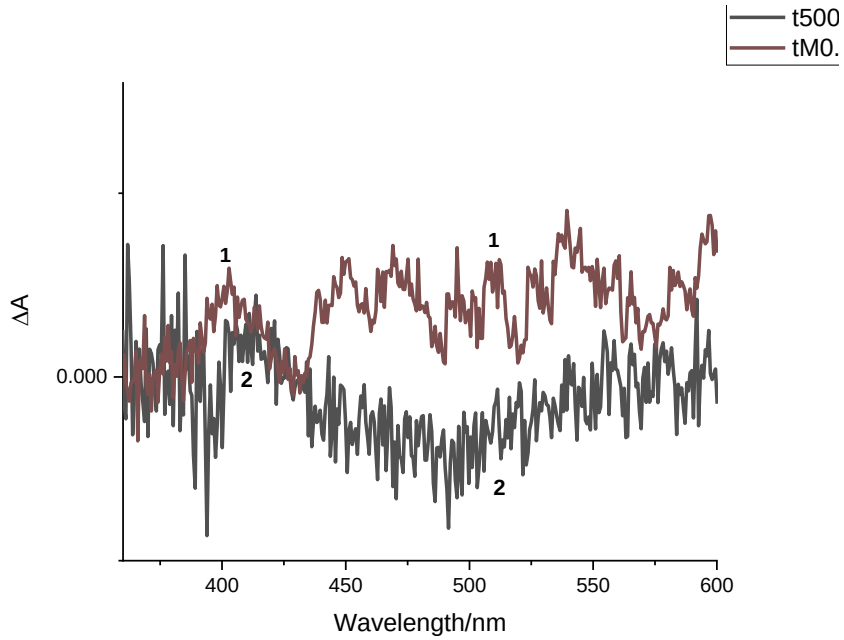

Fig.7b Transient absorption spectra of the dyad-GQD nanocomposite in ACN at the different delay times shown in: 1, 0.2 ps; 2, 500 ps

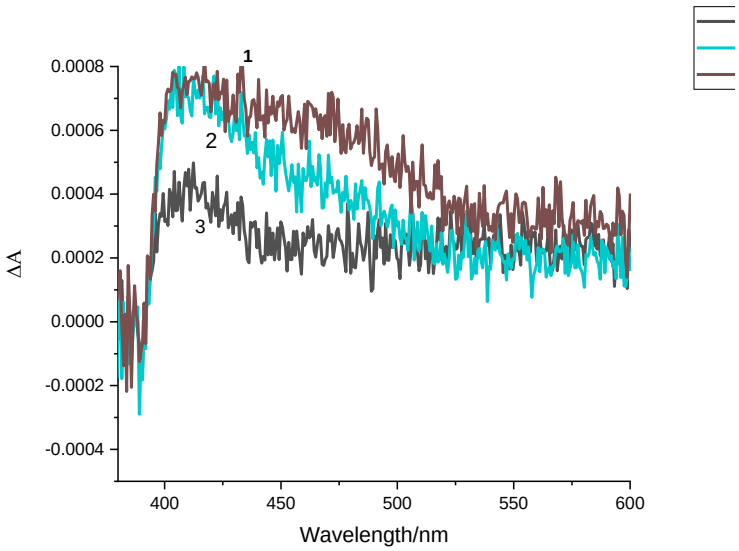

Fig.7c Transient absorption spectra of the dyad-GO nanocomposite system in ACN at the different delay times shown in: 1, 3 ps; 2, 6 ps; 3, 500 ps

Thus additional ET reactions in case of dyad-GQD nanocomposite provides the opportunity to forming relatively stable charge-separated species (Fig 7b), as evidenced from both the transient spectra, and observed larger fractional contributions, f (Table 1) in comparison to pristine as well as dyad-GO nanocomposite systems. It seemingly indicates that dyad-GQD should have the possibility to building up efficient light energy converters where energy wasting charge recombination process plays minor role.

Conclusions

On comparing the dyad-GQD with the pristine dyad, the former looks better light energy converters due to greater ability of retention of trans-conformers even on photoexcitation. This trans conformation being of elongated nature, where the redox partners the donor and the acceptor within the dyad would be far apart, will help to impede energy destructive charge recombination processes within these redox components and may serve as better candidate for artificial light energy conversion systems relative to its pristine form which on photoexcitation converts mostly into folded structure cis-form from its ground extended trans-structure. Graphene based artificial devices appear to be significantly stable in nature and stable trans-conformer in the excited state in case of the nanocomposite dyad NNDMBF-GQD in comparison to the pristine form may primarily arise from the surface trap effects. Involvement of PET reactions of the dyad with GQD (acceptor GQD interacts with the amino donor part of the dyad NNDMBF) appear to change the shape of the trans structure from its extended nature to somewhat new type of conformation altering or quenching the fluorescence lifetimes from ns (observed for tans form of the dyad - CQD nanocomposite system) to ps order. This additional nonradiative transitions may be helpful to stabilize the charge-separated state more efficiently than the pristine dyad and consequently become able to build more stable, proficient artificial light energy converters. The results from the transient absorption measurements further corroborate the presumption.

References

1. I. Mitra, S. Paul, M. Bardhan, S.Das, M.Saha, A.Saha and T. Ganguly *ChemPhys Letts* 726, 1 (**2019**)

2.G. Dutta (Pal), S. Paul, M. Bardhan, A. De, and T. Ganguly, *SpectrochimicaActa Part A*180, 168 (**2017)**

3.G. Dutta (Pal), P. Chakraborty, S. Yadav, A. De, M. Bardhan, P. Kumbhakar,S. Biswas, H.S. DeSarkar, and T. Ganguly,*J Nanosci Nanotechnol*16, 7411 (**2016)**

4.G. Pal, A. Paul, S. Yadav,M.; Bardhan, A.. De, J. Chowdhury, A. Jana, and T. Ganguly,*J NanosciNanotechnol*15, 5775 (**2015)**

5. G. Zaragoza-Galán, J. Ortíz-Palacios, B.X. Valderrama, A.A. Camacho-Dávila , D. Chávez-Flores , V.H. Ramos-Sánchez , and E. Rivera, *Molecules* 19, 352 (**2014)**

6. S. Bhattacharya, T.K. Pradhan, A. De, S.RoyChowdhury, A.K.De, and T. Ganguly, , *J PhysChem A* 110, 5665 (**2006)**

7. E. Allard, J.Cousseau, J. Ordúna, J. Garín, H. Luo, Y. Araki, and O.Ito, ***Phys. Chem. Chem. Phys.,***4, 5944 (**2002)**

8. S.Fukuzumi, K. Ohkubo, H. Imahori, J. Shao, Z.Ou, G. Zheng, Y. Chen, R.K. Pandey, M. Fujitsuka, O.Ito, and K.M. Kadish, *J Am Chem Soc* 123, 10676 (**2001)**

9.S. Paul, I. Mitra, R. Dutta, M. Bardhan,M. Bose, S. Das, M. Saha and T Ganguly *J Nanosci Nanotechnol* 18,7873(**2018)**

10. J P Naik, P Sutradhar, M Saha J Nanostruct Chem 7, 85 (**2017**)

11. C T Smith, M A Leontiadou, R Page, P.O.Brien, D.J.Binks *AdvSci*2, 1500088 (**2015**)

12. Y. Wang, A Hu *J Mater Chem* C2, 6921 (**2014**)

13. H. Zou, C. Dong, S. Li, C. Im, M. Jin, S. Yao, T. Cui, W. Tian, Y. Liu, H. Zhang, *J. Phys. Chem. C* 122, 9312**(2018)**

14. S Paulo, E. Palomares, E M Ferrero *Nanomaterials* 6, 157 (**2016**)

15. C Xie, X Zhang, Y.Wu, Y Wang. W Zhang,P Gao, Y Han, J Jie *J Mater Chem A*1, 8567 (**2013**)

16. A I Taleb, D.Farias *J Phys. Condens Matter* 28, 103005 (**2016**)

17. T Ghosh, S Chatterjee, E Prasad *J Phys Chem A* doi:10.1021/acs.jpca.5b08522

18. T Ganguly, D K Sharma. S Gauthier,D Gravel, G Durocher *J Phys Chem* 96, 3757 (**1992**)

19. D Rehm, A Weller Bur Bunsen-Ges Phy Chem 73, 834 (**1969**)

Chapter: 4

Overall Conclusions

The theoretical predictions along with the steady state and time resolved spectral measurements clearly reveal that in the ground state trans-isomer of the dyad NNDMBF prevails but on photoexcitation cis-isomeric species of the dyad predominates. This cis-form having folded in nature generates from the relatively planar trans conformer through interconversion processes. In presence of GQD, the photoconversion is somewhat hindered resulting the presence of excited trans-isomers along with the cis-ones. The hindrance effect for photoconversion is not as efficient as observed in the case of carbon quantum dots (CQDs) where more than 80% of the ground state trans-conformers were able to retain their identity of trans-configuration even on photoexcitation. Thus dyad-CQD systems appear to be better artificial light energy conversion devices relative to the dyad-GQD nanocomposites. Nevertheless developments of artificial energy conversion devices with GO or GQD could not be avoided. Being very strong due to its electrostatic forces resulted from delocalized electrons flowing through positively charged carbon atoms, Graphenes are the excellent candidates which may be used to form chemically and physically stable artificial devices. However, if the light energy conversion efficiencies of the dyad-GQD is compared with the pristine dyad system, the former looks better light energy converter due to **relative stability** or ability of retention of trans-conformers even on photoexcitation, as evidenced from the observed value of fractional contributions, f (Table 1) and transient spectra. This conformation **of elongated nature** will help to impede energy wasting charge recombination processes and **thus nanocomposites** may serve as better candidates for designing artificial light energy converter relative to the pristine form.

Additional ET reactions in case of dyad-GQD nanocomposite occurs due to involvement of two ET reactions of the donor (amino) part of the dyad with fluorene as well as GQD which also acts as electron acceptor. The simultaneously occurrences of the two reactions facilitate the formation of relatively stable charge-separated species, as evidenced from both the transient

spectra, and observed larger fractional contributions, f (Table 1) of fluorescence lifetimes in comparison to pristine as well as dyad-GO nanocomposite systems.

Table 1: Fluorescence Lifetime data of the short chain dyad NNDMBF in absence (pristine) and presence of GQD at the different excitation and emission wavelengths at the ambient temperature. Values in parentheses besides lifetimes correspond to fractional contributions (f) of the particular species in the total steady state fluorescence emission intensity

Samples	λ_{exc} **(nm)**	λ_{em}**(nm)**	τ_1 **/** (f_1)	τ_2 (f_2)	χ^2
Dyad in ACN	375	480	1.5 ns (0.06)	15 ps (0.94)	1.13
		550	-	1.9 ps (1.0)	1.12
	440	550	-	-	---
Dyad + GQD (1μg/ml)	375	480	54 ps (0.72)	25 ps (0.28)	1.11
		520	50 ps (0.67)	25 ps (0.33)	1.13
		550	56 ps (0.63)	22 ps (0.37)	1.13
	440	550	56 ps (0.10)	26 ps (0.90)	1;07
Dyad + CQD[1]	375	480	6.4 ns (0.84)	256ps (0.16)	1.156
		550	6.0 ns (0.77)	260ps (0.23)	1.077
	440*	550			
Dyad + GO ($1x10^{-6}$ M)	375	480	3.61ns(0.21)	91 ps (0.79)	1.080
		550	3.44ns(0.17)	82 ps (0.83)	1.09
	440	550	3.01ns(0.09)	100 ps (0.91)	1.16

Comparison of the results of GQD is done with those of carbon quantum dots (CQD) and GO